1

Microplastics Formation

Xinxing Zhang, Qinke Cui, and Zhuo Huang

Polymer Research Institute of Sichuan University, State Key Laboratory of Polymer Materials Engineering, No. 24, South Section of 1st Ring Road, Chengdu 610065, China

1.1 Definition of Microplastics

Over the last few decades, plastic contamination has become a major cause of concern among scientists, politicians, and the public. The world production of plastic surpassed the 320 million tons mark in 2016, most of which is intended for packaging, i.e. for immediate disposal. Consequently, these materials significantly contribute to waste generation, and it is estimated that between 5 and 13 million tons leak into the world's oceans every year [1]. When inappropriately dumped or mismanaged, plastic waste can accumulate in both terrestrial and marine environments, and once released, it may be subjected to degradation by several agents or routes, such as solar radiation, mechanical forces, and microbial action. This leads to fragmentation and breakdown of larger materials into plastic debris and eventually nanoplastics (NPs), though the latter has only been recently identified as potentially deleterious toward the environment, and research is currently underway. In addition, these particles can be intentionally produced with micro- and nano-sizes and disposed of directly into the environment [2]. Microplastics (MPs) are defined as debris smaller than 5 mm. Mesoplastics are defined as plastic debris within the 5 mm−20 cm range, while MPs are defined to be less than 5 mm in size, according to the National Oceanic and Atmospheric Administration (NOAA) workshop consensus definition. However, as far as the authors are aware, the lower limit for defining MPs remained undefined for a long time. Recently, two categories have been proposed: large MPs in the 1–5 mm range and small MPs defined as micrometric particles, that is, below 1 mm [3]. These categories were confirmed by Galgani et al. [4] and suggested for adoption by the European Marine Strategy Framework Directive (MSFD) (precisely, large MPs were defined by the range 1–5 mm and small MPs by the range 20 μm–1 mm). Nanosized plastic particles are referred to as NPs (1–1000 nm size range) [5]. In 2008, Klaine et al. defined NPs as particles with at least two-dimensional diameters between 1 and 100 nm [6]. However, some studies defined NPs as plastics with particle sizes between 1 and

Microplastics in the Environment: From Formation to Remediation,
First Edition. Edited by Xinxing Zhang.

1000 nm [7, 8]. Although there are some controversies about the definition of NPs, the definition of NPs with a particle size of 1–1000 nm is generally accepted by researchers. Here, MPs are defined as debris smaller than 5 mm, and our book defines NPs as plastics with particle sizes between 1 and 1000 nm.

When discussed in detail, MPs in the environment are usually categorized as primary or secondary MPs (PMPs or SMPs) depending on their source [9]. PMPs are MPs produced without aging, whose primary source is particulates specifically manufactured for commercial applications such as personal care products and cosmetics [10, 11]. In general, they include plastic pellets used as raw polymer materials, cosmetic microbeads, and sandblasted plastic microbeads [9]. SMP are smaller fragments formed from larger plastic products (e.g. fishing nets, plastic bottles, and films) that have been broken up through the effects of aging processes, biological action, and mechanical wear [12, 13]. Notably, SMPs are being generated in an increasing number of obsolete consumer products, and many studies have shown that SMPs account for the majority of MPs in the environment, including oceans, rivers, mountains, landfills, and even drinking water [14–19].

Due to the small particle size, high specific surface area, remote migration, and contaminant adsorption capacity, these particles can be ingested by several species, leading to direct physical damage and potential toxicity effects [2]. MPs may also leach plastic additives, including persistent organic pollutants (POPs) and potentially toxic elements that are adsorbed in higher concentrations than those found in the surrounding environment. These pollutants may transfer and accumulate in different tissues of organisms, possibly undergoing biomagnification along the food chain. Hence, the consumption of contaminated seafood poses a route for human exposure to MPs, POPs, and potentially toxic elements [20]. POPs, including polychlorinated biphenyls (PCBs) and polycyclic aromatic hydrocarbons (PAHs), have also been shown to accumulate on MPs, thus enhancing their potential toxic effect in the environment [21–23]. Recently, Jovanović reported potential negative effects of the ingestion of MPs and NPs by fish, including possible translocation of MPs to the liver and intestinal blockage, yielding not only physical damage but also histopathological alterations in the intestines and modification in lipid metabolism [24]. Hence, it is of urgent and significant importance to clarify formation mechanisms, transport processes, toxicity of composite pollutants, and control technologies, which can provide meaningful guidance for production and use of plastics and thus prevent MP pollution.

1.2 Types of Microplastics

Many studies have given information about the most widespread species of MPs in terms of the distribution of plastic debris in systems such as soil, freshwater, and oceans. It reveals that polyethylene (PE), polypropylene (PP), polystyrene (PS), polyvinyl chloride (PVC), polyester, polyamide (PA), and polylactic acid (PLA) are found in a variety of locations, and the majority of environmental MPs are concentrated in the top five, which are also the most common types of plastic products

[25–29]. Plastics with simple composition are basically composed of polymers without any additives. Some types require only small amounts of additives, such as PE and PP. However, most plastics are multicomponent systems that contain a wide range of additives, in addition to the basic polymer component (generally 40–100% polymer). The most important additives can be divided into four types: lubricants to help with processing; fillers, enhancers, impact modifiers, plasticizers, etc., to improve the mechanical properties of the material; flame retardants to provide the flame resistance; and various stabilizers to improve the aging resistance during use. Understanding the composition of plastics is essential for the study of MP formation mechanisms, generation behavior, and even toxicological effects.

1.2.1 Polyethylene

PE has sufficient sources of raw materials and has excellent chemical corrosion resistance, low-temperature resistance, and good processing fluidity. Therefore, the production of PE and its products has developed very rapidly. Since 1966, the production of PE has been the first in the world in terms of plastic production. Due to the simple molecular structure of PE and its good flowability at high temperatures, only small amounts of plasticizers need to be added during the molding process. Excellent processing properties and low cost are the advantages of PE being used in a wide range of film products.

1.2.2 Polypropylene

PP and PE are both polyolefins with similar properties and use. Compared to PE, the molecular chain of PP is less flexible and more rigid, so PP is stronger and harder than PE, presenting a more rigid performance. Another characteristic of PP plastic in performance is its low density, which is the lightest of the commonly used plastics and can float on water. The heat resistance of PP is also better, with a long-term use temperature of 100–110 °C. Even PP does not deform when heated to 150 °C without external forces.

The biggest disadvantage of PP films is the poor aging resistance than PE, mainly owing to the fact that PP has many methyl groups on its main chain, and the hydrogen on the tertiary carbon atoms connected to the methyl groups is easily attacked by oxygen [30]. Therefore, PP plastics are usually subject to the addition of antioxidants and UV absorbers, which greatly affect the generation behavior of PP MPs. For example, variable-valent metal ions such as copper and manganese ions accelerate the oxidative aging process of PP. Metal ion inhibitors are a class of additives that can complex with the variable-valent metal ions to reduce the catalytic oxidative activity of these metal ions. Some of the commonly used ion inhibitors are aldehydes and diamine condensates, oxamide compounds, hydrazide compounds, and so on. Light shielding agents, such as titanium dioxide, are also frequently added to PP to protect the polymer, which will directly reflect light or absorb specific light waves and then convert light energy into heat to scatter. The introduction of metal ion inhibitors and titanium dioxide will greatly slow down the photo-aging process of PP plastic products in nature and reduce the generation of PP MPs.

1.2.3 Polystyrene

The main chain of PS is a saturated alkane chain, and its side groups are benzene rings with large spatial positional resistance. The irregularity of the molecular structure increases the site resistance while affecting the orderly arrangement of molecules; thus, PS has large rigidity but is not easy to crystallize, which is a typical linear amorphous polymer. PS plastic is a transparent hard solid at room temperature, whose light transmission rate (88–92%) is second only to Plexiglas. The extremely small water absorption is the distinguishing feature of PS, which hardly absorbs water at room temperature. In addition, due to the absence of polar groups in the molecular structure, PS has excellent corrosion resistance and electrical properties. PS plastics obtain better mechanical strength due to the presence of benzene rings but also face poor impact strength and brittle cracking due to the lack of flexibility of the chain segments caused by the benzene rings. There is another noteworthy aspect of PS plastics related to the generation of MPs. Although PS is one of the most radiation-resistant polymers, it becomes brittle when cross-linked at high doses of radiation. These brittle qualities are potentially important reasons for the breakage of PS into plastic fragments and the generation of MPs. PS plastic is now widely used in industrial decoration, lighting indication, and electrical insulation materials, as well as optical instrument parts, transparent models, toys, and daily necessities. According to the different usage requirements of PS plastic products, coloring agents, plasticizers, light stabilizers, flame retardants, anti-static agents, and other additives will be added in appropriate amounts.

1.2.4 Polyvinyl Chloride

PVC, in terms of molecular structure, has polar chlorine atoms in the molecular chain, which increases the intermolecular force. The chlorine atom on the side group hinders the rotation within the single chain, and thus compared to PE, the flexibility of the molecular chain decreases while the rigidity increases, resulting in high compressive strength, surface hardness, and good rigidity but low elongation of PVC products. When the operating temperature is lower than 0 °C, the products will easily become hard and brittle, and PVC MPs will be generated in large quantities. PVC is divided into rigid PVC and soft PVC according to the requirements of usage performance, which is controlled by the different amounts of plasticizer added during processing and molding. Most commonly used plasticizers are esters synthesized from fatty alcohols with carbon atoms of 6 to 11 and phthalic acid, which are utilized to reduce the intermolecular forces of PVC, thus having the effect of lowering the molding temperature of the polymer, as well as reducing the modulus, rigidity, and brittleness of the product. Industrial plasticizers used in PVC processing are the most major ones, accounting for about 80% of plasticizer usage. Rigid PVC plastic can be made when a small amount of plasticizer is added to the production. It has high mechanical strength and is resistant to acid and alkali corrosion, so it can be used to replace some valuable stainless steel and other corrosion-resistant materials to manufacture various downpipes and joints. It is widely used in agricultural drainage and irrigation, urban downpipes, and exhaust pipes. When plasticizer is added at 30–40%, soft PVC is produced. Although the tensile strength and bending

strength are lower than those of rigid PVC, the elongation is high, and the products are soft. The main disadvantages of rigid PVC plastics are poor processability, thermal stability, and impact resistance. On the other hand, soft PVC plastics are susceptible to plasticizer volatility, migration, and extraction during use. Another significant characteristic of PVC is its very poor thermal stability. In air above 150 °C, PVC degrades and emits HCl, which acts as an autocatalyst and promotes degradation. Macroscopically, the color of the product turns yellow and, finally, black. Therefore, a large number of heat stabilizers must be added to PVC plastics. Organotin compounds are the most common heat stabilizers for PVC products, while others include metal salt compounds. The abovementioned plasticizers and heat stabilizers are generally toxic and can cause adverse effects on living organisms.

1.2.5 Polyester

Polyester mainly refers to PE terephthalate, which is primarily used as the fiber. Polyester is a linear macromolecule with a symmetrical benzene-ring structure and neat arrangement of functional groups on the molecular chain, so it has high density, softening point (230 °C), melting point (250–260 °C), heat resistance, and light resistance. The presence of a benzene ring hinders the internal rotation of the molecular chain, making its macromolecular backbone rigid and resistant to deformation, with high initial modulus and excellent recoverability. In addition, the structure of polyester also contains methylene, so it has a certain degree of flexibility, which endows the fiber with good elasticity. It is worth noting that the ester bond of polyester will be oxidized during the long-term use of the fiber, thus leading to oxidative cleavage of the molecular chain and the generation of carboxyl groups. The result is decreased molecular weight, reduced strength, yellowing of the color, and even the generation of MPs. Particularly, the ester group will undergo hydrolysis or alcoholysis with water and alcohol at high temperatures, which will damage the fiber as well. Due to the regularity of the molecular chain, polyester has the ability to form crystals by the orderly arrangement in three-dimensional space. Although the trait is limited by the benzene ring, the crystals are more stable once polyester has been stretched to form them. Therefore, polyester has a high degree of crystallinity overall, which is also closely related to the formation of MPs. Besides fibers, polyesters are also widely used in the preparation of films and hollow plastic bottles. However, the main drawback of polyester is its poor processability, which is due to its low crystallization rate. Nucleating agents and other additives are now needed to increase polyester crystallization speed to improve molding processability.

1.3 Generation of Microplastics

Due to their small sizes, MPs are easily introduced into the body by organisms through nutrient intake, causing a range of physical effects and toxicological reactions [31, 32]. In addition, the high surface area of MPs tends to complex and enrich with various contaminants such as PCBs, PAHs, antibiotics, heavy metals, and organochlorine pesticides. These adsorbed chemical pollution complexes have been proven in numerous studies to be highly toxic and harmful to marine

organisms, soil microorganisms, and plants [12, 33–38]. Therefore, a detailed and extensive discussion of the degradation processes, formation mechanisms, and generation behaviors of secondary MPs is a very important and urgent task, which is essential to improve our understanding of the threat of environmentally relevant MPs to ecosystems and the biosphere.

1.3.1 Primary Microplastics

Due to the many benefits of plastic, its use has increased, but improper waste management has led to the entry of these materials into the environment. One of the emerging contaminants of plastics is MPs, which are plastic particles smaller than 5 mm. MPs can be present in the environment as manufactured MPs (known as primary MPs) or resulting from the continuous weathering of plastic litter, which yields progressively smaller plastic fragments (known as secondary MPs) [39]. Categorizing MPs into primary and secondary particles is beneficial to help identify their sources and a solution to reduce their entry into the environment.

MPs are released into the environment from both primary and secondary sources [19]. Primary MPs often refer to pellets and personal care and cosmetics products (PCCPs), which are produced and enter the environment with small sizes [9]. However, some studies have proposed a broader range of primary MPs [40, 41]. They proposed that primary MPs include not only intentionally created MPs (e.g. PCCPs) but also by-products during the use of related plastic products (such as microfibers detached from clothing, tire dust from running cars, and MPs discharged from artificial turfs and paints), as well as unintentionally released ones (e.g. pelleted raw materials) [42]. They considered that primary MPs are those as adding new plastic materials of micro size to the environment [43].

Primary MPs are mostly produced as part of the daily plastic product use. The emission process is often invisible but poses potential ecological hazards. Primary MPs are inherently small in size, including resin pellets, micrometer pellets in personal care products, industrial scrubbers used in cleaning materials, and plastic powders used for molding, which contain PE, as well as PP and PS. Furthermore, primary MPs are at least less than 10 μm in size, and their average size is between 150 and 330 μm [39]. On the other hand, primary MPs are generated from the breaking of larger plastic particles. For example, up to 700 000 synthetic fibers can enter the water in a washing process, which falls into this category. These textiles are mainly composed of polyester (78%), followed by PA (9%), PP (7%), and acrylic (5%) [44].

Based on the relevant literature, we identified the main sources of primary MPs [45, 46]. The finalized list generated for this study included the following: (i) synthetic fibers produced during the laundry process and present in household/indoor dust, (ii) microbeads produced in the use of PCCPs, (iii) marine coatings (shedding of paint during the use of the ship or removal of old paint during maintenance), (iv) vehicle paint (flaking and chipping of the paint in original equipment manufacturer (OEM) or paint emissions during refinishing), (v) road markings, (vi) architectural coatings (such as paint falling off during the process of painting buildings), and (vii) plastic dust (pellets) from raw material production or generated during transport [44]. Given the known use of MPs and in view of desired product properties,

consumer product categories containing primary MPs are determined. Synthetic fibers (i) and microbeads (ii) are primary MPs released from consumer products, and others are from industrial processes.

1.3.1.1 Industrial

Primary MPs may be added to coating products to achieve specific functional requirements such as weight reduction, scratch and abrasion resistance, and elasticity. Plastic particles, such as (hollow) microspheres (5 to 80 μm) and microfibers (0.5 to 50 mm) that are artificially incorporated or present in the design in the size range of 1 nm to 5 mm can be added to coatings [47]. These microspheres can reduce the mass of the coating, improve the application function of the coating, allow thicker coatings and provide unique coating film properties such as elasticity and scratch resistance. Microfibers can improve the toughness of coatings, act as a joint in cracks and joints in walls or ceilings and increase the thixotropy of undried coatings. Water-based coatings contain "polymer dispersions in water," which are considered virgin-grade MPs and consist of dispersed polymer particles. They act as a binder in the cured coating but are still the main MPs when the coating is not handled properly; for example, when fluids are poured down the drain [48]. Possible sources of coating-related virgin MPs include the following applications: (i) paints: architectural, industrial, automotive, wood, marine (including antifouling), etc.; (ii) road marking paints; (iii) sandblasting of old coatings using plastic materials [49].

Primary MPs can be released by draining waste waterborne paint down the drain and rinsing brushes and rollers under the tap. This release of polymer particles and intentionally added microspheres/microfibers from liquid waste paint occurs from time to time. It is important to note that the MPs will enter the sewage system and eventually the publicly owned treatment works (POTW), and a proportion of them will enter and be present in the sludge of the sewage treatment plant [50]. In recent years, environmental pressure to control volatile organic chemicals (VOCs) has led to the rapid development of waterborne coatings, and changes in the composition of waterborne coatings have led to changes in other characteristics of the coating products. Waterborne coatings contain MPs (emulsions containing dispersed solid polymer particles), whereas solvent-based coatings do not contain MPs (dissolved polymers) [51]. The change from solvent-based to water-based paints may result in increased environmental releases of primary MPs through the disposal of waste water-based paints in drains.

The main components of coatings are fillers, film-forming resins, additives, and dispersing media. Many natural resins and synthetic polymer resins can be used as film-forming resins in coating products. The film-forming resins used in coatings are usually based on carbon-chain polymers such as alkyd, polyester, acrylic, polyurethane (PU), and epoxy resins, which form a solid coating after the coating has been applied. The chemical properties of the coating MPs will, therefore, depend on the main components chosen for the coating product. In addition, coatings are complex mixtures of many compounds, some of which are associated with potential health effects in biological organisms (e.g. biocides in antifouling coatings) [9]. Whereas solvent-borne paint polymers are dissolved in the paint system, water-borne paints are essentially emulsion systems in which polymer particles are

dispersed. The size of the polymer particles has a different effect on the performance of aqueous coatings, with the fine particles enhancing the film formation and pigment adhesion of the coating, as well as increasing the viscosity of the coating. Polymer particles in aqueous coatings generally range from 80 to 1000 nm [52].

The shapes of primary grade MPs added to marine coatings include microspheres/beads, but most coating formulations do not contain microspheres as a component. Acrylic polymers range from 5 to 80 μm (0.005 to 0.8 mm), and acrylic polymer nanoparticles are used as binders ranging from 50 to 200 nm (0.000 05 to 0.000 2 mm). The polymer particles in aqueous coatings range from 80 to 1000 nm (0.000 08 to 0.001 mm). The particle size of microspheres added to coatings ranges from 5 to 80 μm (0.005 to 0.08 mm) [53]. It has also been reported that the size of microspheres added to coatings can range from "a few to several hundred microns" and that microbeads for reflective purposes can have diameters of up to several millimeters. The size of microfibers added to coatings ranges from 0.5 to 50 mm. PA or polyacrylonitrile fibers are 4 to 50 mm long and have a diameter of 10 μm (0.01 mm). MP coating particles are denser than MPs of the same size. Theoretically, paint particles of the same size and shape as MPs are easier to deposit and less mobile in aquatic systems [54].

Reflective glass spheres collected from San Francisco Bay, US, are part of road marking coatings ranging from 0.25 to 1 mm. In addition to the polymer binder, most coatings usually include fillers (glass beads) that provide abrasion resistance and increase tire grip as well as light reflectivity. Road marking paint granules are "irregularly shaped" chips and road marking paint granules are "colored, rounded and with a rough surface." Road marking paint particles and road dust are also described as fibrous [55]. The density of the MPs associated with road marking paint is approximately greater than 1.2 g cm^{-3}.

Air blasting and industrial abrasive technology are special procedures in which compressed air generates pneumatic velocity for the abrasive material to be pushed to the surface through nozzles. Industrial abrasive technology and air blasting are commonly utilized to wipe out rust, color, and other contaminants from steel surfaces, such as ship hulls, machines, engines, and walls before new coatings are added through the media blasting process. MPs as abrasive media (including acrylic and polyester) are the best media for mold washing. Popular sectors that use air blasting technology include automobile, aircraft, boating, telecommunication, and manufacturing industries. Waldschläger et al. [56] reported that the MP particle size used as abrasive media is around 0.2–2 mm, which can be considered a primary source of MP pollution. This issue is a major concern in harbors and ports because huge tankers are stripped of paint, and the untreated wastewater is released directly into the sea. According to the data, the plastic particles used for sandblasting are in the range of 0.15 to 2.5 mm. In contrast, at the lower limit of the statistical values, the range of plastic media used for sandblasting materials for stripping coatings is 0.012 to 2.03 mm. Microbeads have been used for sandblasting materials. The relative density of sandblasted particles is generally greater than 1000 kg m^{-3}, indicating that they do not float and drift [57]. Similarly, European Chemicals Agency (ECHA) states that the particle size of sandblasted materials "typically ranges from 0.15 to 2.5 mm with

a relative density greater than 1000 kg m^{-3}, indicating that the particles will not float on water."

1.3.1.2 Consumer

Primary fiber MPs are synthetic fibers less than 5 mm in length that are released or shed from the fiber material during the production and processing process. There are two forms of shedding, from the surface of the fabric and the cut edges of the fabric [36]. The two types of shedding coexist during the production of the fabric, and the surface shedding is predominant during daily use due to the hemming design of the fabric. In the first stage of washing, most of the shedding is in the form of floating fibers in the fabric. The amount of fiber MPs release depends to a large extent on the fibers, the yarn, and the processing of the fabric. Fiber MPs that do not leave the fabric in time for the production phase cannot be ignored.

Fiber MPs are produced and spread to the environment at all stages of the textile life cycle. The carding, drafting, and finishing of fibers in the yarn formation and weaving process cause damage to the fibers/yarns and form fiber MPs. Textile mills have special ventilation and dust removal systems that allow fibers and dust to enter the air through ducts. The garment care process also generates a certain amount of fiber MPs, and drying fabrics using a drying cycle increases the release of fiber MPs by a factor of 3.5. Washing one garment in a washing machine makes 100 to 1000 fiber MPs being shed and an increase in fiber MP release during washing. The Norwegian Environment Agency reports that household laundry discharges 600 t of effluent per year, and fibers shed in textile washing are bound to be of concern as an important source of fiber MPs in the water environment [58].

The type of fiber affects the formation of fiber MPs, and it has been found that washing a 660 g polyester fabric can shed between 220 and 260 mg of fiber, while cotton fabrics shed even more fiber during washing. Francesca et al. found that the amount of natural fibers in air and water was 97% and 80%, respectively, mainly because polyester is highly crystalline and does not swell and break significantly in water [59].

The shorter the fiber length, the higher the likelihood of fiber migration to the yarn surface and the greater the release of fiber MPs during the washing process. Polyester filament woven fabrics are made from continuous filaments. As the twist increases, the resistance to fiber migration and elasticity within the yarn increases, resulting in a more compact yarn structure, whereas cotton yarns are short fiber yarns with large length irregularities and a higher number of fiber slips, which leads to more hairiness on the surface of the yarn, which can be stretched to varying degrees during the washing process, resulting in fiber shedding [60]. At the molecular level, the macromolecules in the amorphous zone are stretched, the bond lengths and angles become larger, other molecules are broken or even pulled out, and eventually, the macromolecules are unevenly stretched and slip off until they break.

Fabric structure is also an important factor in the shedding of fibrous MPs. Woven fabrics are more compact than knitted fabrics and produce less fiber MPs. Plain fabrics are less susceptible to abstraction at higher warp and weft densities because of the relatively high number of interweaving points, the strong attachment of fibers

to the fabric, and the narrow inter-fiber spaces; satin fabrics also release the least amount of fibers into the atmosphere at higher warp and weft densities, but are more likely to produce fiber MPs than plain fabrics; twill fabrics shed the least fibers at moderate warp and weft densities [61]. Because the fabric structure affects the flatness and feel of the fabric and the amount of friction that exists during washing is influenced by the flatness of the surface, fabrics with low abrasion resistance, high hairiness, and low yarn breakage strength have a higher tendency to pile up and release fiber MPs during mechanical washing, with the broken fibers forming a short layer of fuzz on the surface of the fabric, which is subjected to various mechanical forces during washing and becomes less able to adhere to the fabric and eventually falls off. Eventually, they fall off. The production of fiber MPs in knitted fabrics is also very closely related to the tissue, and the basic rules are the same as for woven fabrics.

The yarns are bent and stretched by external forces in the course of use, resulting in damage and the formation of hair feathers on the yarn surface that break off and produce fiber MPs. During daily wear and use, loose fibers protrude from the surface of the textile and are then subjected to mechanical forces such as friction between the fabric and the laundry, between the laundry and the cylinder wall, between the laundry and the water, and the force of the water flow [62]. In a domestic drum washing machine, when the laundry is placed in the drum, the inertia causes the laundry to move slowly, increasing the contact area between the laundry and the water, and the laundry is deformed by the difference in speed between the laundry and the water flow, resulting in bending and elongation of the fibers and eventual damage and breakage [62]. The friction between the clothes causes relative movement between the clothes and the stains, which promotes the removal of dirt from the surface of the clothes, while the microplastic fibers fall off under mechanical action.

Friction between garments causes the most wear and tear, and damage caused by friction can be divided into two types: superficial damage and decolorization damage. Superficial damage is caused by the frictional force of washing, resulting in the surface of the clothing in the yarn of the fibers disperse into extremely fine hair-like feathers, which fall off. If not removed these fibers will form small balls, and under the action of mechanics, this process will extract a certain amount of hair feathers, and friction is very easy to make it break, thus accelerating the formation of fiber microplastic, mainly in the softer fine fabrics. The damage occurs on garments that have been washed over a long period of time, where the surface is white or even worn, and where the fibers are easily dislodged [63]. The ability of the fibers to shed MPs is therefore largely dependent on the formation of lint and the ease with which these fibers can be broken off by external forces in the washing machine before forming a hairball.

As primary MPs have a high surface-to-volume ratio (which increases with the decreasing linear dimension); their role in ecological impact is crucial, especially as vectors for pollutants and viruses or substrates for biofilm. One can classify them further as those originating from industrial dust, washed-out from synthetic textiles, transferred to waters as a spillage of nurdles, or being an ingredient added to cause surface abrasion (in cosmetics or detergents). Particles originating from those sources are persistent and ubiquitous, freely passing the wastewater treatment

plants (WWTP) [64]. One can estimate the number of microbeads added to domestic sewage in a single use is >200 000. Primary MPs dominate environmental samples filtered from waters, soils, or airborne. The MPs from cosmetics, comprising >90% PE and also PP, PET, polymethyl methacrylate (PMMA), and nylon, were already studied locally in many research studies [42]. According to the European Cosmetic Ingredient Database, currently added abrasive agents in cosmetics include, among others, the following: PE, PLA, hydrogenated poly (c6–20 olefin), ethylene/propylene copolymer, ammonium acryloyldimethyltaurate/laureth-7 methacrylate copolymer, and 1,4-butanediol/succinic acid/adipic acid copolymer. Research conducted in the UK estimated the number of microbeads released in a single use to be between 4594 and 94 500 particles. This considerable amount of particles varies in size, shape, roughness, and sorptive properties comparable with the transport potential. Primary MPs are potential vectors for hydrophobic pollutants with a considerable affinity to dichlorodiphenyltrichloroethane (DDT) [65]. The transfer of hydrophobic substances (PAHs, PCBs, and PBDEs) from plastic to biota was already proved. Fortunately, the increasing awareness of the problem caused the systematic reduction in primary MPs on the market. The EU has reduced primary MPs in cosmetics from 4360 tonnes in 2012 to 793 tonnes in 2015. From 2020, MPs as exfoliating agents in cosmetics are entirely forbidden. The bans in the US and UK prohibit the use of MPs microbeads in rinse-off cosmetics. However, there is still a need to extend these strategies and policies [66].

Singers, celebrities, models, performing artists, and not to mention many ordinary people use makeup materials, clothing, and objects extensively containing glitters to achieve a more attractive look [67]. These products are promoted, advertised, and sold with the help of beauty, makeup, and shopping websites, as well as influencers using their social media accounts and bloggers. To boot, many childrens movies entail animations with characters composed almost completely of glitter. That is why this shiny material's popularity increases each day, leading to increased use of an expanding range of products.

Shows, fashion events, celebrations, marches, and festivals take days and even weeks (Mardi Gras – United States, Coachella Valley Music and Arts Festival – United States, Rio Carnival – Brazil, Carnival of Venice – Italy, Halloween, etc.) see excessive use of glitters. For example, in 2011, nearly 70 kg of glitter was used in the Toronto Santa Claus Parade alone. Between 1989 and 2009, more than 4.5 million kg (10 million lbs) of glitter were purchased in the United States [68].

People do not content themselves with the use of glitters on themselves alone but apply them to animals as well. For instance, there are a number of firms applying various patterns and figures using glitters on the bodies of horses, including their eyes, trunk, legs, hooves, mane, and tail. At times, glitter madness reaches extreme levels, and some people cover their whole body with glitter, from head to toe (even their tongues). It is obvious that a person who covers their hair and whole body with glitter would be shedding millions of MP particles all around, as well as into the sewer system during a shower. Therefore, "MP litter" could be an apt description for glitter.

Glitters are used not only in makeup and cosmetics products but also in kindergarten, preschool settings, and primary schools for various art class purposes.

Thinking that these activities are guided by otherwise educated and informed teachers is a true source of pessimism. Glitters are used as a coating material for new puzzles, ornaments, metal objects, masks, ethylene–vinyl acetate (EVA) stickers, various toys, doll hair, crayons, and much more [69]. Moreover, play-dough, a material hitherto reported to be swallowed by children, and materials marketed as kinetic sand can also contain excessive amounts of glitter. It is widely known that children younger than the age of 3 are inclined to put into their mouths and swallow whatever they can put their hands on, including various objects, paints, and articles. Indeed, today, kindergartens are at the stage of excessive use of glitters along with similar ornamental materials, craft, and do it yourself (DIY) materials such as flakes and beads, which had hitherto been popular items in these activities [69]. Today, these materials are almost universally made of plastic. Products such as Slime, which are favorites among children and known to contain borax – widely considered a health hazard – are also characterized by the involvement of plastic glitters, not to mention other types and forms of plastic polymers (PET, PE, PP, PS foam [Styrofoam]). Yet the dangers of MPs in these products are almost completely ignored.

Glitter is not a basic need. In a psychological hierarchy of needs, the need to use glitters can arise in the sixth stage (esthetic needs) and above of the extended hierarchy of Maslow. Based on Maslow's beliefs, it is stated in the hierarchy that humans need beautiful imagery or something new and esthetically pleasing to continue up toward self-actualization. Humans need to refresh themselves in the presence and beauty of nature while carefully absorbing and observing their surroundings to extract the beauty that the world has to offer. Glitters are pleasing to human beings as they allow one to stand out among the crowds of ordinary people and thus see extensive use [70]. Maybe its sparkle reminds us of water resources or sunlight. Shiny objects have hitherto been associated with spiritual powers. Glitter symbolizes vividness, joy, and hope. Shiny materials can attract people and even animals. There is a rough consensus that human beings love to stand out with a shiny look and play with shiny things, likely because glitters are associated with wealth and status or a glittering of nature.

In recent years, the increasing use of glitters can be observed in many products, including textiles, shoes, bags, ornaments, and more. Manufacturers apply glitter-coated patterns even on children's clothing made of 100% cotton, 100% organic materials, and not to mention other textile products. To make the matters worse, such glittery and shiny products attract substantial consumer interest. As these clothes are washed a few times, the glitters are shed into the water and eventually find their way into sewer systems. In addition, the microfibers shed by synthetic textile products, which are produced by thousands of tons each year, are also an undeniable source of MPs.

On top of all these, nowadays, most haberdashery products such as sequins, beads, and buttons are made of plastics such as PET, recycled PET, PVC, nylon, polyester, and melamine. The fact that some of these are made of recycled PET, is a small consolation from an environment perspective. Sequins are used widely on various evening dresses for special occasions such as proms, weddings, and other ceremonies, as well as on other goods. They even find their way into daily clothing items

produced for children in the form of patches ornamented with sequins or sequined fabrics (e.g. multicolored reversible sequins) [71]. It should be evident by now that plastic glitters and similar small particle materials such as sequins and beads, used in excessive quantities in the textile industry, are almost always produced from plastic polymers, and the use thereof pose major sources of plastic litters, which can affect land-based and aquatic ecosystems (biotopes and biocenosis) for centuries to come.

The term glitter refers to an assortment of small, flat, and reflective particles. Glitter is made of a plastic polymer known as Mylar™, which refers to a specific type of polyester film known as Biaxially oriented polyethylene terephthalate(BoPET). BoPET is a polyester made from stretched PET and is used for various purposes. The glitter (PET) particles have a true density of 1.38 $g\,cm^{-3}$ and a melting point of 260 °C. They are also insoluble in water. The particles are coated with metal (aluminum-coated PET glitter) in order to obtain high reflectivity.

Plastic glitters can be found in all colors, including gold and silver. They can even exhibit holographic qualities. The glitters can be produced in different shapes (in precision-cut pieces of uniform size, sometimes with notches): the most common shapes are hexagonal, including square, triangle, stripe, heart, star, crescent moons, diamond/rhombus, flower, snowflake, butterfly, irregular, and so on. Indeed, on e-commerce sites, suppliers often talk about providing 10 000 combinations of glitter colors, shapes, sizes, and materials. In the case of polyester glitters, 200 μm (0.008″) standard glitter flake size is the most popular and versatile one. As glitters are produced on a commercial scale using PET films, with marketed sizes below < 5 mm, they can indeed be categorized as MPs.

Used widely in cosmetics products and household applications, glitters are known to be messy and easy to spill away. Thus, they are often sold in boxes with holes punched at the top. As soon as they are applied, the glitters shine, not only on the body, clothing, or objects they were applied on but also all over the place and often "on the ground" as well. Indeed, upon mere contact, they may be transferred from one carrier to another. It is found that glitters can effectively serve as forensic evidence, which can freely circulate in the environment and which is capable of contamination through contact with someone or something.

Regular glitters are manufactured from PET polymer. There are also varieties made of acrylic, PMMA, PVC plastic epoxy resin mixture, or melamine and phenolic resin mixture. However, renewable plant-based raw materials such as soluble seaweed, regenerated cellulose (sourced mainly from Eucalyptus trees), and glycerin (plant-derived) are also produced as alternatives to glitters [72]. Biodegradable glitters made of plant-derived materials and painted with mineral pigments are rather limited in terms of color and shape options, compared to what is on offer in the case of plastic ones, and are approximately 35% softer compared to the latter group. The plastic glitters, in turn, can be subjected to toxic finishes.

It is true that different types of natural phlogopite and synthetic fluorphlogopite mica glitters for cosmetic uses (shimmers) and edible glitters (mixtures of sugar, gum arabic, and cornstarch for food and cake decorations) also exist.

A large number of studies show that the source of primary MPs are microbeads from personal care products, followed by the spillage of preproduction pellets from

industrial operations. The first element that one thinks of in the context of MPs in cosmetic products is microbeads. Their use in cosmetic products is currently prohibited. Yet, there is another major source of MPs, comparable to microbeads in the sense that they are also composed of primary MPs, albeit receiving only a muted interest. These are glitters, which are used often in all kinds of cosmetic and textile products, not to mention craft activities [73]. Commanding a very low price, glitters start to get into the environment directly or indirectly (discharge into sewage systems following washing/cleaning activities) from the time of their first use. Had each and every glitter particle that found its way into the environment were self-luminous or phosphorescent, enabling the ability to trace them (such as radiotracers or thermal cameras), their prevalence in the environment would have been obvious.

A glance at the life cycle of glitters could start with their manufacturing from petroleum-derived polyesters, followed by their shipping to suppliers, to find their way eventually to consumers in a wide range of products (such as textiles, craft and DIY materials, EVA stickers, jewelry, shoes, and bags). Once they start to be used by the consumers, they are often prone to shedding away from the objects they are attached to. If not, they would still be transferred to landfills, where they can continue to contaminate the air, water, and clean soil, where they would remain intact for years. If they had been initially used in makeup materials applied to the face and body, they would, sooner rather than later, be washed with water and reach wastewater treatment plants through sewer systems. If the treatment plant applies secondary treatment processes, a portion of the glitters could be kept in the sludge. Yet, the remaining would still be released into natural sources of water, and affecting living organisms.

Even though there are some studies aimed at understanding the level of microbeads contamination in water sources and to assess the amount of microbeads ingested by organisms, comparable studies on glitters are just starting to take off and are few in number. The figures presented in three new and distinct studies on the analysis of MPs from different cities of Iran suggest the presence of hexagonal film-like MPs in the samples and presume these to be probably from a primary source.

Paints and coatings generally contain polymers. The binder in waterborne emulsion paints (latex paints) may consist of (nanosized) MPs. Different polymeric binders are used. Waterborne emulsion paints (latex) may contain dispersed micro-sized polymers as a binder for pigments. In solvent-borne paints (e.g. lacquer), the binder polymers are dissolved and, after hardening, form polymer films. Waterborne emulsion paints have replaced many solvent-based paints [41]. In the Netherlands in 2008, five times as much waterborne as that of non-waterborne acryl or vinyl polymer paints were produced; in 2013, this ratio increased to six times as much [41]. MP contents in paint have been reported to be 14–30% [37]. Wall paints are reported to have binder content up to 30% [42]. The various scenarios are calculated with plastic content of 14, 20, and 30%. Exact numbers on the market penetration of MP-containing paints are unknown. Based on the scattered product information available, the minimal scenario uses a market penetration of 9%, the average at 13%, and the maximum at 17%.

1.3.2 Secondary Microplastics

Over the past decades, plastics have been widely applied in packaging, construction, electronics, aerospace, and agriculture due to their high performance, low cost, and easy processing [74–76]. In 2020 alone, nearly 367 million tons of plastics were produced globally; however, the recycling of plastics is heavily dependent on national policies and consumer awareness, and the degradation time of petroleum-based alkane chains is counted in years, resulting in most of these plastics being difficult to recycle and degrade until they become environmentally unaffordable and, thus, biohazardous [77]. Therefore, in such a current situation, the inevitable logical consequence of plastic production and release is the generation of secondary MPs [78]. While the U.S. first passed the Microbead-Free Waters Act of 2015 to cut and hinder the release of most primary MPs, secondary MPs have been still measured in all types of water environments, such as natural waters, wastewater, and even drinking water, over the past few years [79].

The degradation mechanism of plastic products is the basis for the study of the formation and generation behavior of secondary MPs, which have been extensively studied in the field of polymers. Conventional petroleum-based plastics feature complex chain structures and condensed state structures, the former including sequence distribution of structural units, stereoisomerism, bonding mode, chemical composition, branching/crosslinking structure, molecular weight, and molecular weight distribution. The latter includes phase structure, orientation structure, liquid crystal structure, crystalline state, and amorphous state. Among these, the cross-linking structure, high molecular weight, crystalline state, and other physicochemical properties such as hydrophobicity, chemical, and biological inertness are important factors that seriously hinder the degradation of traditional petroleum-based plastics, making them pollutants that accumulate in large quantities in the environment when they are discarded [80, 81]. For polyolefins, for example, the estimated half-life of plastics on land ranges from two years (e.g. Low-density polyethylene) to 780 years (e.g. PP), even with the contribution of aging factors and microbial action [82].

The studies point out that the accumulation of MPs in the ocean over long periods of time is attributed to their resistance to chemical, photochemical, and mechanical degradation, as well as biodegradation [83, 84]. Conversely, some researchers have shown that plastics degrade precisely through photodegradation, thermal degradation, hydrolysis, and biodegradation to form MPs [19]. These are two general views in the environmental field, depending on a basic understanding of the process of MP formation. In fact, from the perspective of polymeric materials, environmental factors may include photo-oxidation due to UV light, thermal degradation owing to temperature, and hydrolysis in high humidity or water environments (Figure 1.1) [85]. Although the mechanisms of these processes vary, they generally have a negative impact on the properties of plastic products, such as the generation of oxygen-containing groups, improvement of hydrophilic properties, molecular chain breakage, and decrease in molecular weight [86]. The most obvious macroscopic manifestation is the significant decrease in mechanical properties accompanied by color changes and cracks [87]. It is, therefore, reasonable to assume that they can

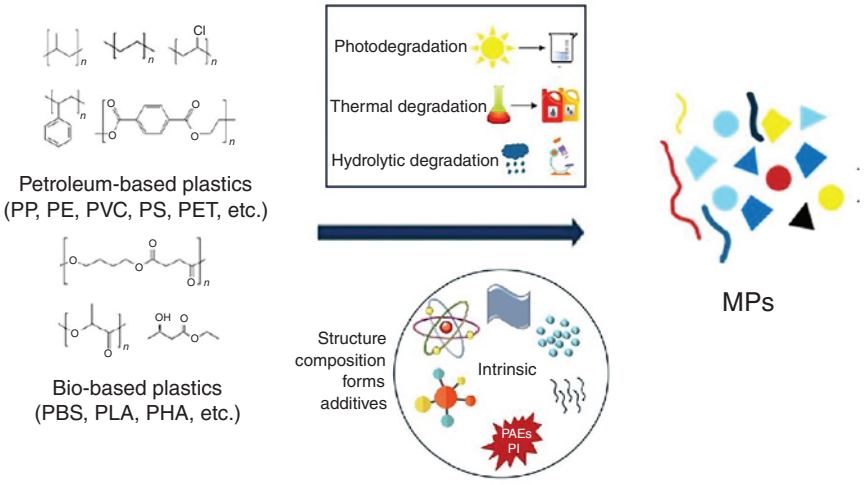

Figure 1.1 Degradation of plastics to microplastics is influenced by environmental factors and intrinsic elements. Source: Reproduced from Liu et al. [85]/with permission of Elsevier.

all be classified as environmental "aging factors" and that the logical consequence of aging processing is a certain degree of change in the properties and performance of polymeric materials, often toward the detrimental side of the use properties.

In addition, while plastic products are subjected to the aging process, various natural mechanical forces in the environment are constantly impacting plastic products. Some have detailed that such forces can be the impact of ocean waves, river scouring, and wind blowing [86–89]. The technical term weathering is often mentioned in many articles that attempt to study the mechanisms of MP generation [90]. In line with the increase in the amount of plastic waste, weathering of plastics in the environment has reportedly led to the generation of large amounts of MPs, which are now distributed globally, including in the atmosphere, polar regions, freshwater, marine, and terrestrial ecosystems (Figure 1.2) [81, 90, 91]. In fact, the process of degradation and fragmentation of plastics by weathering is accompanied by two objective phenomena: physical and chemical changes in plastic products and constant impact of wind on plastic products. The change in the physicochemical properties of the plastic products can be attributed to the aging factors mentioned above, while the latter explains the importance of "mechanical wear" in nature for the generation of MPs; however, the two are usually lumped together in a large number of studies, thus neglecting the importance of either of them. Combining the two key points of aging factors and mechanical wear, it is not difficult to accept the possible and approximate actual process of secondary MP generation: first, due to the chemical and biological inertia of plastics, it is difficult for plastic products to degrade completely in nature, resulting in accumulation in soil, seas, and rivers; furthermore, plastic products that are discarded in various environments still receive the adverse effects of aging factors all the time, while suffering from the impact of mechanical wear, until the performance caused by aging decreases to the extent that it is

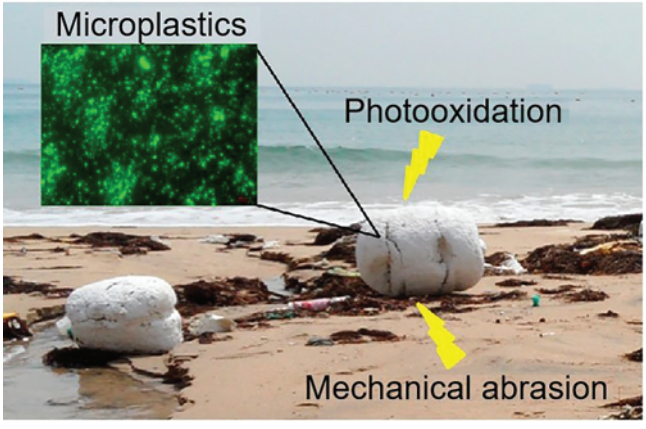

Figure 1.2 Typical weathering process along the coast, involving mechanical wear from sand and waves and photo-oxidative degradation from UV light. Source: Reproduced from Song et al. [91]/with permission of American Chemical Society.

not enough to resist the impact of mechanical wear, and finally, plastic products are broken to form secondary MPs.

It is now becoming more and more accepted to study the formation mechanism and generation behavior of secondary MPs by accelerated aging experiments in the laboratory through aging chambers [10, 11, 79, 81, 92–94]. However, such studies often also face the challenge that the laboratory environment is significantly different from the real natural environment and does not truly reflect the generation of MPs in nature. For example, aging chambers can simulate natural light, water mist, and temperature, but they cannot control and regulate the growth of microorganisms. It has been reported that once plastics enter the environment, they may be susceptible to fragmentation and degradation via abiotic and biotic processes (Figure 1.3) [95]. Abiotic degradation caused by environmental aging leads to loss of structural and mechanical properties, and creates surface irregularities, providing favorable conditions for microorganisms to colonize and alter the physicochemical properties of the polymer surface [96]. Biotic processes include the secretion of extracellular enzymes that produce oligomers and monomers that can be mineralized by several microorganisms [97]. Biological action plays a crucial role in the generation of secondary MPs in the natural environment, especially in the soil, but this is often overlooked by studies of MP generation behavior conducted through laboratory aging.

Up to now, researchers have already monitored the plastic degradation and MPs generation in different environments [98, 99]. However, most of these studies have focused on the changes in size, quantity, and distribution of the MPs over time. We still know very little about the essential mechanism of the process by which plastics transform into secondary MPs.

Yet the reality is becoming more and more complex, with recent and increasing research findings indicating that the degradation of plastic debris is not expected to stop at the MP level [100]. This means that the study of MPs is gradually moving into

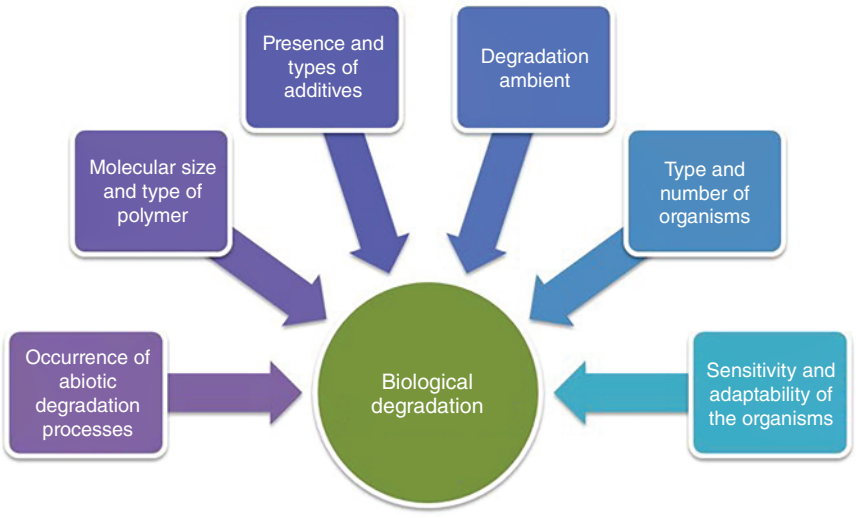

Figure 1.3 Main factors responsible for the biodegradation of polymers. Source: da Costa et al. [95]. Reproduced with permission of Elsevier.

the nanoscale. It has been proposed that MPs subsequently degrade into nanometer range plastics, so-called nanoscale MPs or NPs. The definition of nanoscale MPs has not been formally established, but there is a growing tendency to report nanoscale MPs as undesirable products of plastic degradation, ranging in size from 1 nm to 1 μm, with colloidal behavior [8, 101]. Similarly, nanoscale MPs can be divided into two categories based on their origin: primary nanoscale MPs are manufactured NPs, and secondary nanoscale MPs are the result of the fragmentation and degradation of macro- and microplastics into nanoparticles. Due to their smaller size and specific colloidal properties, nanoscale MPs may pose a greater hazard than MPs because of their ability to cross biological barriers. Some studies have demonstrated that MPs and nanoscale MPs ingested by marine organisms can reach their circulatory system [102, 103]. Even nanoscale MPs can penetrate cell walls, leading to cellular stress and oxidative damage [104]. In addition, there is growing evidence that nanoscale MPs can be transferred across biological barriers and accumulate in organs and tissues, thereby affecting human health [105]. Currently, researchers are increasingly interested in nanoscale MPs, but are mainly focused on bioaccumulation and ecotoxicology studies.

Polymers are allowed to be processed into various products, such as plastics, rubber, fibers, and foams, depending on the actual application scenario and different application needs, and are widely used in our daily lives. Strictly speaking, plastics are only one of the most common products made from processed polymer materials. However, in a large number of studies, MPs prefer to include all polymer fragments smaller than 5 mm in size, not only for plastics. Taking common personal medical protective equipment as an example, disposable masks, N95 masks, gloves, and face masks are mainly made of polymers such as PP, PS, polyacrylonitrile, polyester, and PU [106, 107]. Most surgical masks have three layers: an inner layer of soft fibers,

a middle layer of melt-gusted filters, and an outer layer of nonwoven fibers that are usually colored and waterproof [108]. These personal medical protective devices are heavily used but easily discarded. If they are not properly disposed of and recycled after use, they will be left in the environment to produce large amounts of MPs. These large amounts of polyester microfibers that flow into the environment are also referred to as MPs in the study. Therefore, this section will discuss in detail the formation mechanism and generation behavior of secondary MPs from the perspective of different polymeric product forms, combining aging factors, mechanical wear, and biological action. Polymer product forms include four types: plastic, rubber, fiber, and foam. The formation mechanism and generation behavior of secondary MPs will be discussed in the context of MP generation kinetics studies and recent advances related to nanoscale MPs. In addition, since biodegradable plastics (recognized by enzymes present in nature independent of whether their source is renewable or fossil) are considered to be the best candidates to replace conventional plastics, related topics are also discussed in the field of plastics-derived MPs research [109].

1.3.2.1 Plastics-Derived Microplastics

Plastics are generally defined as materials that can be molded into a specific shape under certain conditions (temperature, pressure, etc.) and retain their shape at room temperature, using synthetic or natural polymer compounds as the basic components. Plastic is an important class of polymer materials, with characteristics of light weight, electrical insulation, chemical resistance, and easy processing [25]. However, the significant disadvantages of plastics are low mechanical properties, flammability, and poor heat resistance. Understanding the properties of common plastics from the perspective of their microscopic molecular structure is of significant importance to explore the mechanisms and behaviors of MPs generation through degradation process. In addition, various additives in plastics processing have a significant contribution to the MP generation behavior, including time, morphology, and size, which may be either facilitative or mitigating effects. However, sometimes additives do not receive enough attention or are often considered together within polymers for MP generation research.

1.3.2.1.1 Influence Factors of Microplastics Generation Understanding the formation of secondary MPs is essential to control their emissions. Aging factors, mechanical wear, and biological action are the three key influences on the formation of MPs. Due to the excellent processability of plastics, the diversity of shapes of plastic products is also a very important influencing factor for plastic-derived MPs.

1.3.2.1.1.1 Aging Factors Photodegradation of plastics caused by UV radiation and oxygen is the potential basis for plastic aging (Figure 1.4a) [110]. Visible light and UV radiation absorbed by the plastic activate its electrons to enhance reactivity, promote its oxidation and cleavage, and cause chain breakage and cross-linking reactions [100]. For example, the phenyl rings of PS get excited by UV radiation and form triplet state, leading to dissociation of the phenyl group or its transfer to the nearest C—H or C—C bonds [111]. PE, PS, and PP have strong absorption in the 300, 318,

and 370 nm bands, respectively [91]. UV irradiation has enough energy to break the C—C (375 kJ mol^{-1}) and C—H (420 kJ mol^{-1}) bonds and form radicals that subsequently interact with oxygen [110, 112]. Thus, in nature, the specific wavelengths of energy of visible and UV light induce the beginning of the photo-oxidative degradation process of waste plastics, with the formation of free radicals in the process and the further role of oxygen in changing the structure and properties of plastics. Oxidation of C—H bonds can lead to the formation of new functional groups, such as hydroxyl (—OH) and carbonyl (C=O). PE and PP itself do not have chromophores; however, impurities or structural defects present in plastic products during processing or aging can be used as chromophores [113]. Cui and colleagues investigated the differences in MP generation behavior of PP plastics with different crystalline forms under UV irradiation [87]. It is shown that during the photo-oxidative degradation initiated by natural light (UV plays a major role) and oxygen, the hydroxyl and carbonyl peaks of PP appear at 3417 and 1677 cm^{-1}, respectively, in Fourier transform infrared spectroscopy (FTIR). Thus, the degree of photo-oxidation of plastics can usually be described by carbonyl index (CI) and hydroxyl index (HI), which are expressed according to the Eqs. (1.1) and (1.2), respectively.

$$CI = A_{1645-1725}/A_{2700-2750} \tag{1.1}$$

$$HI = A_{3385-3465}/A_{2700-2750} \tag{1.2}$$

where $A_{1645-1725}$ is the area of the carbonyl absorption band (1645–1725 cm^{-1}), $A_{3385-3465}$ is the area of the hydroxyl absorption band (3385–3465 cm^{-1}), and $A_{2700-2750}$ is the area of the reference band in the range of 2700–2750 cm^{-1}, which is associated with CH bending and CH_3 stretching. The rise of oxygen-containing groups is further accompanied by changes in molecular weight and molecular structure. Gardette et al. showed that oxygen and UV light are more likely to act preferentially on the PP molecular chains in amorphous regions than in the crystalline regions [114]. The degradation of molecular weight in the amorphous regions leads to an increase in relative crystallinity and a macroscopic decrease in the mechanical properties, especially the tensile strength. The decrease in molecular weight and the breaking of molecular chains make the mechanical properties of the waste plastic develop in an unfavorable direction on a macroscopic scale, while the surface of plastics will successively have the appearance of many small microcracks, as well as changes in roughness, which can be visually observed through scanning electron microscopy (SEM) and laser scanning confocal microscopy (LSCM) (Figure 1.4b) [87, 115]. The presence of many irregularly arranged tiny dense microcracks makes the microcracks on the surface of plastic products expand when subjected to natural forces and then rapidly join in a short period of time until the plastic breaks and MPs are produced. The process of generating MPs is often accompanied by whitening phenomena, hydrophobic changes, etc., which are broadly attributed to the generation of oxygen groups, changes in crystallinity, refraction of light by microcracks, etc. Since UV irradiation has sufficient energy to break covalent bonds to form alkyl radicals, which in turn react with oxygen, the crystalline structure of plastics that can reduce UV transmission is expected to reduce the generation of MPs.

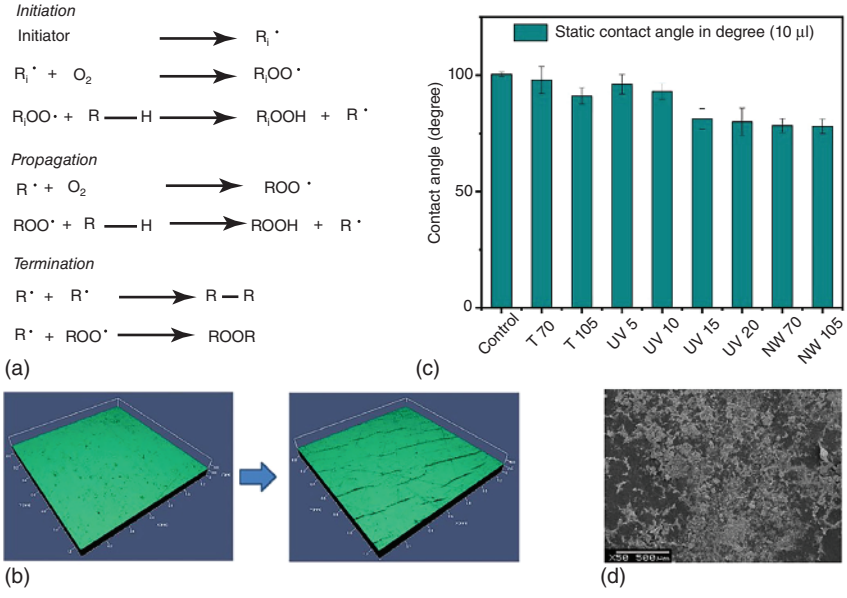

Figure 1.4 (a) Mechanism of photo-oxidative degradation involves auto-oxidation cycle comprising various steps. Source: Singh and Sharma [110]. Reproduced with permission of Elsevier. (b) LSCM 3D images for microcracks on the surface of PP before and after aging. Source: Reproduced from Cui et al. [87]/with permission of Elsevier. (c) water contact angle of packaging PE film in different abiotic conditions. Source: Jaiswal et al. [94]. Reproduced with permission of Elsevier. (d) SEM micrograph of packaging PE film with biofilm coverage on the surface. Source: Reproduced from Jaiswal et al. [94], with permission from Elsevier.

In addition, Kaelsson et al. and Pushkar et al. revealed that UV radiation can lead to chain breakage and new bond formation, thus promoting higher biofilm coverage (Figure 1.4c,d) [94, 116]. Meanwhile, PO_4^{3+} has been reported to inhibit —OH production in plastics, suggesting that inorganic compounds in specific environments (e.g. seawater) may influence the photodegradation aging process [117].

Similar to the UV-induced photo-oxidative degradation process, the main effect of high temperatures on the aging of plastics can be attributed to thermal oxidation reactions. The heat energy provided by the natural high temperatures forces the covalent bonds of the polymer to break, producing free radicals, and further reaction with oxygen leads to changes in the structure and properties of the plastic product [118, 119]. Thermal degradation is closely related to the thermal properties of the plastic (e.g. glass transition temperature and melting point). The activation energy determines the temperature at which the thermal degradation of the plastic is triggered. Natural light and ultraviolet (UV) light mainly have a significant effect on plastics with high light transmission (e.g. PMMA, PE, PP, and polycarbonate) and will act deeper inside the plastic in a very short period of time, rather than just staying on the surface. In contrast, the natural thermal aging process is generally inefficient due to low levels of thermal radiation, except in extremely high-temperature environments [120, 121]. However, the natural photo-oxidation

process is often accompanied by a thermal-oxidative aging process, both of which are important for the degradation of waste plastics and the generation of MPs. Andrady and his coworkers have revealed that temperature and UV radiation can have a synergistic effect on the degradation of plastics [122]. Odhiambo et al. more clearly stated that the rate of oxidation reaction increases with the increase in temperature [123]. In addition, it is worth noting that the thermal energy provided by high temperatures may not only have a thermal oxidation effect but also play a role as a thermal catalyst. During the thermal processing of PVC, a small amount of HCl is often released from the broken macromolecular chains before reaching melt flow, and HCl acts as a thermal catalyst to further accelerate the reaction of molecular chain breakage. Adding appropriate alkaline substances to neutralize the decomposed HCl can prevent further chain breakage of macromolecules, which is the principle of the role of heat stabilizers. Therefore, PVC is also the plastic type with the largest amount of heat stabilizers. On the one hand, heat stabilizers will alleviate the breakage of PVC molecular chains caused by HCl and the deterioration and brittleness of plastic products, reducing the generation of MPs. On the other hand, the use of additives will also create internal defects in plastic products, leading to stress concentration and promoting the generation of MPs.

Plastics are widely present in the aquatic environment, both from the surface to submarine sediments and from coastal areas to the open ocean. Even differences in humidity between regions and changes in humidity between day and night in nature can affect the generation of MPs due to the action of water molecules. The effect of water on plastics is mainly reflected in the attack of water molecules on specific groups in the polymer to undergo hydrolysis, such as ester bonds and amide bonds. In general, plastics with hydrolysis-prone groups in the polymer backbone are more likely to break under water attack to generate MPs, and often these polymers (e.g. nylon) also have other hydrophilic groups that are susceptible to water absorption and deliquescence to exacerbate this negative effect. PET is one of the three most detected MPs in the environment, along with polyolefins and PS. Arhant et al. showed that water molecules are more likely to attack the amorphous region of PET [10]. Hydrolysis in the amorphous phase leads to chain breakage, which reduces the molar mass (Figure 1.5a). In addition, an increase in crystallinity was observed during the hydrolysis process (Figure 1.5b). There exists a critical molar mass above which PET is observed to behave ductile and vice versa, exhibiting brittle behavior. By exploring the effect of hydrolysis on PA 6 and the formation of its MPs, Le Gac and colleagues found a strong chemical coupling between oxidation and hydrolysis [124]. The much faster chain breakage of PA 6 in water with oxygen compared to water without oxygen and the increase in air humidity leading to an increase in degradation rate provide theoretical guidance for studies related to the generation of PA 6 MPs. In addition, it is worth noting that there is often a crossover overlap between plastics highly affected by hydrolysis and those that are biodegradable. For example, poly(butylene adipate-*co*-terephthalate) (PBAT), the raw material of the now very popular biodegradable plastic bags, is largely influenced by the hydrolysis of the ester situated between the terephthalate and adipate groups during the formation of MPs [125]. Other biodegradable plastics, such as poly(glycerol

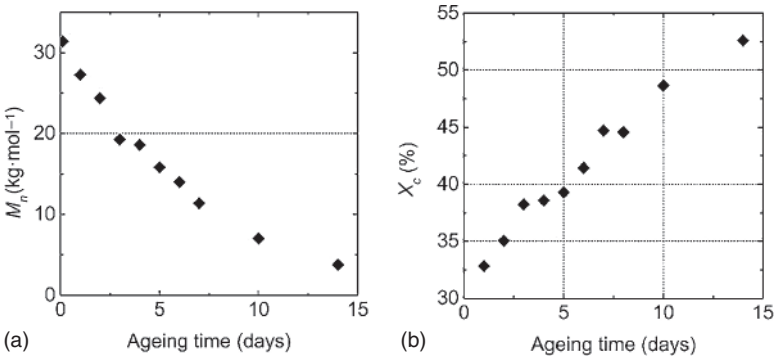

Figure 1.5 (a) Changes in molar mass of PET as a function of aging. Source: Arhant et al. [10]. Reproduced with permission of Elsevier. (b) Changes in crystallinity of PET as a function of water aging. Source: Arhant et al. [10]. Reproduced with permission of Elsevier.

maleate) films and poly(aspartic acid-*co*-L-lactide) bioadditives, have also been studied in detail for their degradation behavior in various aqueous environments (e.g. different salinity and pH conditions) [126, 127]. Notably, Guo et al. determined, through 2D-FTIR COS analysis, that the aging of plastics is higher in seawater compared to pure water, implying that ions in the marine environment contribute to the aging and hydrolysis of plastic products [128].

1.3.2.1.1.2 Mechanical Wear Here, we define mechanical wear as a process in which a plastic product is continuously subjected to mechanical forces in nature. It may be caused by waves, tides, wind, sand, rocks, permafrost, and even animal movements [87, 91, 129]. In many of the available reports, mechanical wear or mechanical force action is often classified as abiotic effects along with photodegradation, thermal-oxidative aging, hydrolysis, etc. In fact, aging factors and mechanical wear do play a continuous role in the formation of MPs. However, the detrimental effects of mechanical wear only become evident visually when the mechanical properties of the plastic degrade due to aging to a level that is insufficient to withstand the mechanical wear of the environment depending on the mechanical properties of plastic [25]. From the perspective of polymer degradation, understanding of MP formation requires consideration of the relationship between the degradation of polymer mechanical properties due to prolonged aging and the natural mechanical forces to which plastics are continuously subjected in the environment. These two are logically distinct, and mechanical wear is an important and essential step, so mechanical wear needs to be categorized separately and highlighted [10]. Many existing studies have focused on the role of external forces. Bläsing et al. pointed out that MPs may be worn away by mechanical forces during their migration along soil pores at the surface [130]. Ter Halle et al. also showed that plastic fragments exposed to the sea surface can break up due to mechanical wear from external shear and tension forces (Figure 1.6) [131]. Enfrin et al. revealed that the stress of water flow shear and mechanical mixing promotes the fragmentation of MPs in WWTPs [89]. They elaborated the mechanism of MP fragmentation in

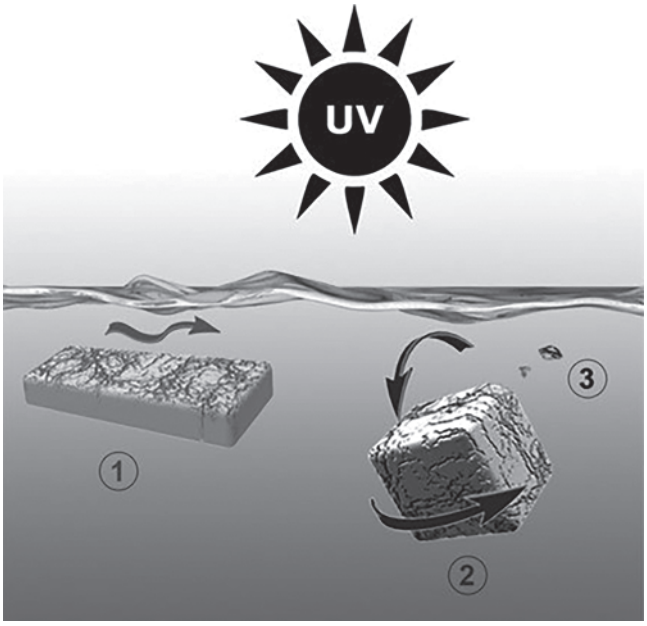

Figure 1.6 Plastic fragments exposed to the sea surface can break up due to mechanical wear from external shear and tension forces. Source: Reproduced from Ter Halle et al. [131]/with permission of American Chemical Society.

water by the model established from experimental data. The model was developed on the basis of the theory of solid failure through crack propagation and fracture, which is expressed according to the Eq. (1.3).

$$X_s = \left(\frac{K_c \sqrt{24}}{\rho c_0 \varepsilon} \right)^{\frac{2}{3}} \tag{1.3}$$

where X_s is the fragment size resulting from crack fracture, K_c is the stress intensity factor and relates to the fracture toughness of a material, and ε is the strain. The strain ε and the stress σ are related to the energy density E according to the Eq. (1.4).

$$E = \frac{1}{2} \sigma \varepsilon \tag{1.4}$$

It is pointed out that mechanical abrasion triggers MP production by causing plastic products to break up through internal defects in the material. The importance of defects and residual stresses generated during the plastic manufacturing process for plastic fragmentation was similarly emphasized in the study by Briain and colleagues [13]. It is worth noting that the "external force" of plastic fragments colliding with each other can also be categorized as a causal factor in the generation of MPs [88]. In addition, many scholars have investigated the relationship between mechanical wear and plastic types, product styles, and microstructure during the generation of MPs under external forces. Song et al. abraded polyethylene, PP, and PS with sand for 2 months after 12 months of UV exposure to simulate mechanical wear

on the beach [91]. The results show that the mechanical wear sensitivity of MPs is closely related to the type of plastic, with PS being more susceptible to sand abrasion compared to PE and PP. Cui et al. showed that the crystalline structure of PP can significantly affect the MP generation behavior [87]. β-crystalline PP can significantly reduce the generation of MPs under the mechanical force of human stepping compared to α-crystalline PP, which is an inspiration for material design with the aim of MP reduction. Xu et al. pointed out that special attention should be paid to plastics with smaller thicknesses due to the higher susceptibility to external forces, such as thin film plastics [11]. In particular, a growing body of literature recently suggests that the mechanical wear MPs undergo during fragmentation accelerates natural aging, both in the marine and soil environments [88, 130, 132].

1.3.2.1.1.3 Biological Action Aging of laboratory systems can simulate aging factors and mechanical wear but still cannot fully reproduce the complex natural aging process in the environment. The recently reported discharge plasma technology can not only simulate the multiple aging processes of MPs in the environment but also reduce the external energy input, effectively improving the above problems [133]. However, the biological action is still rarely mentioned in laboratory aging, although it also plays an important role in the generation of MPs in nature. Biological action is the biodegradation of plastics by organisms (including bacteria, fungi, and insects) that break them into MPs. The breakdown of the polymer backbone into short-chain molecules by aging factors and mechanical wear or extracellular enzymes can have the same effect [134]. The organism then takes up the chain-break products as a carbon source to achieve final degradation or mineralization [135]. The calculation of biofilm density is often involved in these studies and can be determined according to the Eqs. (1.5) and (1.6):

$$\frac{M_s}{D_d} = \frac{M_f}{D_f} + \frac{M_v}{D_v} \tag{1.5}$$

$$\frac{1}{D_w} = \frac{W_{ds}}{D_d} + \frac{W_{tw}}{\rho_w} \tag{1.6}$$

where D_d is the dry biofilm density; D_w is the wet biofilm density; M_s is the dry mass of a biofilm; D_f is the density of fixed mineral solids in a biofilm; M_f is the dry mass of any fixed mineral solids in a biofilm; D_v is the density of any volatile solids in a biofilm; M_v is the dry mass of volatile solids in a biofilm; W_{ds} is the biofilm dry solids content; W_{tw} is the biofilm water content; and ρ_w is the density of water. Wu et al. demonstrated that the generation of cracks and pores on the polymer surface can accelerate the biodegradation process and promote the generation of MPs (Figure 1.7a–c) [136]. Pushkar and coworkers indicated that partially oxidized PE films, when subjected to microbial sources, become precursors for microbial attachment and further increase the level of oxidation [94]. Napper noted that biofilm formation in seawater results in slow degradation [137]. Many studies have screened for strains that are biologically active on PE, PP, and PS plastics [135, 138]. However, the aim of current biodegradation research is mainly to improve the disposal of MPs to provide available technologies for reducing MP pollution, rather than to

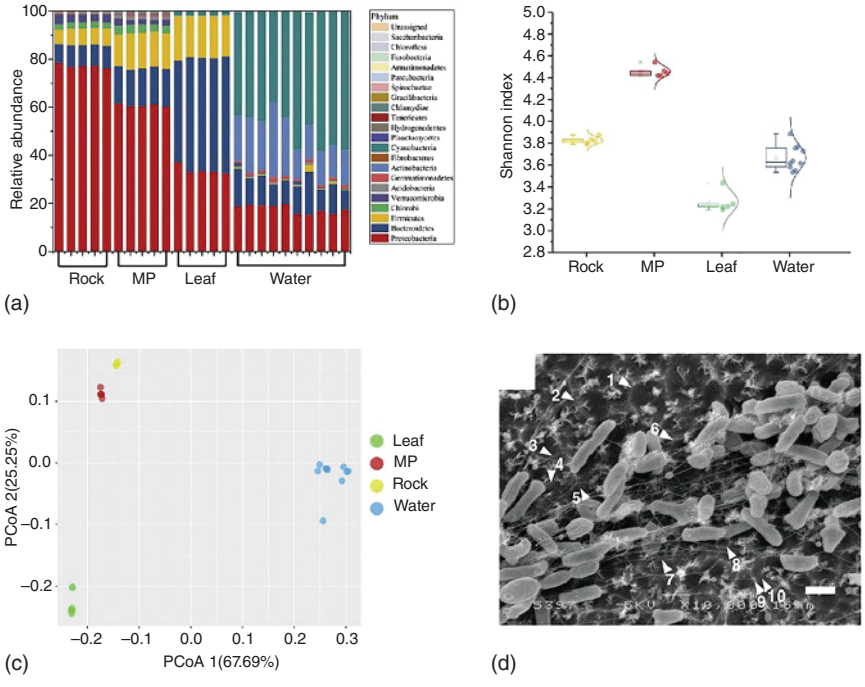

Figure 1.7 (a) Histograms of phyla abundances in three types of biofilm and river water. Source: Wu et al. [136]. Reproduced with permission of Elsevier. (b) Within-sample diversity measurements indicate a decreasing gradient in microbial diversity from the microplastic biofilm to leaf biofilm. Source: Wu et al. [136]. Reproduced with permission of Elsevier. (c) Principal coordinate analysis based on the weighted UniFrac distance matrix indicates a clear separation between the three types of biofilm communities and planktonic communities in river water. Source: Wu et al. [136]. Reproduced with permission of Elsevier, (d) SEM images of *Ideonella sakaiensis* cells grown on PET film for 60 hours. Source: Reproduced from Yoshida et al. [84]/with permission of American Association for the Advancement of Science – AAAS.

accelerate the aging of MPs [121]. For extracellular enzymes, hydrolyzable polymers are more susceptible to enzymatic degradation to form MPs (Figure 1.7d) [84]. Extracellular hydrolases, currently involved in cellulose and protein degradation, have been shown to be useful in the degradation of PET [134].

1.3.2.1.1.4 Shape of Plastics Product Plastics initially take the form of pellets, before being processed into plastic products with a specific shape. It is understandable that most secondary MPs are generated from these plastic products, including sheets, films, hollow bottles, and pipes. Differences in shape, in fact, influence the behavior of MP generation.

The plastic sheet and plastic film are so similar, with almost the only difference being thickness (sheet thickness of several millimeters and more, film on the contrary), that they are not emphasized and distinguished in studies related to MPs. In general, MPs associated with film products have received more attention due to their wide range of applications in daily life, such as packaging film, agricultural

films, and plastic bags. Chen et al. investigated the aging mechanisms of thin-film plastics (10 μm) compared to thick-film plastics (200 μm) in aqueous and terrestrial systems and the effects on controlling MP formation [11]. The results of the MPs collected after 23 weeks indicate that the mechanical action of the water flow in the aqueous system greatly influenced the formation of MPs to generate more debris, but complete fragmentation was only observed in thin-film plastics. In terms of chemical structure, thin-film plastics and thick-film plastics demonstrate significantly different responses, mainly reflected by changes in functional group and molecular chain breaks in the amorphous region, which may lead to deterioration of strength and promote thin-film plastics fracture. Moreover, a recent study comparing MPs released from PBAT/PLA and PE bags clearly indicated that film thickness plays a key role in the degradation pattern and rate [90]. The abovementioned study can be used as a reference for the difference in MP generation behavior between plastic sheet and plastic film.

It is worth noting that films are generally stretched during processing, resulting in an oriented structure or a special crystalline structure. Compared to simple PE, PP has a variety of configurations due to the different spatial arrangement of the methyl groups, including atactic, isotactic, and syndiotactic PPs. Depending on the crystalline phase, they can be divided into α-crystalline PP, β-crystalline PP, and γ-crystalline PP. Huber et al. studied isotropic PP films commonly used in packaging to better understand the process by which the films form MPs [139]. In accelerated UV aging, fragmentation into MPs can be observed in a fairly short period of time, accompanied by a significant amount of oxidative degradation. By combining Weather-Ometer results with an independent Arrhenius study, the time of MP formation and degradation to wax-like products in the natural environment was estimated, depending on UV intensity and temperature effects. Oxidized wax-like particles are more susceptible to further degradation by microorganisms than nonpolar polymers, which may help in the control of MP contamination. Julienne et al. proposed a new method for preparing micron-thick PE films with different thicknesses and controlled crystal morphologies using a dip-coating process [140]. PE films with different spherical crystal sizes were subjected to accelerated aging tests, and the results showed that the spherical crystal size had little effect on the photo-oxidation rate. However, films with large spherical crystal morphologies appeared to be more sensitive to surface erosion and crack extension, suggesting that such films are more vulnerable to mechanical forces when undergoing aging in the environment. Julienne et al. pointed out that studying the effect of crystal morphology on various semicrystalline polymers under different aging conditions can contribute to a better understanding of plastic fragmentation and MP generation in the environment. A similar study was conducted by Cui et al. to investigate the MPs generation behavior of PP films with different crystal structures under UV irradiation [87]. The typical spherical crystal structure imparts good light transmission to α-crystalline PP (α-PP), leading to more severe photo-oxidative degradation and decrease in mechanical properties in the amorphous region under UV irradiation, which is macroscopically manifested by an increase in relative crystallinity and a decrease in mechanical

properties. On the other hand, β-crystalline polypropylene (β-PP) is relatively less affected, as the curled bundle-like crystal structure is more reflective of UV light.

Numerous studies have reported that almost all water in plastic hollow bottles was contaminated with MPs. Dicke's team investigated 21 mineral water bottles from 32 different brands in Germany, where PET was the main MP type [141]. However, similar studies have only investigated the types and amounts of MPs in plastic bottles, and little is known about the causes of MP generation and the control of MP formation in hollow bottles. Ferrante et al. reported for the first time that the release of MPs was closely related to the pH of the water and the plastic density of the bottle [142]. And the amount and diameter of MPs were strongly influenced by the thickness of the plastic. The estimated daily intake (EDI) of MP concentrations in mineral water through drinking water was calculated using the equation:

$$EDI = (C \times IR)/BW \tag{1.7}$$

where IR, the ingestion rate, is assumed to be $2\,l\,day^{-1}$ for adults and $1\,l\,day^{-1}$ for children; C is the MP concentration ($\mu g\,l^{-1}$ and $p\,l^{-1}$), and BW is the body weight assumed to be 70 kg for adults and 16 kg for children. Further, Giese et al. focused on the unique screw cap system that accompanies the hollow bottle as having a large potential for MP release, thanks to the mechanical forces generated by the screw cap in use to abrade the plastic bottle [143]. A recent novel study on hollow plastic bottles containing carbonated beverages, reported by Chen et al. has similar ideas, with the difference that they attribute the release of MPs associated with plastic bottles to high pressure in order to store carbon dioxide, which significantly increases the presence of MPs [144]. In addition, carbon dioxide brings a combined effect of carbonic acid and air bubbles, which are also noted to promote the generation of MPs, with the adverse effect of carbonic acid on pH coinciding with the study reported by Ferrante et al.

In contrast, the release of MPs from plastic pipes has been somewhat less studied. However, plastic pipes are often used in municipal water systems, which means that MPs may be more easily released into drinking water. Plastic pipes are produced and processed generally using polyolefins or PVC as raw materials. Zhang et al. showed that the release potential of MPs from plastic pipes exposed to ozone was ranked as follows: LDPE > PP > HDPE > PVC [145]. With the large number of plastic rainwater facilities in use, MPs will also inevitably be released into the stormwater system during the aging and hydraulic flushing process. Zhang et al. found that plastic pipes of different materials subjected to UV aging and hydraulic scouring exhibited an increase in surface roughness and cracks [146]. In particular, the formation of oxygen-containing functional groups on the surface was an important factor affecting the release of MPs. The size of MPs released from different shapes of plastic pipes showed distinct trends with increasing aging. The release potential of MPs from typical rainwater facilities during aging process was ranked as follows: HDPE > PP > PVC. While the MP release potential of PP and PE differs in practical scenarios, PVC has the smallest of all. However, this does not mean that PVC poses the least amount of environmental pollution, as it is a plastic that contains high levels of toxic plasticizers and stabilizers with additional potential hazards. In addition,

the use of disinfectants is closely related to drinking water safety; however, residual disinfectants have been shown to promote plastic aging and the release of MPs [147].

1.3.2.1.2 Microplastics Generation Kinetics of Plastic Since polymers do not have a definite end-of-life and only undergo major performance degradation, the effect between the widespread degradation of plastics and the kinetics of MP generation must be considered. The onset of plastic fragmentation is particularly important if we wish to develop reliable models to predict the generation of MPs. Kalogerakis et al. monitored the weathering process of PE films from single-use plastic bags under simulated terrestrial and nearshore conditions for a period of six months [93]. The initiation of fragmentation and the level of weathering leading to complete fragmentation of the PE film was determined by means of tensile strength, molecular weight, and mass loss. Halle et al. investigated MPs floating in the ocean and fragmentation patterns through a combination of physicochemical characterization and mathematical methods with mass distributions, which differs from the size distribution usually used in this field [131]. Researchers assumed that the smaller MPs were mostly the cubic and fragmented much faster than the parallelepipeds. Models and experiments demonstrated the existence of a discontinuity in the rate of fragmentation. This lays the foundation for initial kinetic and mechanistic studies of MP generation.

Using the mask as a study object, Liang et al. found that the release kinetics of MPs were well described by the Elovich equation, which is expressed according to the Eqs. (1.8) (Figure 1.8a,b) [148]:

$$Q_t = a + b \ln t \tag{1.8}$$

where t represents time (d), Q_t represents the MP quantity released at time t (particles/piece), a and b represent the rate constant. The highest release of MPs was observed for 100–500 μm, followed by <100 μm. The photodegradation process of PS MPs in natural water with the presence of common inorganic anions was investigated in detail by Zhu et al. [150]. The inorganic anions promote more pronounced changes in the morphology, functional groups, and molecular weights of the MPs under the action of light, mainly caused by the formation of reactive radical species. Moreover, the evolution of CI values of photodegraded MPs is consistent with a pseudo-first-order kinetic model, and the photoaging rate constant in the presence of anions is higher than that of ultrapure water. The pseudo-first-order kinetic model is expressed according to the Eqs. (1.9):

$$\ln\left[\frac{(CI)_t}{(CI)_0}\right] = kt \tag{1.9}$$

where $(CI)_t$ and $(CI)_0$ is the CI value of PS–MP at time t (d) and time 0, respectively, and k (d^{-1}) is the pseudo-first-order rate constant. Liu et al. further quantified the particle number and dynamic size changes during aging of MPs by applying single particle inductively coupled plasma mass spectroscopy (spICP-MS) (Figure 1.8c) [149]. Aging kinetics of PS MPs accelerated by UV light, and a large number of nano/microsize fragments were revealed. And the aging process exhibited a

decrease in size from 5 to 1 μm with a simultaneous threefold increase in particle number concentration. These are crucial for assessing the ecotoxicological risk of MPs and NPs. Arhant et al. emphasized that the understanding of MP formation needs to consider new open problems related to fracture mechanisms in polymers due to extended aging [10]. Using polyester as an example, aging results were described by molar mass change, crystallinity, and tensile behavior under hydrolysis conditions, and a general explanation for fracture stress reduction was proposed. This work has considered the mechanical behavior of typical polymers at high levels of degradation and predicted the degradation through a kinetic model. Specifically, for high levels of degradation, the fracture stress decreases linearly with molar mass, which can be described by a simple mathematical expression (1.10):

$$\sigma_{\max} = A + B \times M_n \tag{1.10}$$

where $\sigma_{\max}$ is the maximal stress in Mpa; M_n is the molar mass in kg mol^{-1}; A and B are constants identified with experimental data.

Environmental degradation will significantly affect the mechanical properties of plastics, particularly elongation at break, which reduces the external force requirements for plastic fragmentation and promotes mechanical degradation of plastics [151, 152]. The synergistic accelerated aging effects of mechanical agitation and UV irradiation on plastics have been discussed in detail by many researchers [77, 91]. Song et al. counted different types of MP particles (PE, PP, and PS) after UV irradiation and mechanical stirring [91]. The number of fragmented polymer particles increased with the decrease in size, and the size-normalized abundance of the particles was predictable. By combining Weather-Meter results with an independent Arrhenius study, which is expressed according to the Eq. (1.11), Huber et al. studied isotropic PP films commonly used in packaging and the time of MP formation was estimated [139].

$$k = A \cdot e^{-\frac{E_a}{RT}} = \frac{1}{IP} \tag{1.11}$$

where k is the rate constant; IP is the induction period; R is the universal gas constant; T is the temperature; and E_a is the activation energy. The kinetics and mechanism of mechanically degraded secondary NPs related to size distribution have also been widely investigated [77, 100]. Enfrin et al. reported the release of NPs formed by the fragmentation of MPs extracted from personal toiletries [89]. Researchers have investigated turbulence-induced MPs fragmentation and NPs release under low shear, finding the increase in the number of particles in water by an order of magnitude. And the size of resulting NPs was correlated to the energy density given to the particles using the model of solid failure through crack propagation. Chen et al. found that MPs can be degraded in a frozen environment with extremely fast kinetics, attributed to the fact that radicals excited by the limited space between ice crystals attack the MPs and promote degradation (Figure 1.8d,e) [129]. The degradation rate of MPs in ice is more than 60 times that in aqueous solutions at room temperature, which is surprisingly competitive with most artificial techniques and may provide an efficient pathway for the degradation of MPs.

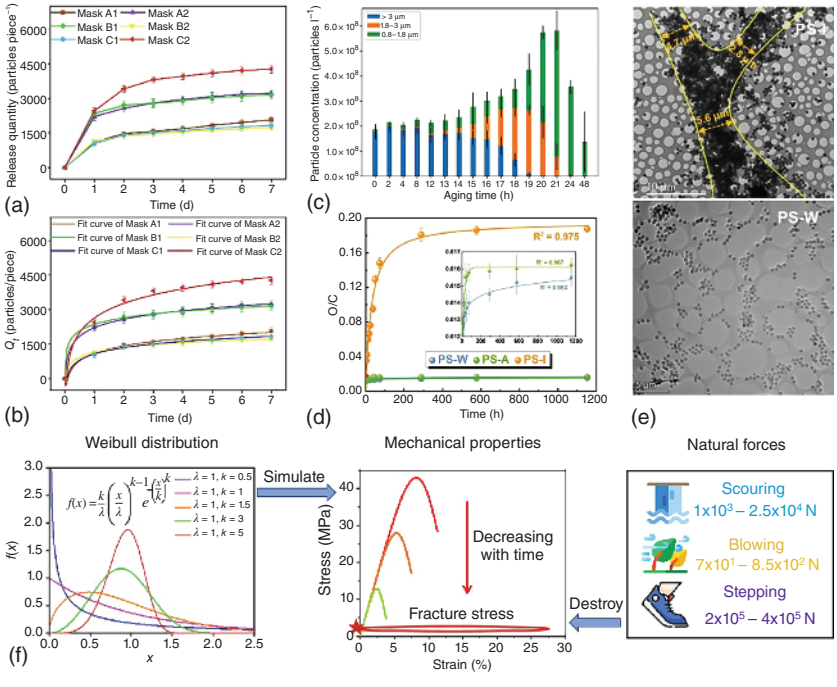

Figure 1.8 (a) Actual quantity and (b) fit curves from Elovich equation for microplastics released from masks. Source: Reproduced from Liang et al. [148]/with permission of Elsevier, (c) PS MPs particle number concentration along the aging process determined by spICP-MS. Source: Reproduced from Liu et al. [149]/with permission of American Chemical Society, (d) correlations between the O/C ratio and degradation time in different environment (W-water, A-air, I-ice). Source: Reproduced from Tian et al. [129]/with permission of John Wiley & Sons, (e) TEM images of PS-I at −20 °C and PS-W at 25 °C. Source: Reproduced from Tian et al. [129]/with permission of John Wiley & Sons, (f) schematic illustration for the evaluation model of microplastics generation behavior via quantitatively matching aging behavior and mechanical failure. Source: Reproduced from Cui et al. [87]/with permission of Elsevier.

Recently, Cui et al. and Huang et al. presented a kinetics evaluation model containing parameters representing environmental aging factors and mechanical wear to predict MP generation [86, 87]. The evaluation model of MPs generation behavior via quantitatively matching aging behavior and mechanical failure was demonstrated (Figure 1.8f). The modified Weibull formula was used to simulate the ultimate fracture stress of aged films, which can be expressed according to the Eq. (1.12), and the finite element analysis quantified the magnitude of natural forces:

$$\sigma(\varepsilon) = E \cdot \varepsilon \cdot e^{-\left(\frac{\varepsilon}{\varepsilon_{td}}\right)^m} \tag{1.12}$$

where $\sigma(\varepsilon)$ is the simulated stress; ε is the actual strain of the material; E is the elastic modulus; m is the shape parameter, which controls the shape of the fitted function image; and ε_{td} is the characteristic parameter, which reflects the decay of material failure strain with increasing aging time. As a result, the MPs are considered to be generated when the magnitude of above fracture stress and natural

force match. Based on the time variable introduced by the method, the time point of MP generation can be predicted. If the time parameter is linearly related to ε_{td}, the formula can be expressed according to the Eq. (1.13):

$$\sigma(\varepsilon) = E \cdot \varepsilon \cdot e^{-\left(\frac{\varepsilon}{kt+b}\right)^m} \tag{1.13}$$

where t is aging time; k and b are two parameters of a linear function fitted to time using fracture strain.

1.3.2.1.3 Nanoplastics Generation from Plastic Currently, more and more researchers are focusing on the generation of NPs, besides MPs. Determining the fate of larger particles (e.g. MPs) could help to understand the formation, release, and distribution of NPs in the environment. For example, some researchers have quantified the processes and fluxes of the ocean–atmosphere micro(nano)plastic cycle (Figure 1.9) [153]. However, assessing the fate of nanoparticles in the environment is inherently difficult due to the size of nanoparticles [95].

On the one hand, NPs can be generated along with MPs during the use of plastic products. Because the size of NPs is so small, even slight external forces will cause them to come off. Chen et al. demonstrated that a common polyester plastic bottle containing carbonated beverages released both MPs and NPs due to the synergistic effects of carbonation and high pressure, ranging from 68 to 4.66×10^8 particles l^{-1} (Figure 1.10a) [144]. Repeated freeze–thaw cycles even considerably exacerbate the release of MPs and NPs. Luo et al. showed that MPs could easily mask and shield NPs [155]. To address this issue, Raman imaging was applied to the study related to the generation of NPs. They found that thousands of MPs and billions of NPs might be released by cutting of one PVC pipe. On the other hand, NPs can also be formed by the fragmentation of MPs. Peller et al. reported a method for the formation of NPs in aqueous conditions using agitation and ultrasound mixing of these plastics in the presence of simple organic liquid solubilizers, which provides valuable insights into the research related to the mechanism of NP formation (Figure 1.10b) [154]. Song et al. exposed three major plastic films (PE, PP, and PS) to simulated sunlight in

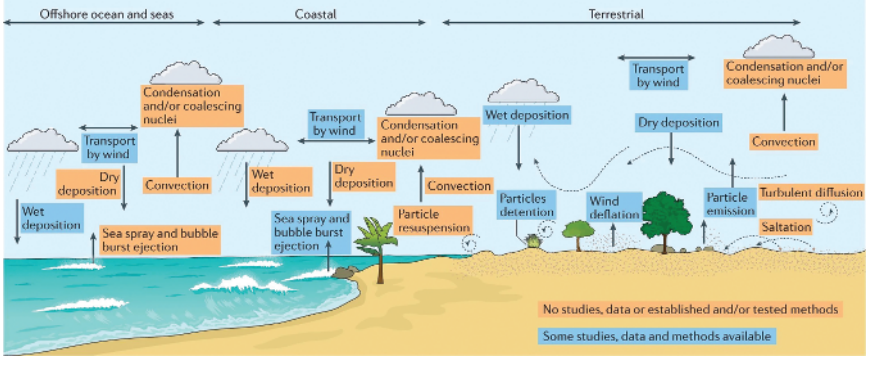

Figure 1.9 Critical known and unknown atmospheric processes. Source: Allen et al. [153]. Reproduced with permission of Springer Nature.

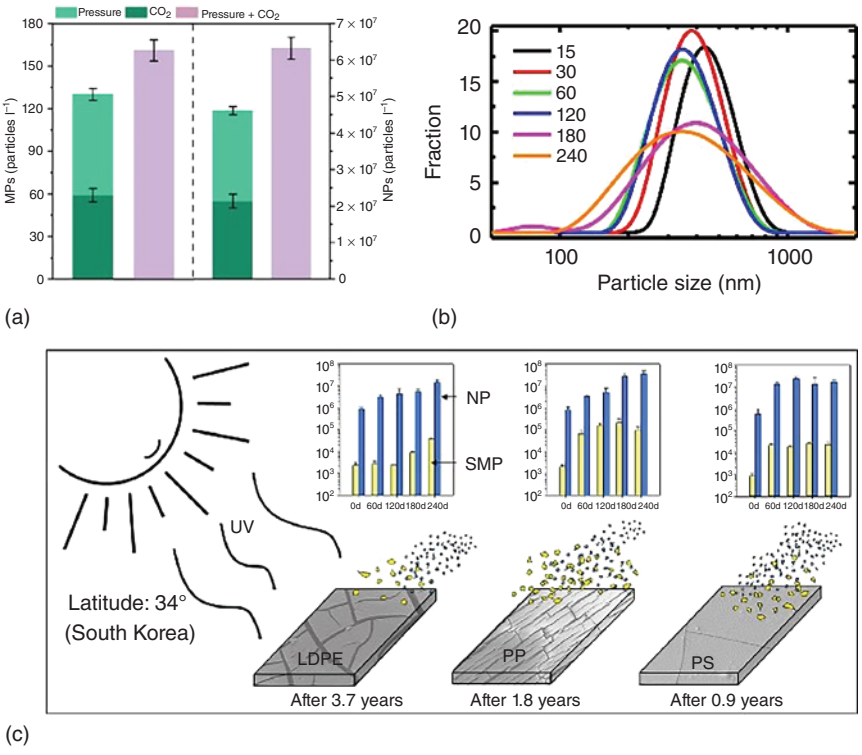

Figure 1.10 (a) The number of MPs/NPs released under single and combined factors was counted. Source: Reproduced from Chen et al. [144]/with permission of Elsevier. (b) Specific particle size distributions generated for PE as a function of sonication time. Source: Reproduced from Peller et al. [154]/with permission of Elsevier. (c) The assessment of the speed of photooxidation-induced fragmentation of three major plastic films. Source: Reproduced from Song et al. [81]/with permission of Elsevier.

an accelerated weathering chamber to assess the speed of photooxidation-induced fragmentation (Figure 1.10c) [81]. PS has a faster initiation of fragmentation than the other polymers but a lower total abundance and increasing ratios than PP. The increasing ratio between MPs and NPs of PP films was significantly different from that of other polymers. And it is worth noting that the surface cracks generated by photo-oxidation do not directly reflect the onset of MPs, which is much slower. Quantitatively determined data on the fate of plastics exposed to simulated sunlight as a function of polymer type are valuable for estimating secondary NPs and MPs production in the environment. In addition, Hadri et al. prepared NPs using mechanical degradation of various MPs and characterized them in terms of size distribution, shape, surface charge, and environmental stability [100]. The resulting NPs were polydisperse, polycrystalline, and negatively charged at pH ranging from 4 to 11. The fragmentation efficiency depends on the properties of the plastic (e.g. glass temperature and molecular weight) and also on the pre-degraded state of the plastic prior to the grinding process.

The kinetics of MP generation from different types of mulch films in agricultural soil, including conventional non-degradable, oxodegradable, and biodegradable films, was studied by Yang et al. [99]. A dose-dependent relationship for MP generation upon UV irradiation strictly following the Schwarzschild's law was demonstrated. The formula can be simplified to the Eq. (1.14):

$$\ln It = \text{constant} - a \cdot \log I \tag{1.14}$$

where I is the irradiance intensity; and t is the exposure time. If the Schwarzschild's law is obeyed, then a linear relationship should be obtained between the logarithm of photo response versus the logarithm of light intensity, and the slope of the line indicates the Schwarzschild p-coefficient factor. Under the experimentally set conditions, the average number of MPs released from biodegradable, oxodegradable, and nondegradable films in size range of 0.02–0.10 mm was 475, 266, and 163 particles cm^{-2}, respectively. It is worth noting that the MPs from the oxodegradable mulch films were more concentrated at the size range of 0.20 μm to 0.20 mm, which has started to enter the nanoscale. This means that the abovementioned equations may be applicable to NP kinetics studies. In addition, Enfrin et al. proposed a simple method to describe the agglomeration behavior of NPs in water by calculating the agglomeration rate coefficient k (s^{-1}) depending on the particle minimum size d_0 (m), the size of agglomerate d_{max} (m), and the time t (s) according to the Eq. (1.15):

$$d(t) = d_{max} - (d_{max} - d_0)e^{-kt} \tag{1.15}$$

Understanding which type of force induces NPs agglomeration in water would indicate how strong these agglomerates are and whether they can be easily dispersed under low shear forces.

1.3.2.1.4 Microplastics from Biodegradable Plastics Biodegradable plastics include PLA, poly(butylene succinate) (PBS), and PBAT, which can be degraded by microbial action and eventually turn into carbon dioxide and water under natural or specific conditions. However, they may persist in the environment for long periods under inappropriate degradation conditions. And regardless of the degradation rate, both conventional and biodegradable plastics generate MPs or NPs during plastic aging under natural environmental conditions.

Tong et al. evaluated the formation of secondary micro- and NPs during the degradation of various biodegradable plastics (PBAT, PBS, and PLA) and conventional plastics (PE, PS, and PVC) and the effect of aging factors and mechanical wear [90]. The results have shown that relatively more secondary MPs were generated from biodegradable PBS and PLA than other types (Figure 1.11). PBAT/PLA and PE were more prone to degrade to MPs through photo-oxidation than mechanical forces. Therefore, most of the problems associated with conventional plastics in the field of MPs are also related to biodegradable plastics, and the risk assessment of secondary MPs and NPs of biodegradable plastics should be taken into account. Recently, Wang et al. revealed the health risks of the "eco-friendly" biodegradable plastic PLA and its effects on the gastrointestinal tract, where hydrolyzed oligomers can cause intestinal damage and acute inflammation [156]. Napper et al. further explored MP

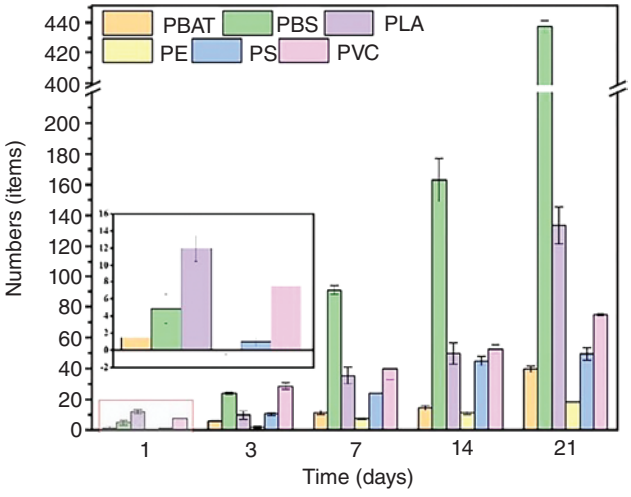

Figure 1.11 The number of secondary microplastics produced by various plastic materials under UV conditions. Source: Reproduced from Tong et al. [90]/with permission of Elsevier.

generation from biodegradable, oxo-biodegradable, compostable, and conventional plastic exposed to three natural environments (open air, soil, and seawater) over a three-year period [137]. However, neither biodegradable nor oxo-biodegradable plastic bags, nor conventional single-use plastic bags, degrade sufficiently to reduce the negative impact on the environment or biota. Researchers pointed to no clear evidence that oxo-biodegradable or biodegradable formulations provide sufficiently high degradation rates for an advantage over conventional plastics in reducing marine litter. Degradable plastic bags degraded more rapidly when exposed to open air and buried in soil than when immersed in seawater; however, there is still a need for a comprehensive discussion of what the breakdown products are, such as MPs or NPs. Potential environmental consequences should also be considered, and it remains to be determined whether fragmentation into MPs poses a greater environmental risk than the original intact waste. It was recently pointed out by Shen et al. that recycling biodegradable plastics is a preferable alternative to biodegradation in settings where collection is easy, which not only reduces the environmental risk of MPs but also reduces carbon emissions (Figure 1.12a–c) [157].

In addition, the MP emission of the biodegradable plastics polyhydroxybutyrate (PHB) and starch-based biodegradable plastics were analyzed by Pleiter et al. and Innocenti et al. [92, 158]. PHB MPs generated secondary PHB NPs (75–200 nm) through abiotic degradation under environmental conditions, which were harmful to the tested organisms, suggesting that the biodegradable plastic PHB is not meant to be completely safe for the environment. On the other hand, Innocenti et al. defined a parameter called microplastic emission potential (MPEP), applied to cellulose, PE, and starch-based biodegradable plastics [158]. The MPEP values were equal for cellulosic and biodegradable plastic materials but 1827 times higher for PE.

Traditional petroleum-based plastics are not capable of later processing and degradation to reduce the generation of MPs and the negative impact on the environment.

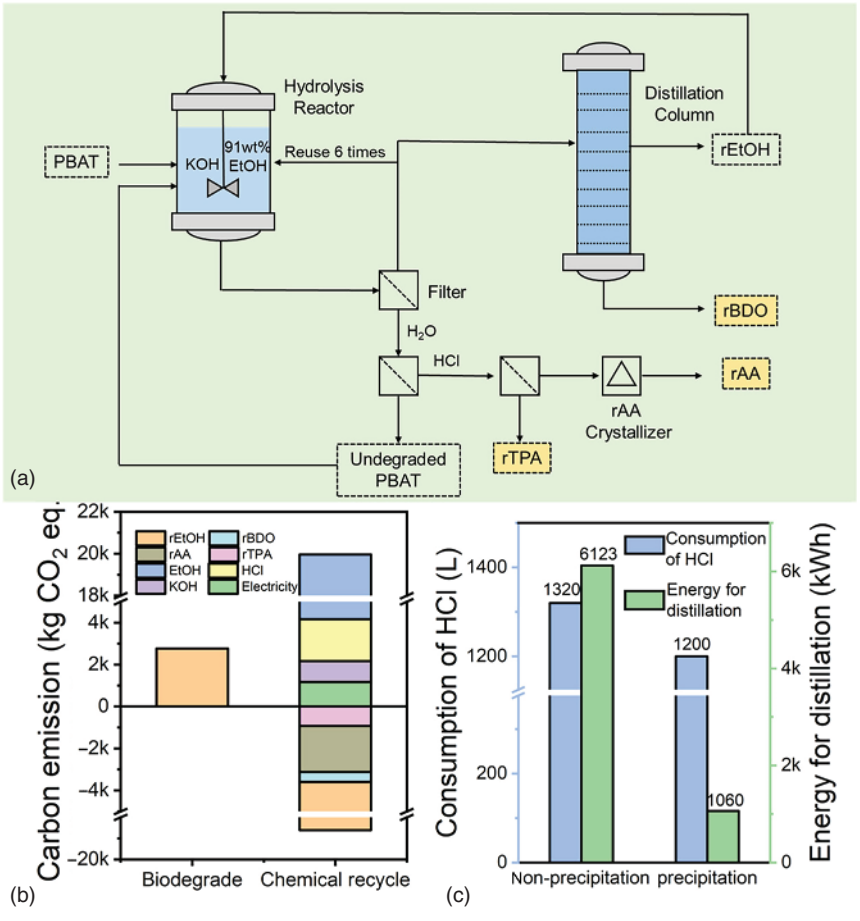

Figure 1.12 (a) Chemical process model of PBAT recycling. (b) Carbon emission during the biodegradation and chemical recycling of 1200 kg PBAT. (c) Comparison of the consumption of HCl and energy for distillation between the precipitation process and nonprecipitation process of diacid products. Source: Reproduced from Shen et al. [157]/with permission of American Chemical Society.

Recently, Jaiswal et al. used a two-stage oxidation process connecting abiotic and biotic treatment by using enriched cultures from landfills to upgrade the degradation process [94]. The main effect of abiotic aging on PE films was more prominent under natural weathering conditions than thermal aging, leading to the formation of oxidized functional groups. Further, the enriched cultures increased the oxidation level of naturally weathered films through biotic treatment. The importance of enriched cultures for efficient biooxidation of PE packaging films under suitable abiotic degradation conditions was elucidated by analyzing the changes in chemical components of the films with the observation of surface biofilm formation. This has implications for the development of methods to mitigate the environmental pollution caused by plastic waste and MPs.

Overall, biodegradable plastics do not show significant advantages over traditional nondegradable plastics in terms of the amount of MPs generated and their toxicity to the environment. Even under certain conditions, biodegradable plastics will generate more MPs if they are not properly disposed of after disposal. Therefore, various topics related to MPs and NPs from biodegradable plastics, such as plastic degradation mechanisms, MPs generation behavior, and NPs characteristics need to be discussed under the framework of life cycle assessment (LCA). MP emission potential and physiological toxicity should be compared with conventional plastics for a comprehensive risk assessment.

1.3.2.2 Rubbers-Derived Microplastics

Rubber is a highly elastic polymer material with reversible deformation, elastic at room temperature, capable of producing large deformations under small external forces and recovering after removing them. Rubber is a completely amorphous polymer with a low glass transition temperature (T_g) and often a large molecular weight greater than several hundred thousand. Rubber is divided into two types: natural rubber (NR) and synthetic rubber [159]. NR is made from rubber trees, rubber grass, and other plants after gum extraction; synthetic rubber is made from various monomers by polymerization. Rubber products are widely used in various industries or daily life, such as tires, hoses, tapes, and cables.

Since 1960, when DuPont introduced the first generation of thermoplastic elastomers (TPUs), TPUs have been a class of rubber materials with a wide range of applications. Compared to vulcanized rubber, TPUs have the properties of both rubber and thermoplastic. At room temperature, they are soft, similar to rubber, tough and elastic, and at high temperatures, they become fluid and can be molded. It is the so-called third generation of rubber after NR and synthetic rubber. The plastic segments form physical cross-linking points by virtue of the forces between the chain segments, and this physical cross-linking is reversible with temperature, thus demonstrating the plastic processing properties of TPUs. The rubber segment is a highly elastic chain segment, and the elasticity of the TPU is determined by the rubber segment [160]. PU products have many excellent properties, such as good low-temperature flexibility, high impact resistance, radiation resistance, wide rebound range, and good adhesion, which are widely used. Compared with traditional plastics, rubber, and even metal, they have obvious performance advantages. With economic development and consumer upgrading, it will gradually become a rational alternative to traditional materials. Because of their dual properties as rubber and plastic, TPUs are used in rubber shoes, adhesives, automotive parts, wires and cables, hoses, coatings, extruded products, and so on [161]. They are used in all areas of automotive, electrical, electronic, construction, and craft, as well as in everyday life. In addition to being unsuitable for the manufacture of inflatable tires, many rubber products can be replaced by TPUs, so the application of TPUs is very promising.

PU is a polymer with repeating structural units of urethane segment chains made by reacting isocyanic acid esters with polyols. TPU (thermoplastic PU elastomer) is a block copolymer composed of isocyanate (curing agent), polyether

(or polyester), a large polyol (forming the main chain structure of the soft segment), and a small polyol (or amine) as a chain extender (forming the hard segment structure) [162]. The main component of the block copolymer is the polyether (or polyester) [163]. Different varieties of raw materials, curing agents, polyols, and chain extenders can synthesize a variety of TPU products with different performances and processing. TPU can be made into high-modulus specialty plastics, high elasticity rubber, films, and fibers.

Styrene butadiene rubber (SBR) is a copolymer of butadiene and styrene. According to the different production processes, SBRs can be divided into two kinds: emulsion polymerization and solution polymerization. SBR is mainly used in the production of tires, footwear, auto parts, hoses, tapes, and other rubber products and has a wide range of applications. It shows characteristics such as low rolling resistance, good anti-slip properties, and good wear resistance. It is widely used in the tire industry, especially in green tires, anti-skid tires, ultra-light tires, and other high-performance tires. Compared with NR, it has uniform quality, less foreign matter, better abrasion, and aging resistance; however, it has weaker mechanical strength and can be mixed with NR. It is a low-cost, non-oil-resistant material with good water resistance, good elasticity below 70 hardness, and poor compressibility at high hardness.

NR is made from latex collected from rubber trees and is a polymer of isoprene. It has good abrasion resistance, high elasticity, strength and elongation, and good overall performance. NR is chemically reactive because it has unsaturated double bonds. Light, heat, ozone, radiation, flexural deformation, and metals such as copper and manganese, and other metals can promote the aging of rubber. NR is easily aged in air, becomes sticky in heat, swells and dissolves easily in mineral oil or gasoline, and is resistant to alkalis but not to strong acids. Its advantages are good elasticity and resistance to acid and alkali. The disadvantage is that it is neither heat-resistant nor oil-resistant (can be resistant to vegetable oil), and it is the raw material for making tape, hose, and rubber shoes, and is suitable for making shock-absorbing parts, products used in automobile brake fluid, ethanol, and other liquids with hydroxyl roots.

1.3.2.2.1 Influence Factors of Microplastics Generation Rubber and its products in the process of processing, storage, and use, due to the combination of internal and external factors caused by the physical and chemical properties of rubber and mechanical properties of the gradual deterioration, finally lose the value of their use. This change is called rubber aging, which is caused by cracking, stickiness, hardening, softening, chalking, discoloration, and mold. Aging factors include oxygen, ozone, heat, light, mechanical stress, moisture, and oil. Oxygen reacts with rubber molecules by a free base chain lock reaction, which leads to a molecular chain breakage or excessive cross-linking, causing changes in rubber properties. Oxidation is one of the important causes of rubber aging. The chemical activity of ozone is much higher than that of oxygen and more destructive. Ozone also breaks the molecular chains, but its effect on rubber varies depending on whether the rubber is deformed or not. When used in deformed rubber (mainly unsaturated rubber), there is a straight crack with the direction of the stress, the so-called "ozone

cracking"; when acting on deformed rubber, it leads to only the surface generation of oxide film and not cracking [164]. Increasing the temperature can cause thermal cracking or thermal cross-linking of rubber. However, the basic effect of heat is still activation, which leads to increase in the rate of oxygen diffusion and activation of oxidation reaction, thus accelerating the rate of rubber oxidation, which is a prevalent aging phenomenon known as thermal oxygen aging. The shorter the light wave, the greater the energy. The destructive effect on rubber is the higher-energy UV light. In addition to UV light directly causing the breakage and cross-linking of rubber molecular chains, rubber produces free radicals due to the absorption of light energy, which triggers and accelerates the oxidation chain reaction process. The external light plays a heating role. Another characteristic of light action (different from thermal action) is that it mainly affects the surface of the rubber [165]. Specimens with high gum content will have a network of cracks on both sides, which is called "light outer layer cracking." Under the repeated action of mechanical stress, the rubber molecular chain breaks to generate free radicals, which trigger the oxidation chain reaction and form a forceful chemical process that involves mechanical breakage of molecular chains and mechanical activation of the oxidation process. The one that dominates depends on the conditions under which they are located. In addition, it easily causes ozone cracking under stress. The role of moisture is twofold: rubber is easily destroyed when wet air is drenched or immersed in water, which is caused by water-soluble substances, hydrophilic groups, and other components in rubber being dissolved by water extraction, hydrolysis, or absorption. Especially under the alternating effect of water immersion and atmospheric exposure, the destruction of rubber will be accelerated [166]. However, in some cases, water does not have a destructive effect on rubber and even has the effect of delaying aging on rubber. In long-term contact with oil media, oil can penetrate the rubber, causing internal swelling of rubber, resulting in the reduction of rubber strength and other mechanical properties. Oil can make the rubber swell because the oil penetrates the rubber, leading to molecular diffusion so that the network structure of vulcanized rubber changes. Other factors that act on rubber are chemical media, variable metal ions, high-energy radiation, electricity, and biological factors.

Even when designed to be chemically and biologically inert, synthetic polymers fragment into micro- (<5 mm) and nano-sized (<100 nm) particles under mechanical forces and when exposed to (photo-)oxidizing agents. Direct sunlight, particularly in the UV range, induces changes in polymer brittleness, density, size, and surface charge, leading to loss of bulk mechanical properties. These changes are the result of oxidative processes initiated by free radicals activated by light in the presence of oxygen. These processes compromise the polymer structure by (i) incorporating oxygen-containing functionalities, (ii) initiating chain scissions that reduce the number-average molecular weight of plastics, and (iii) introducing cross-links. Specifically, reactive oxygen species activated by light in the UV range initiate the photolytic cleavage of a C—H bond on the polymer backbone to produce a polymer alkyl radical (P·). Reaction with molecular oxygen leads to the formation of unstable polymer peroxy radicals (POO·), which decompose into hydroxyl radicals (OH·) and polymer oxy radicals (PO·) that can decay into chain scission products. The reaction

terminates when polymer radical species couple mutually or form crosslinks with polymer peroxy radicals [167]. In particular, chain scissions can release oligomers, monomers, and additives into the environment surrounding MPs, contributing to the pool of dissolved organic carbon (DOC) available to microorganisms with potentially unaccounted consequences on marine ecosystems.

PU is a family of synthetic copolymers obtained by a condensation reaction of polyisocyanates and polyols to give a urethane linkage (—NH—COO—). Although not as abundant as major consumer plastics such as PE, PP, and PS, PU MPs are commonly found in marine environments, including coastal areas, seafloors, and remote areas. If exposed to sunlight, the urethane linkage will photo-oxidize. Following a characteristic initial yellowing, the homolytic scission of the urethane bond will form free radicals, whose decomposition and recombination ultimately generate short polymer chains, monomers, and low molecular weight photo-oxidized products that partition into the surrounding environment.

Surface properties were investigated, especially as UV radiation that first causes degradation on the surface and, in this way, degradation can be detected more sensitively than for the characterization of bulk properties. After radiation for 1000 hours in dry, humid, and wet conditions, TPU becomes yellowish. Under humid conditions, cracks appear. The most significant change appears between 3650 and 3000 cm^{-1}, where the signal at 3328 cm^{-1}, characteristic of the stretching vibration of H-bonded N—H group, broadens with two maxima at 3451 and 3200 cm^{-1}, respectively, suggesting the formation of hydroxyl groups (—OH) induced by UV radiation. However, these two bands could also be characterized as a stretching vibration of N—H group in primary amine [168]. The 3451 cm^{-1} band has been attributed to the hydroperoxidation of the methylene bridge. Attenuated total reflectance- Infrared radiation (ATR-IR) spectra of both TPUs show a significant decrease in the N—H deformation band and the C—N stretching vibration band of the urethane group (1534 cm^{-1}). Also, both carbonyl regions, 1734 and 1700 cm^{-1}, corresponding to free and H-bonded states, respectively, became weaker with increasing exposure time, along with the formation of new carbonyl groups. Peaks between 1652 and 1638 cm^{-1} were attributed to C=O stretching vibrations of oxidized methylene bridge. Furthermore, the intensity of the peak at 1110 cm^{-1}, attributed to the C—O—C vibrations of the ether groups, strongly reduces irradiation. Also, the peak at 1597 cm^{-1}, which can be ascribed to —C=C— stretching vibration of aromatic ring, loses intensity with increasing exposure time. Similar decrease is detectable for the aromatic =C—H out-of-plane deformation vibration at 817 cm^{-1} (Figure 1.13).

All irradiated PU MPs developed yellowing by receiving a UV dose of 175 MJ m^{-2}, an unambiguous indicator of photo-oxidation. Most commonly, PU yellowing results from the oxidation of aromatic isocyanate residues to monoquinone imide and diquinone imide. Less commonly, yellowing can result from photo-Fries rearrangement of the urethane linkage. Overall, the results of the ATR-FTIR analysis aligned well with the scientific literature. For all PU MPs, yellowing via the quinonoid route was supported by the emergence of a band at 814 cm^{-1} (out-of-plane C—H bending vibration in 1,4-disubstituted aromatic rings) that had decreased by receiving a UV dose of 350 MJ m^{-2}, indicating that aromatic

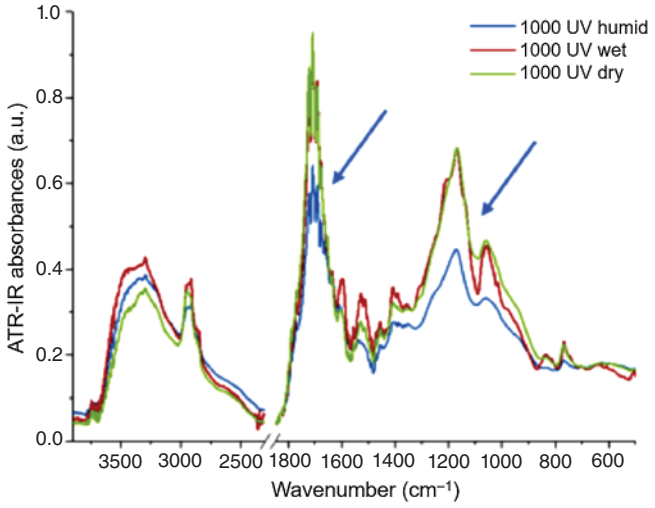

Figure 1.13 FTIR spectra of TPU before and after irradiation in dry, humid, and wet conditions. Source: Theiler et al. [169]. Reproduced with permission of Elsevier.

rings were degraded. Additionally, evidence of quinone formation was found in the bands at 2856 and 2941 cm^{-1}, which are characteristic of the methylene group bridging diphenyl diisocyanate residues' asymmetrical and symmetrical stretching vibrations, respectively. Decreases in these bands were unambiguous for polyether TPU and not observed in polyester TPU. However, polyester TPU also showed a decreasing amide II band at 1527 cm^{-1}, an indicator of photo-Fries rearrangement of the urethane linkage. Finally, the increasing band at 1597 cm^{-1} was assigned to quinonic C=C stretching vibrations, indicating the accumulation of quinone structures in all PU MPs. This result is in partial agreement with the literature, as other studies have reported a decreasing 1597 cm^{-1} band, attributing it to C=C stretching vibrations in aromatic rings. Other notable changes in the irradiated samples were the increasing carbonyl peak at 1704 cm^{-1} wavenumber in all PU MPs, a strong indicator of photo-oxidation; the increasing and broadening 3200–3600 cm^{-1} wavenumber region in all PU MPs, consistent with hydroxyl stretching vibration; and the decreasing band at 1100 cm^{-1} in polyether TPU, characteristic of C—O stretch in ethers, reflecting the degradation of ether bonds [170].

The solubility of photo-weathered ether-based TPU decreased due to cross-linking while observing a stabilization of molar mass loss. Cross-linking competed with chain scission in ether-based TPUs under high-energy radiation. Cross-linking reduces interchain distances (e.g. via hydrogen or covalent bonds), preventing oxygen diffusion and UV light penetration, conferring a de facto resistance to photo-oxidation. Studies on other cross-linked PUs showed that chemical oxidation produced short-chain scission products that reorganized and cross-linked, whereas UV photo-oxidation induced only minor chain scissions.

The features of the TPUs differed in (i) degree of saturation expressed as H/C ratio, which was lower in TPU_Ester, and (ii) oxygen content, expressed as O/C ratio,

which was lower in TPU_Ether. These differences aligned with the chemistry of TPU elastomers: ester-based segments contain less hydrogen and more oxygen than ether-based segments of the same chain length due to the carbon-to-oxygen double bond of ester functional groups. Based on literature data, UV photo-oxidation of ester-based flexible segments can induce decarboxylation to give alkene group-containing products. The data showed that the features of PU_Hardened had fewer carbon atoms, and, in line with the literature on cross-linked PU degradation, indicated that only low molecular weight photo-oxidation products were generated. The literature indicated that the organic carbon leached from weathered polymers can photodegrade to low molecular weight by-products, partially oxidized DOC and CO_2. According to the literature, the soft segments of TPU_Ether are very sensitive to photo-oxidation; their degradation is initiated by radical attacks followed by hydrogen abstraction, forming alkoxy radicals and hydroperoxides, and culminating in chain scissions [169]. As UV radiation induces photo-oxidation of ester segments with chain scissions through Norrish type II reactions, it gives products with unsaturated chain ends.

In NR and SBR, a broad —OH stretching band is observed between 3660 and 3125 cm^{-1} in the unaged material due to the hydroxyl groups. The signal intensity increases up to 168 hours, possibly due to oxidation or hydration, but reduces thereafter as the additives are consumed. A direct result of weathering in both materials is the occurrence of a carbonyl band at about 1713 cm^{-1} after 168 hours of weathering, which is prominently present in the skin at 504 hours but disappears in the core. In NR, the asymmetric =C—H stretching band at 3035 cm^{-1} (i) decreases from 0 to 504 hours, while the skin shows its complete loss at 504 hours. Likewise, the asymmetric —CH_3 stretching (2959 cm^{-1}), (ii) asymmetric —CH_2 stretching (2918 cm^{-1}), and (iii) bands also reduce with weathering. Further, the symmetric —CH_3 stretching and symmetric —CH_2— stretching bands are seen as a single peak at 2849 cm^{-1}, which shows a decrease in intensity and suppression in the skin region at extended weathering. To put this into context, in a thermo-oxidatively aged NR study, the —CH_2— stretching vibration demonstrated peak retention, contrary to the observation made in the present work [171]. Using only UV radiation, dos Santos et al. summarized the formation of different groups in polyisoprene (cis, trans, and NR) subjected to various wavelengths. It was concluded that apart from the wavelength, the type of isomer and the precondition (presence of groups characteristic of partial oxidation) of the polymer dictate the effects of UV. The —C=C— stretching vibration occurs at 1662 cm^{-1}, whose intensity decreases with weathering. In the fingerprint region, the IR spectra are dominated by —CH_3 and —CH_2— bending vibrations at 1452 and 1375 cm^{-1}, respectively, and the rocking vibration of —CH_2— at 724 cm^{-1}. As stated before, these peaks also decrease upon increasing the time of weathering, representing a likely explanation for the appearance of the skin in the Gram–Schmidt maps. In SBR, the —C=C— stretching of the vinyl group at 1640 cm^{-1} tends to become stronger with successive weathering due to cross-linking. The aromatic —C=C— stretching vibration peak occurs at 1601 cm^{-1}, and its contribution is masked by the presence of the —C=C— vinyl stretching. It has been noted that an increase in the intensity of the —COO—

stretching vibration at 1541 cm^{-1} in thermo-oxidatively aged SBR is an indication of the carboxylate formation as the main product on the material surface [172]. However, such a conclusion cannot be drawn in this study due to the broadening of the —C=C— stretching. Lastly, the —C=C— vibrations of butadiene at 966 and 909 cm^{-1} present in the unaged sample disappeared completely after weathering [173]. This is in line with the gas chromatography flame ionization detector (GC/FID) studies on similar samples by Kano et al. which revealed that the relative amount of butadiene with respect to the pristine sample completely disappeared after 100 hours of accelerated weathering. From these observations, it can be appreciated that the reactions caused by weathering, mainly involving oxygen, lead to chemical modifications that affect the surface preferentially. Nevertheless, several changes occurring within the core lead to unique physical properties that affect the macroscopic moduli, as observed in the previous section (Figure 1.14).

The highest percentage of SBR in the respective tire formulations can be attributed to its less susceptibility to UV-weathering compared to NR. Osswald et al. reported that the higher double bond content and the aromaticity in SBR made it more resistant to weathering than NR. However, the presence of fillers, such as carbon black, in the tire cryogrind interfered with the analysis due to the near complete IR

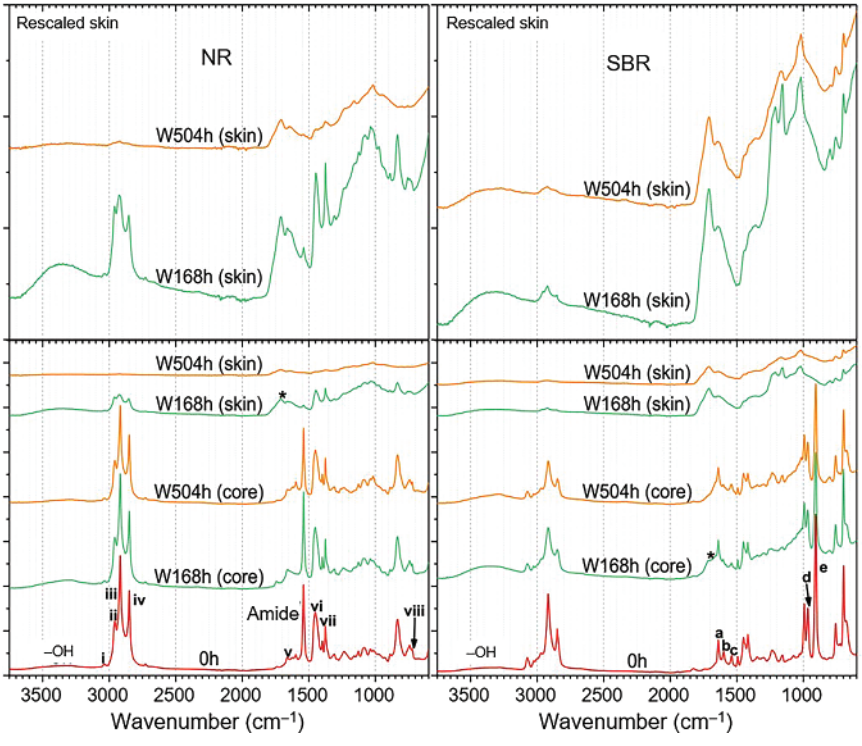

Figure 1.14 ATR-FTIR spectra of NR (left) and SBR (right) weathered for various durations (bottom boxes). The top boxes contain skin-specific spectra rescaled vertically (and equally). Source: Reproduced from Karekar et al. [172]/with permission of Elsevier.

light absorption, as previously reported. Carbon black also decreases the impact of UV exposure. For instance, Sahu et al. reported that carbon black in high-density PE decreased UV weathering of solar photovoltaic structures. Although effective in mitigating some of the impacts of UV exposure, Kim et al. recently reported that carbon black might also be released through the continuous abrasion of tire particles. After the accelerated weathering tests, GC–MS results showed the presence of several degradation intermediates in all the cryogrinds. Sufficient heating helps breakdown of long polymer chains, generating radicals, which react with oxygen to form peroxy radicals and then hydroxy peroxides upon hydrogen abstraction. Further, they dissociate into alkoxy and hydroxy radicals, and several intermediates are formed. Ketones and chain scission products such as acids are also produced, and epoxides are also formed by decomposition of the peroxy alkyl radicals [172]. Aldehydes, carboxylic acids, and ketones are the most prominent and possible tire degradation intermediates due to the photo-oxidation of the elastomers during the two exposure times corresponding to 1-year and 3-year natural aging. The 3-year natural aging results also provided a way to assess the impact of weathering time on the tire cryogrind. As expected, more carboxylic acid degradation intermediates were formed after extended UV weathering times. This observation can be attributed to the fact that under prolonged photo-oxidation, ketone groups can be converted to carboxylic acid groups by Norrish type 1 reactions. The pertinent photo-oxidation degradation mechanisms of elastomer in tire particles are shown in Figure 1.15.

1.3.2.2.2 Microplastics Generation Kinetics of Rubber TPU is a versatile elastomer that is used in various commercial applications. TPU has great potential in materials for underwater applications. However, TPU encapsulants can be torn or broken apart due to the degradation of mechanical properties in seawater, resulting in hydrophone failures. Accelerated lifetime tests (ALTs) have been adopted in various industrial and academic fields with increasing demands for rapid service life assessments. ALT is useful for characterizing the service life of manufactured items that have a considerably long failure time, such as structural materials and components. Several studies have successfully estimated the lifetime of polymeric components by implementing ALT. For example, the lifetime of a NR engine mount compound was predicted to be 31 years by ALT. PE pipes were aged in a chlorine dioxide solution, and its lifetime was estimated to be 50 years. Accelerated aging was performed in distilled water on poly (3-hydroxybutyrate-*co*-3-hydroxyvalerate), and its lifetime was estimated. A glass fiber/PU composite was aged in an accelerated condition, and the dependence of the flexural strength on the temperature was predicted [175]. In addition to these materials, the lifetime of TPU encapsulants can also be estimated using ALT. The ALT of polymeric components is conducted as follows: The polymeric components were aged at accelerated conditions, and then the failure times were obtained, followed by calculating the lifetime at use conditions using acceleration and life distribution models. Degradation of mechanical properties of polymeric components is observed during the ALT and can be chosen as a failure criterion. In addition, 50% of the initial value of mechanical properties is commonly chosen as the failure criterion, according to the International Organization for Standardization (ISO) 11 346. Several studies have examined the changes in

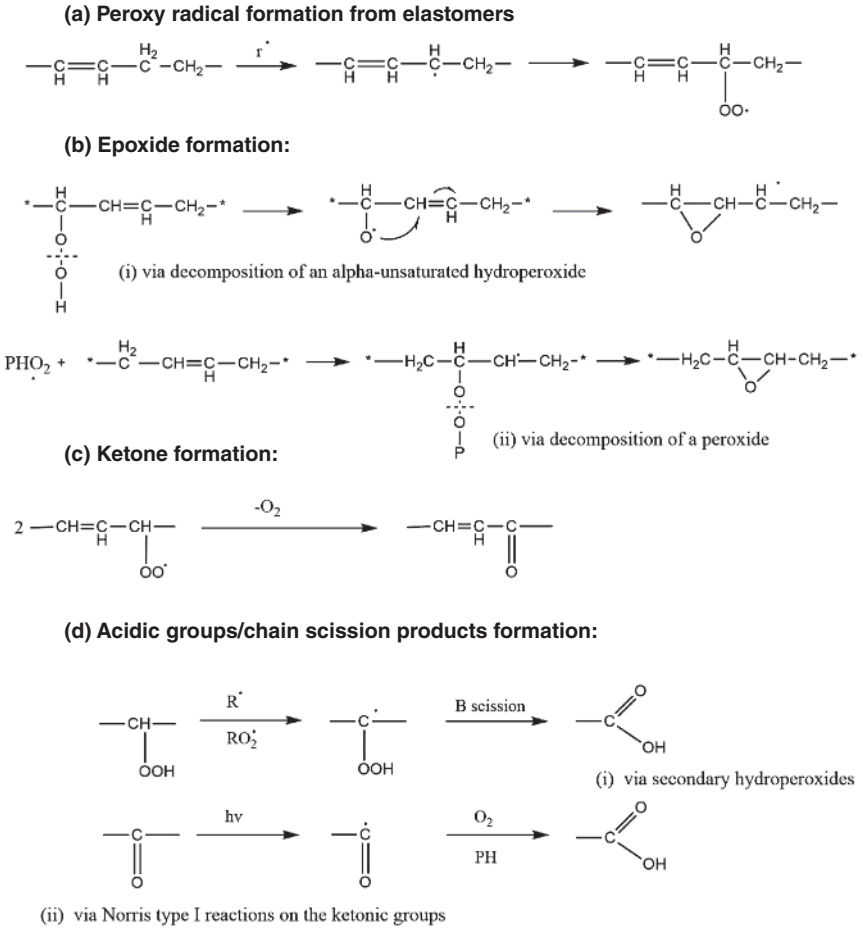

Figure 1.15 Possible degradation pathway and mechanisms of elastomers post weathering tests. Source: Reproduced from Thomas et al. [174]/with permission of Elsevier.

mechanical properties of TPU by aging in seawater, with hydrolytic degradation as the main reason for mechanical degradation. For the ALT of TPU encapsulants in underwater acoustic sensor (UAS), the change in TPU mechanical properties should be examined in terms of hydrolytic degradation in seawater. TPU encapsulant was aged in seawater, and then the failure times were obtained from the changes in mechanical properties to predict its lifetime. The degradation of TPU encapsulant by aging in seawater was explored from changes in the chemical structure and molecular weight of TPU. Molecular dynamic (MD) simulations were conducted to confirm the degradation effect on the TPU mechanical properties [176]. The lifetime of TPU encapsulant in a use-stress level was estimated by using acceleration and life distribution models supported by commercial software for the ALT.

Degradation of TPU encapsulants used in an UAS was examined by aging in seawater, and the lifetime of TPU encapsulants was estimated using an empirical approach based on ALT. The TPU encapsulants were placed in seawater and aged

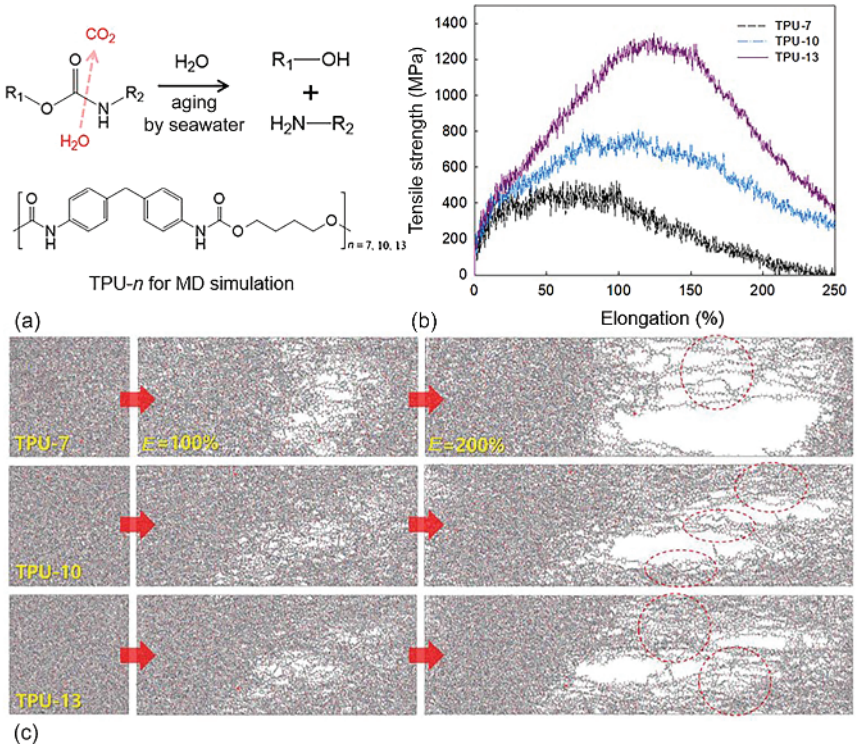

Figure 1.16 (a) Hydrolysis reaction of TPU by aging in seawater and molecular structure of TPU for MD simulation, and (b) stress–strain curves of TPU-7, TPU-10, and TPU-13 examined by the MD simulation, (c) image of MD simulation cells containing TPU-7, TPU-10, and TPU-13 at strains of 0, 100, and 200%. Source: Reproduced from Choi et al. [175]/with permission of Elsevier.

at temperatures of 85, 100, and 110 °C. TPU encapsulants underwent a hydrolysis reaction during aging in seawater, changing the chemical structure and molecular weight of TPU. MD simulation results described the hydrolysis degradation of TPU that leads to a decrease in tensile strength. Tensile tests were conducted on the aged TPU encapsulants, and then failure times for each of the accelerated conditions were estimated from the changes in tensile strength over aging time. The accelerated failure times were used for the lifetime prediction of TPU encapsulants at a use-stress level by using ReliaSoft's ALTA software. An empirical prediction model based on the Arrhenius equation and Weibull distribution was determined for the lifetime prediction of the TPU encapsulant, facilitating lifetime estimations of TPU encapsulant at various failure criteria. A decrease in the tensile strength to 50% of the initial value was established as the failure criterion for lifetime prediction, indicating that half of TPU encapsulants will fail after aging about 20 years. Therefore, this result helps to determine the appropriate time for replacement of TPU encapsulant before failure (Figure 1.16).

Strain-induced crystallization affects the tensile behavior of elastomers and prevents crack propagation. Chain scissions of elastomers, such as hydrolysis result in slower strain-induced crystallization kinetics. Therefore, seawater-induced hydrolysis of TPU encapsulants hindered strain-induced crystallization, resulting in reduced tensile properties. MD simulation was performed on the TPU to examine the effect of TPU degradation on the mechanical properties. The effect of TPU degradation by seawater on the mechanical properties was examined by MD simulation. The large-scale atomic/molecular massively parallel simulator (LAMMPS) package was used to perform the MD simulation. TPU simulation cells were built and stabilized as follows: The TPU chain was constructed with a repeat unit containing MDI and 1,4-butanediol. The MD simulation cell consisted of 100 TPU chains under a periodic boundary condition. A general assisted model building with energy refinement (AMBER) force field (GAFF) was assigned to the TPU cell, and then the TPU cell was stabilized under the constant number of particles, volume, and temperature (NVT) ensemble at 800 K for 25 ps with a time step of 0.5 fs. Subsequently, the cell was relaxed under the constant number of particles, pressure, and temperature (NPT) ensemble at 1 atm with a cooling rate of 1.0 K ps^{-1} until the system temperature reached 300 K. The resulting TPU cell was further stabilized under the NPT ensemble at 1 atm and 300 K for 50 ps with a time step of 0.5 fs. Finally, tensile deformation along the Z-direction was applied to the TPU cell at a strain rate of 1×10^4 s^{-1} for 50 ps to obtain the stress–strain curve [177]. A simple TPU structure was constructed by using MDI and 1,4-butanediol as hard and soft segments, respectively. The ends of repeated units were terminated with amine and hydroxyl groups. TPU molecules with repeated units numbering were constructed and examined (hereafter referred to as TPU-7, TPU-10, and TPU-13, respectively, according to the number of repeated units). The MD simulation cell was constructed with 100 TPU molecules, and tensile deformation was applied to the simulation cell under the periodic boundary condition. It shows the stress–strain behavior of TPU-7, TPU-10, and TPU-13 examined by the MD simulation. The tensile strength of TPU obtained by the MD simulation was much higher than the experimental results because the MD simulation assumed a defect-free condition, and a faster strain rate was applied. As the number of repeat units of TPU was low, the maximum tensile strength and strain at this point were low. This tensile behavior is reasonably consistent with the experimental results because the aged TPU encapsulant exhibited a decrease in molecular weight and tensile properties (Figure 1.17).

TPU encapsulants were aged at 85, 100, and 110 °C for certain periods, and their tensile behavior after aging was evaluated for lifetime prediction. The accelerated failure times of TPU encapsulants were obtained from the tensile test of aged specimens and used for the lifetime prediction of TPU encapsulant. Changes in tensile strength were examined as a function of aging time by using regression models in Sigmaplot-10 software. Then, the time required to reach 50, 60, 70, and 80% of the initial tensile strength was recorded as the accelerated failure times. The acceleration and life distribution models for TPU encapsulant were determined from accelerated failure times by using ALTA 9 Pro-software. According to the mathematical background of the ALTA software, four acceleration models, including exponential,

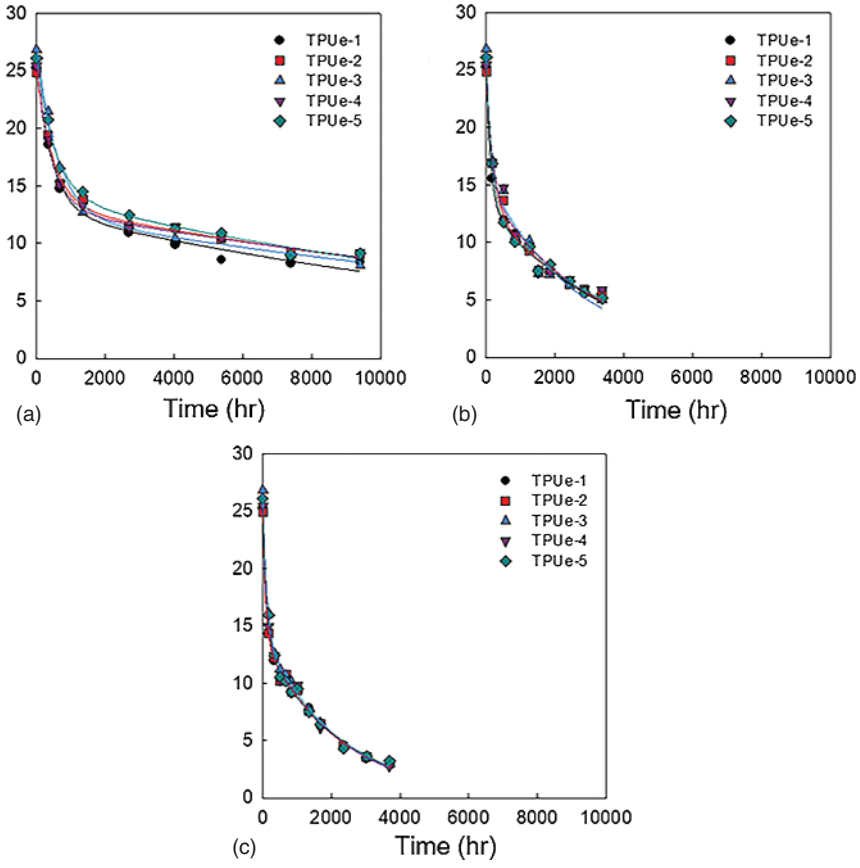

Figure 1.17 Decrease in the tensile strength of TPU encapsulants upon aging time in seawater at temperatures of (a) 85 °C, (b) 100 °C, and (c) 110 °C. Source: Reproduced from Choi et al. [175]/with permission of Elsevier.

Arrhenius, inverse-power law (IPL), and Eyring equations, were examined. Three models, exponential, Weibull, and log-normal distributions, were examined as life distribution models. Maximum log-likelihood estimation (MLE) was used to estimate the parameters of acceleration and life distribution models. Interested readers may refer to the detailed mathematical procedures of lifetime prediction by ALTA software explained in our previous study. Aging was performed at high temperatures to facilitate fast water diffusion in the TPU encapsulants, which led to homogeneous hydrolytic reaction and degradation behavior. Since the TPU encapsulants have a substantial thickness, aging at low temperatures may not be suitable for the ALT due to slow water diffusion. Five TPU encapsulants produced at different times were examined for the ALT, and results showed different rates of decrease in tensile strength, resulting in different aging times to reach failure criteria. In other words, TPU encapsulants have varying failure probabilities; therefore, a number of TPU encapsulants were examined for the ALT to obtain lifetime distribution and predict failure rate. The tensile strength of TPU encapsulants decreased as aging time in

seawater increased. Curve fittings describing the decrease in tensile strength upon aging time were obtained using an exponential regression model in the Sigmaplot-10 software. The exponential regression model for the curve fittings is given as follows:

$$S(t) = Ae^{-Bt} + Ce^{-Dt} \tag{1.16}$$

where $S(t)$ is the tensile strength, and A, B, C, and D are the parameters for the exponential regression model. The average R-squared value for the curve fittings at aging temperatures of 85, 100, and 110 °C were 0.99, 0.98, and 0.99, respectively. This suggests that the exponential regression model was the best fit for the decrease in tensile strength of TPUe. From the curves, the accelerated failure times were estimated at the points corresponding to 50, 60, 70, and 80% of the initial tensile strength (hereafter referred to as tf50, tf60, tf70, and tf80%, respectively) [175] (Figure 1.18).

The accelerated failure times of TPU encapsulants were fitted by using the Arrhenius equation, which is given as follows:

$$\mathrm{In}(L(V)) = A_0 + \frac{A_1}{V} \tag{1.17}$$

where $L(V)$ is the lifetime; V is the stress; and A_0 and A_1 are model parameters. The average values of accelerated failure times and aging temperatures were used as $L(V)$ and V, respectively. It shows that the Arrhenius plot and the accelerated failure times decreased exponentially as the aging temperature increased. R-squared values of Arrhenius plots were 0.982, 0.980, 0.977, and 0.973 for tf50, tf60%, tf70%, and tf80%, respectively [175]. This result indicates that the ALT of TPU encapsulants exhibited a high degree of correlation between the accelerated temperature and failure time. The lifetime of TPU encapsulants at a use-stress level was estimated from the accelerated failure times using the ALTA software. The lifetime prediction of TPU encapsulants was performed using an empirical approach based on life distribution and acceleration models. Life distribution models, including exponential,

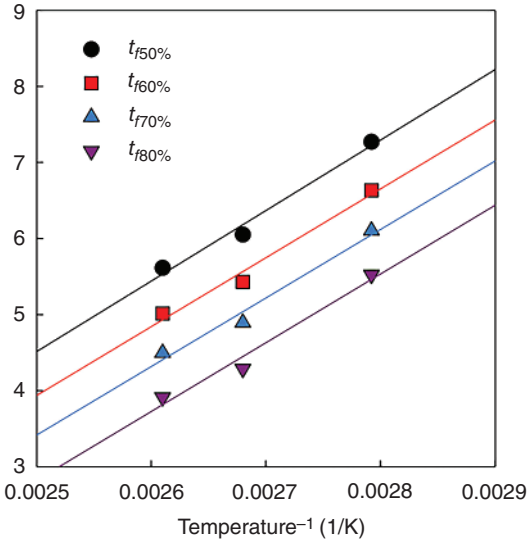

Figure 1.18 Arrhenius plot for the changes in accelerated failure times of TPU encapsulants with aging temperature. Source: Reproduced from Choi et al. [175]/with permission of Elsevier.

Weibull, and log-normal distributions, are described in the ALTA software and were examined for the statistical analysis of accelerated failure times. Cumulative density functions (CDF, $F(t)$) for the failure time can be expressed by the life distribution models as follows:

$$F(t) = 1 - e^{-\frac{t}{m}} \tag{1.18}$$

$$F(t) = 1 - \left(\frac{t}{\eta}\right)^{\beta} \tag{1.19}$$

$$F(t) = \frac{1}{2} + \frac{1}{2}\mathrm{erf}\left(\frac{\mathrm{In}(t) - \mu}{\sqrt{2\sigma}}\right)^{\beta} \tag{1.20}$$

where Eqs. (1.18)–(1.20) are the CDFs of exponential, Weibull, and lognormal distribution models, respectively. m is the mean life for the exponential distribution. η and β are parameters for determining the scale and shape of the Weibull distribution, respectively. σ is the standard deviation, and μ is the mean of natural logarithms for the lognormal distributions. The MLE results obtained by ALTA software indicated that the Weibull distribution model was best suited for the accelerated failure times of TPU encapsulants. Acceleration models, including exponential, Arrhenius, Eyring, and IPL equations, are described in the ALTA software. Those acceleration models were combined with the Weibull distribution model to characterize the lifetime of TPU encapsulants as a function of stress and aging time. The CDFs of acceleration–Weibull models are given as follows:

$$F(t) = 1 - e^{-\left(\frac{t}{\exp(A_0 + A_1 V)}\right)^{\beta}} \tag{1.21}$$

$$F(t) = 1 - e^{-\left(\frac{t}{A_0 \exp\left(\frac{A_1}{V}\right)}\right)^{\beta}} \tag{1.22}$$

$$F(t) = 1 - e^{-\left(\frac{t}{\frac{1}{V}\exp\left(A_0 + \frac{A_1}{V}\right)}\right)^{\beta}} \tag{1.23}$$

$$F(t) = 1 - e^{-\left(tA_0 V^{A_1}\right)^{\beta}} \tag{1.24}$$

where Eqs. (1.21)–(1.24) are the CDFs of exponential–Weibull, Arrhenius–Weibull, Eyring–Weibull, and IPL–Weibull models, respectively. V represents stress, and A_0 and A_1 are model parameters. The model parameters and maximum log-likelihood values (Λ) estimated from tf50% by using the ALTA software are listed. According to the mathematical background for the maximum loglikelihood method, the acceleration–life distribution model achieves a better fit to accelerated failure times since the values are higher. Therefore, the Arrhenius–Weibull model was determined for the lifetime prediction of TPU encapsulants, as it shows the highest value among the models examined. According to the CDF plot for tf50% of TPU encapsulants calculated from the Arrhenius–Weibull model (lines) and the CDF plot obtained from tf50% (filled symbols), the result indicates that the CDF plot predicted by the Arrhenius–Weibull model achieved a reasonable fit with

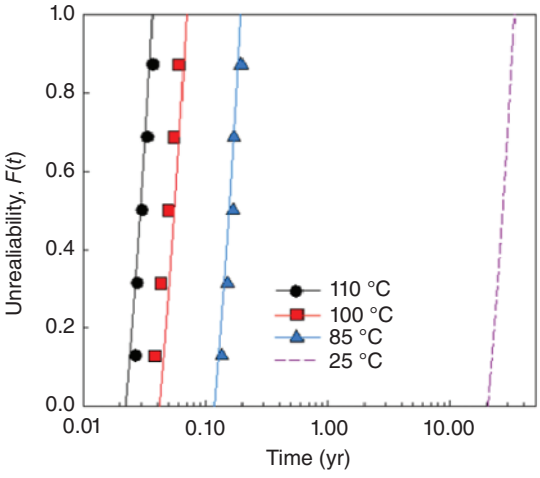

Figure 1.19 Plots for tf 50% of TPU encapsulants calculated by the Arrhenius–Weibull model (lines) and the plots obtained from tf 50% of TPU encapsulants (filled symbols). Source: Reproduced from Choi et al. [175]/with permission of Elsevier.

experimentally obtained accelerated failure times of TPU encapsulants. The CDF plot for tf50% of TPU encapsulants at room temperature (25 °C) calculated by the Arrhenius–Weibull model (dashed line) was examined to characterize the lifetime of TPU in seawater at the use-stress level. The failure rate of TPU encapsulant at 25 °C increases significantly when the aging time reaches approximately 20 years. This result indicates that the tensile strength of TPU encapsulant decreases to 50% in seawater in at least 20 years, and failures can occur. The time required for *x*% of failure of TPU encapsulants (B*x*% lifetime) was estimated by using ALTA software. B10%, B50%, and B90% lifetimes refer to the time at which 10, 50, and 90% of TPU encapsulants will have failed in seawater, respectively. The B*x*% lifetimes of TPU encapsulants in seawater at failure criteria for 50, 60, 70, and 80% of the initial tensile strength were calculated from the CDFs for tf50%, tf60%, tf70%, and tf80%, respectively. The B*x*% lifetimes increased as the percentage of the initial tensile strength was examined as the failure criterion decreased. For instance, the B10% lifetimes for the failure criterion corresponding to 70% of the initial tensile strength (5.07 years) is approximately twice as higher as that for 80% of the initial tensile strength (2.68 years). This result indicates that the B*x*% lifetime varies depending on the failure criterion, so the failure criterion should be carefully determined. We determined the B*x*% lifetime for the 50% decrease in the initial tensile strength as the lifetime for TPU encapsulants in seawater, which is widely chosen as the failure criterion for elastomers and rubbers, according to ISO 11346. The B50% lifetime for the failure criterion for 50% of the initial tensile strength is 27.31 years, indicating that half of TPU encapsulants will fail in seawater 27.31 years later [175] (Figure 1.19).

NR-based blends, which have excellent resilience, are commonly used in industrial applications, for example in tires and resistant products. These types of blends are generally compounded by mixing NR and butadiene rubber (BR) to satisfy both tensile and fatigue characteristics. However, rubber hardens when exposed to sunlight and oxygen for a long period of time. As aging occurs, the tensile properties and the strain-energy density (SED) function of the rubber products

change, greatly reducing the safety of industrial equipment in contrast to the initial design conditions. The mechanical properties directly affect the performance of rubber products, so research at the development stage is very important. Therefore, in the design stage, it is important to evaluate the physical changes due to the aging characteristics. In general, the exposure of rubber to real conditions for a long time is the most accurate method for evaluating the aging property; however, this is difficult to conduct realistically in terms of time and cost. Therefore, in most product-development stages, accelerated test methods are mainly used, which are tested with aged rubber material under severe conditions [178]. The physical-property change parameters for the aged rubber are typically evaluated using the hardness, tensile strength, permanent set, and elongation. However, as the mechanical behavior is only apparent through experimental analysis and cannot demonstrate the fundamental reaction of the aged rubber, researchers have attempted to evaluate the aging characteristics using the crosslink density. Furthermore, only a few experiments and tendencies were studied; studies analyzing the organic relationship of changes in the mechanical (stress–strain curves, SED, etc.) and chemical (cross-linked structure, crosslink density, etc.) properties are lacking. A swelling test was performed to analyze the relationship between the SED, obtained by a mechanical experiment, and the crosslink density, obtained by a chemical experiment. The swelling test results were substituted into the Flory–Rehner equation to obtain the crosslink density, and an equation assuming the crosslinked structure as a spring model was presented. Finally, the relationship between the SED and the crosslink density was summarized as a formula, and a method for predicting the aging behavior of NR/BR blends using the crosslink density was proposed. A master curve that can predict the behavior of the SED function, based on the results of previous experiments was proposed. By deriving a SED function with a specific aging temperature or aging time, we can predict its behavior under all conditions with the equivalent aging conversion using the Arrhenius Eq. (1.21), where R is a constant (8.314), t is a time, and T is the absolute temperature. The exponent value (n) is selected as 1.69, using the average, and the constant value (k) affecting the SED function is fitted to the arc tangent and expressed as (1.22). Finally, the Arrhenius equation is substituted into Eq. (1.22) to derive the aged master curve as Eq. (1.23). In addition, by substituting (1.20), which shows the relationship between the crosslink density and the SED constant, into the SED function, the crosslink-density master curve is derived as Eq. (1.24) [179] (Figure 1.20).

Finally, the experimental results were compared with the predicted SED function using the master curve. The SED function was derived by substituting the average temperature (17 °C) and the number of days (365, 730 days) into the aged master curve [6]. The crosslink density of the aged specimen at room temperature was substituted into the crosslink-density master curve [7], and the SED function was derived and compared. It was confirmed that the real test results were within 2.3% of the mean error when predicted using the aged master curve and within 5.8% of the mean error when predicted using the master density curve [180] (Figure 1.21).

A swelling test for accelerated-aged and room temperature-aged specimens was performed to obtain the crosslink density of the NR/BR blends. The results

$$T_1 = f_1(T_2, t_2) = \frac{T_2(294.3 \cdot l_n(t_2) + 292.2)}{1125 - 0.0867RT_2(2.83 - l_n(t_2))} \quad (6)$$

$$f_2(T_1) = 1.32 - 0.39 \times tan^{-1}\left(\frac{355 - T_1}{16}\right)$$

$$SED = f_2(T_1) \cdot \varepsilon^{1.69} \quad (7)$$

$$SED = [1.32 - 0.39 \times tan^{-1}\left(\frac{355 - f_1(T_2, t_2)}{16}\right) \cdot \varepsilon^{1.69} \quad (8)$$

$$SED = [0.514 + 0.00818 \times v] \cdot \varepsilon^{1.69} \quad (9)$$

Figure 1.20 Process of predicting the behavior of the SED function.

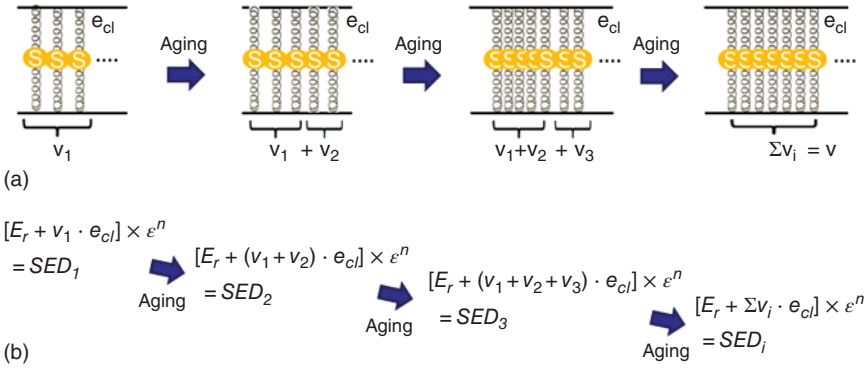

Figure 1.21 (a) Crosslink density expressed as a parallel spring model. (b) SED function expressed as a parallel spring model. Source: Reproduced with permission of Moon et al. [180]/MDPI/CC-BY-4.0.

confirmed that the rubber properties affected the mechanical properties, based on the chemical change due to aging. As the aging progressed, the SED and the crosslink density increased. Therefore, we assumed that the increase in the crosslinked structure was a parallel connection model to the spring, and a linear relationship was found between the SED and the crosslink density. We proposed a method for predicting the aging characteristics of NR/BR blends using a swelling test by summarizing the relation between the SED function and the crosslink density. By using this method, we derived an aged master curve that could obtain the behavior of the SED function according to the aging and the strain condition and a crosslink-density master curve that could predict the behavior of the SED function by the swelling test. When the experimental and predicted values were compared, it was confirmed that the SED value predicted using the aging master curve had a mean error of 2.3% or less, which was highly effective. The tensile properties of rubber and the behavior of the SED function could be predicted by aging. Therefore, it is possible to design in advance for the safety of mechanical

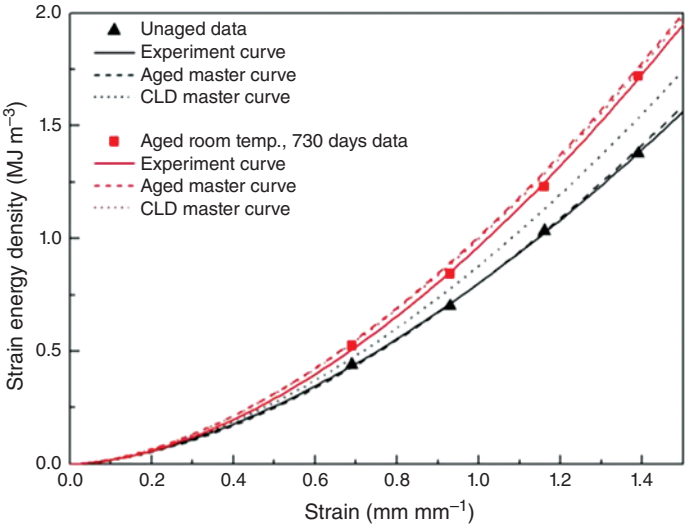

Figure 1.22 Master curve and validation. Source: Reproduced with permission of Moon et al. [180]/MDPI/CC-BY-4.0.

equipment, tires, etc. In addition, the sustainability can be evaluated by predicting the SED by measuring the crosslink density of NR/BR blends (Figure 1.22).

MPs have become an emerging new pollutant of rising concern due to the exponential growth of plastics in consumer products. Most MP and NP pollution comes from the fragmentation of plastics through mechanical stress, chemical reactions, and biological degradation that occur during use and after disposal. MPs and NPs can be fragmented from macroplastics through mechanical degradation, a process that can be accelerated by chemical and biological weathering. MP fragments have been found to undergo further degradation under UV solar radiation, followed by chemical, thermal, and biological changes that weaken the plastic and may accelerate the release of additives [179].

To simulate mechanical stress, a custom abrasion setup was created as previously described in Bossa et al. and NIST SOP and is briefly summarized here. A weight presses down on a rod, providing a normal force on the plastic sample attached to the bottom of a plate. The power input to the abrasion process can be characterized in a scalable fashion through knowledge of this normal force and the torque measured on the rotating abrading element. The sample is pressed onto the abradant and is enclosed in the space, allowing for abraded MPs to be collected for further analysis. The abrasion rate was measured by weighing the sample before and after one minute of abrasion, changing the weight applied to the sample (from 0.1 to 3 kg), and keeping speed constant around 800 rpm. Aluminum oxide sandpaper (P100) was used as the abradant and was attached to the lower plate. After cleaning out the inside of the machine and placing the machine under a hosed fume hood, collectors were placed for the abraded MPs. The sandpaper was changed after every test to ensure that it is not too worn down. Using the value of torque measured produced on the stem of

the sample holder attached to the motor, and the normal gravitational force from the top weight, power input was calculated. Abrasion rates were measured over a range of power input from 0 to 50 W.

When the polymers were abraded, particles were generated from the abrasion testing method. The particles for each plastic were then characterized via size and shape in order to see if they would be indicative of how they were abraded or of the material and if they were comparable to MPs collected in field samples. Volume distributions of the abraded materials are summarized for the six plastics. The volume distribution of abraded nylon particles, with a mode of about 200 μm, differed most from the other plastics, which tended to have a mode of approximately 100 μm [177]. The particle sizing method does not allow for the detection of any possible nano-scale fraction in the abraded material. As described below, Nylon produced some fibrous abrasion products that may not be adequately represented as a spherical equivalent as implied by the measurement technique. The SEM images show the relative size distributions and shapes of the MPs produced. The most distinguishable results are the fibrous shapes of the nylon MPs and the spherical "eraser-shaving" particles from the TPU polymer (Figure 1.23).

It brings into scope that more use tests have to be performed with this new standard operating procedure on future polymer products in order to better understand their breakdown during use and in the environment. Studies on the breakdown from MPs into smaller NPs will also be important to better understand fragmentation in the environment and during use. This is especially true with the increasingly popular TPUs. Also, weathering of polymers and their abrasion rate can once again improve models. In the future, abrasion tests after environmental degradation and exposing to UV, hydrolysis, and other environmental chemical exposures should be investigated. More future tests need to be done on plastic products with additives, such as

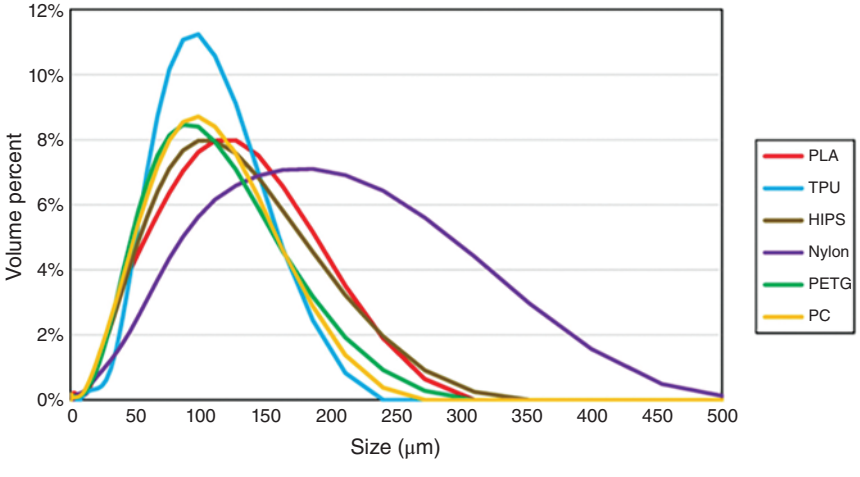

Figure 1.23 TPU microplastic particle size distribution. Source: Reproduced from Sipe et al. [177]/with permission of Elsevier.

nanomaterials, in order to try to estimate their release and if they impact abrasion and release in consumer products.

1.3.2.3 Fibers-Derived Microplastics

Fibers are fine filamentary substances, natural or synthetic. In modern life, fibers are used everywhere. Fibers are substances consisting of continuous or discontinuous fine filaments. In plants and animals, fibers play an important role in maintaining tissues. Fibers are used for a wide range of purposes and can be woven into fine threads, threads, and twine and into fiber layers when making paper or weaving felts; they are also commonly used to make other materials and to form composites with other materials. The chemical composition of synthetic fibers and natural fibers is completely different, some synthetic fibers do not contain cellulose or protein substances such as petroleum, coal, natural gas, limestone, or agricultural by-products. The production of synthetic fibers involves first synthetic units, and then followed by chemical synthesis and mechanical processing methods. Examples of synthetic fibers are polyester fibers (polyester), PA fibers (nylon or nylon), polyvinyl alcohol fibers (vinylon), polyacrylonitrile fibers (acrylic), PP fibers (polypropylene), and PVC fibers (chlorine spandex). Fiber-forming polymers are linear polymers (tensile orientation), and the polymers are easily stretched along the longitudinal direction of the fiber arranged in an orderly manner. When the fiber is stressed, the macromolecules can simultaneously withstand the force so that the fiber has a high tensile strength and suitable elongation, while maintaining flexibility in the direction perpendicular to the longitudinal axis of the fiber. Fiber-forming polymers have a suitable relative molecular weight (processing and physical and mechanical properties); very high relative molecular weight is not suitable for spinning processing, whereas very low physical and mechanical properties are not good. Most fiber-forming polymers contain polar side groups (interaction, moisture absorption, dyeing, and thermal properties), and the presence of polar groups has a great impact on intermolecular chain interactions, fiber moisture absorption, thermal properties, and dyeing [181]. The stronger the intermolecular force, the greater the fiber strength. Meltability or solubility (processing methods) is the ability to melt or dissolve polymers into a melt or solution, spinning, cooling, or solidifying into fibers. The general requirement is a semicrystalline structure of the polymer (comprehensive performance): the presence of crystalline areas enhances its strength and modulus, whereas the presence of noncrystalline areas provides the fiber with a certain degree of elasticity, fatigue resistance, and can be dyed; the semicrystalline structure can fix the original irregular arrangement of molecular chains, during processes like spinning and drawing, these chains orient along the fiber axis to achieve an orderly arrangement and becomes fixed in this state.

PET is a thermoplastic polyester formed by polymerizing terephthalic acid and ethylene glycol; it shows excellent mechanical properties and thermal stability, which make it widely used in textile fibers. Polyester fiber, commonly known as "polyester." This synthetic fiber is made by spinning polyester condensed from organic diacids and diols, referred to as PET fiber, which is a polymer compound. Invented in 1941, it is the first major variety of synthetic fiber [182]. The biggest

advantage of polyester fiber is good wrinkle resistance and conformability, with high strength and elasticity recovery ability. It is firm and durable, wrinkle resistant and non-iron, and non-stick lint. As a textile material, polyester staple fiber is suitable for pure spinning, and can also be suitable for blending with other fibers, not only with natural fibers such as cotton, hemp, and wool but also with other chemical staple fibers such as viscose fiber, acrylate fiber, acrylonitrile fiber, and other short fibers. Its pure spinning or blending form is made of imitation cotton, imitation wool, and imitation linen fabric and generally has the original excellent characteristics of polyester fiber, such as fabric wrinkle resistance, pleat retention, dimensional stability, wear resistance, and washability, and some of the original shortcomings of polyester fibers are static electricity in the textile processing and dyeing difficulties, poor sweat absorption and breathability, easy to melt into a cavity when encountering a spark. To improve these shortcomings, polyester can be mixed with hydrophilic fibers to a certain degree To a certain extent, polyester can be reduced and improved. Polyester twisted filament (DT) is mainly used to weave a variety of imitation silk fabrics, can be interwoven with natural fibers or chemical staple fiber yarn, can be interwoven with silk or other chemical fiber filaments. These interwoven products maintain a series of advantages of polyester. Polyester-deformed yarn (mainly low-stretch DTY) is the main species developed in China in recent years. It differs from ordinary filaments in its high fluffiness, large curl, strong hairiness, softness, and high elastic elongation (up to 400%). The fabric woven with it has good warmth, excellent coverage and drapability, soft luster, etc. [183]. It is especially suitable for weaving imitation tweed, beech, other suit fabrics, outerwear, coats, and various decorative fabrics such as curtains, tablecloths, and sofa fabrics. Polyester air deformation silk (ATY) and network silk shows good huggability and smoothness, and it can be directly used in the form of tube silk on water jet looms, making them suitable for weaving simulation silk and thin fabrics. These can also be woven into thick fabrics. Polyester fibers in industry, agriculture, and new technological applications are also widespread, such as cords, conveyor belts, ropes, and electrical insulation materials. Polyester strong yarn has high strength and initial modulus, good heat resistance, fatigue resistance, and morphological stability, and is especially suitable for spinning tire cord. Using polyester cords ino tire manufacturing can reduce the flat spot phenomenon.

1.3.2.3.1 Influence Factors of Microplastics Generation In the processing, storage, and use of polymer materials, a phenomenon called "aging" occurs where its physical and chemical properties gradually deteriorate due to the combination of internal and external factors. This leads to the final loss of its utility value PET is a semicrystalline polyester material. Its molecular chain mainly contains benzene ring, ester bond, methylene fatty chain, end shuttle group, and end warp group, and the degradation (or cross-linking) of polyester materials and the breakage of chemical bonds (and generation). Therefore, the greater the bond energy of the chemical bonds that make up PET, the more stable the polyester material is and the more resistant it is to aging. In the polyester PET macromolecule, the bond energy between C=O is the weakest. In the presence of external environmental factors, such as UV light, heat, oxygen,

and water can lead to the breakage of the ester bond and then the degradation of PET macromolecule. PET macromolecules in the presence of moisture undergoes bond hydrolysis, and its hydrolysis process is accelerated with the increase in temperature, and in long-term exposure to high temperature and hot and humid environments. Sammon C et al. investigated the hydrolysis process of PET films in pure water and 1% KOH water solution by FTIR above its glass transition temperature (90 °C), and showed a strong degradation behavior after 4–8 days in pure water, whereas in 1% KOH water solution in less than 2–4 hours. The endopolycool process initiate the degradation of PET molecules. Specifically, the nucleophilic reagent, OH, attack the carbonyl carbon (C=O) on the PET macromolecule to form an unstable tetrahedral intermediate, which is hydrolyzed and broken to form the terminal carboxyl portion and the hydrocarbon-containing portion [184].

The thermal degradation of polyester PET is inevitable and the degradation process is quite complicated during the actual polyester processing and molding and its application. Foti S. et al. and Montaudo G. et al. investigated the pure thermal degradation mechanism of polycool PET macromolecules by direct thermal analysis by mass spectrometry technique and concluded that the thermal degradation of PET macromolecular interchain occurs first in the breakage of β-methylene; specifically, the β-methylene. The H atom on the β-methylene group undergoes cyclization, which leads to decomposition of the terminal carboxyl group and a terminal vinyl group. In addition to the breakage of interchain ester groups, the breakage of interchain C—C bonds may also occur between polyester PET chains. One of the interchain thermal degradation reaction products, end-vinyl polyesters, will be further degraded into polyesters containing end-carboxyl groups with small molecule products such as CO_2, and other small molecules at high-temperature state. The thermal oxidative degradation products of PET are very similar to its thermal degradation products; however, the thermal-oxidative aging process is more complicated by the influence of, for example, oxygen, heat, and trace impurities. Oxygen first generates peroxides in the polymer interchain or chain end active centers, and then the free radical chain reaction mechanism eventually leads to cleavage of the PET from the interchain or chain end regions. The thermal oxygen degradation process is shown in Figure 1.25. After oxidation of PET macromolecule (RH), —ROOH is first generated, and —ROOH is further decomposed into RO— and OH or R and OOH, where the generated RO— reacts with RH to generate ROH and R, and R can undergo free radical chain reaction and further decompose into end-vinyl polyesters and end-radical-containing polyesters [185] (Figures 1.24–1.26).

1.3.2.3.2 Microplastics Generation Kinetics of Fiber The service life of many materials is often decades long, and data cannot be obtained by natural environment exposure or natural environment simulation exposure experiments alone, so it is necessary to conduct accelerated life tests in a simulated environment and to establish a methodology for service life prediction. The basic idea of material service life prediction is to use various research tools and experimental data, such as natural environmental exposure, accelerated laboratory exposure, and degradation mechanism analysis, to establish communication channels between information sources and to

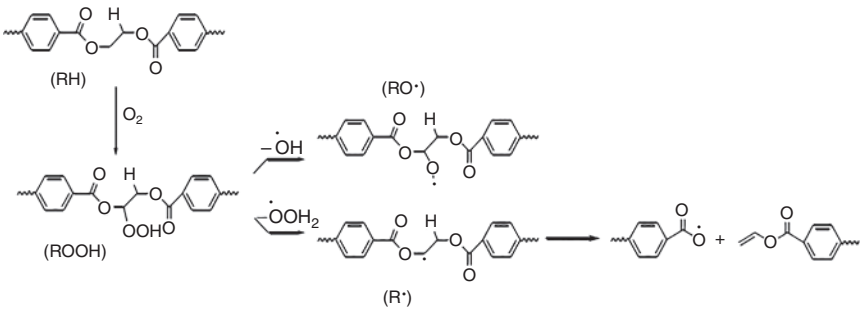

Figure 1.24 PET interchain degradation mechanism.

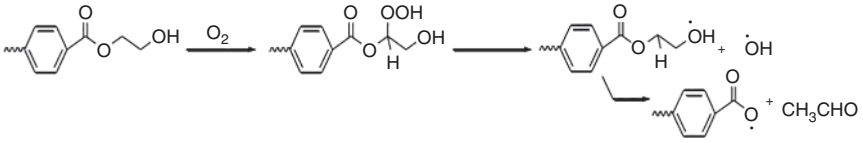

Figure 1.25 PET chain end thermal oxygen degradation mechanism.

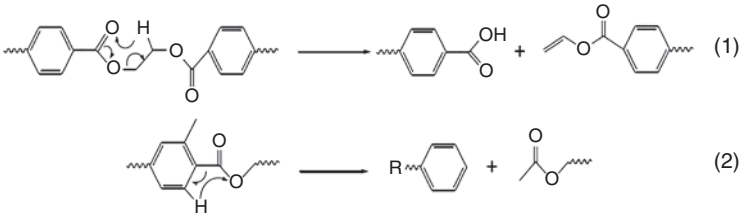

Figure 1.26 PET degradation mechanism.

integrate them using modern statistical analysis methods, so as to establish material life prediction models. The reliability indexes are calculated and compared with the extrapolated reliability indexes based on the accelerated experiments using the measured data from the natural environmental exposure experiments to determine the prediction accuracy of the model. Finally, the established models are applied to production practices such as selecting materials and their constituents to improve the system service life. Using the life data obtained at each accelerated stress level, the analyst is able to use standard life data analysis techniques to extrapolate the parameters of the life distribution (e.g. Weibull, exponential, or log-normal distribution) at each accelerated stress to best fit the data at each stress. This result will lead to a probability density function at each accelerated stress level [186]. In addition, based on the probability density function characteristics at each accelerated stress level, a mathematical model, i.e. the life–stress relationship, is used to infer the probability density function under normal use conditions. The lifetime characteristic can be any lifetime measure, such as the average or median lifetime, expressed as a function of stress. A life–stress relationship model must be selected so that it is appropriate for the type of data being analyzed. Commonly used life–stress relationship

models include Arrhenius, Allen, and inverse power-law models. These models are designed to analyze one type of stress data (e.g. temperature, humidity, or voltage). The Arrhenius model is the most typical and widely used acceleration model, with the expression given by.

$$L(V) = Ce^{\frac{B}{V}} \tag{1.25}$$

Clothes also contain MPs. Clothes comprise polyester, nylon, and microfiber. The fiber from clothing is also a kind of MP that contributes large quantities to MP pollution through washing processes. According to De Falco et al. [60], around 124–308 mg kg^{-1} of microfiber is separated from clothes during washing; the average length and diameter of this microfiber are 360–660 and 12–16 μm, respectively. Henry et al. reported that the effluent from laundry is a substantial source of microfiber released into the environment. Small-sized microfiber can pass through the wastewater treatment system and accumulate in the marine area.

Several studies have provided evidence of polymers being shed from synthetic fibers, such as nylon, polyester, and spandex, during cloth washing. This type of polymer can be cracked by the pressure of washing machines and can produce microfibers. The average amount of microfibers produced from washing activities is 100 items/discharged water, with around 100 particles of MPs being produced per kilogram of washed cloth. Fleece is the highest producer of MP fibers among all cloth materials. Filter utilization is effective in reducing the escaped number of MPs from washing activities.

The process of cloth washing releases not only MPs into the aquatic ecosystem but also MPs into the air. MPs in the air are suspected to originate from the drying process of clothes after washing. The abundance of MPs as microfiber particles in indoor environments reaches up to 1–60 particles m^{-3}, whereas outdoor abundance is slightly lower, with 0.3–1.5 particles m^{-3}. The study conducted by Dris et al. [60] found that the average deposition of MPs in air is 190–670 microplastics as microfibers/mg of collected dust.

1.3.2.4 Foam-Derived Microplastics

Foam is a type of polymer material formed by a large number of gas micropores dispersed in solid plastic and has several advantages such as light weight, heat insulation, sound absorption, shock absorption, and other characteristics, and dielectric properties better than base resin. Almost all kinds of plastics can be made into foam; foam molding has become an important area of plastics processing. Foam is also called porous plastic. It is a plastic with numerous micropores inside made of resin as the main raw material. It is light, heat-insulating, sound-absorbing, shockproof, and corrosion-resistant. These are soft and hard. It is widely used for heat insulation, sound insulation, packaging materials, and car and boat shells. Compared with pure plastic, foam has low density, light weight, high specific strength, and its strength increases with density, the ability to absorb impact loads, excellent cushioning and shock absorption performance, sound insulation and sound absorption performance, low thermal conductivity, good thermal insulation

performance, excellent electrical insulation performance, corrosion resistance, and mold resistance performance. Soft foam has excellent elasticity and other properties. Plastic has many tiny pores inside. It is made by mechanical method (air or carbon dioxide is introduced while mechanical stirring to make it foaming) or chemical method (foaming agent is added). There are two types: closed pore type and open pore type. In the closed-cell type, the pores are isolated from each other and float; in the open-cell type, the pores are connected to each other and do not float. It can be made of PS, PVC, PU, and other resins [187]. It is a widely used material for thermal insulation and sound insulation. The advantages of foam are very low weight, can reduce the weight of packaging, reduce transportation costs, has excellent shock and vibration energy absorption, used for cushioning in shockproof packaging, which can greatly reduce product damage, temperature and humidity changes in adaptability can meet the requirements of the general packaging; with low water absorption, moisture absorption, and chemical stability, foam itself will not produce corrosion of the contents, and is resistant to acids, alkalis, and other low thermal conductivity, which makes it suitable for thermal insulation packaging, such as ice cream cups, fast food containers, and insulated fish boxes. It is easy to be molded and processed, and can be made into various foam liners, foam blocks, and sheets by molding, extrusion, and injection methods. Easy to secondary molding processes, such as foam sheets by thermoforming, can be made into a variety of items, such as fast food containers. In addition, foam blocks can also be bonded with adhesives or bonded with other materials to make a variety of products such as cushion liners [188].

Expanded polystyrene (EPS) is a common plastic marine debris found in oceans worldwide. The unique "foamed" structure of EPS, which is composed of thin layers, makes it more vulnerable to fragmentation than bulk plastics. Foamed PS that may be either expanded or extruded is a rigid, lightweight, insulating thermoplastic that has a variety of use in consumer products, packaging, construction, and marine sectors. The properties of the material also result in waste that is readily generated, dispersed, and fragmented into the environment. In the ocean, foamed PS is subject to wind-assisted transport and fracturing via photolytic degradation. The material may also act as a substrate for rafting organisms while being exposed to elevated concentrations of natural and anthropogenic surface-active chemicals in the sea surface microlayer. In the littoral setting, fragmentation is accentuated by milling in the swash zone and abrasion when it is beached. Wind transport further leads to the temporary burial of significant quantities of materials. PS is a rigid, amorphous thermoplastic produced by free radical vinyl polymerization of styrene. The structure of the polymer can be written as: $[CH_2CH(C_6H_5)]_n$, where C_6H_5 is a pendant phenyl group, which restricts rotation and is responsible for many of the physical and mechanical properties of the polymer. Both expanded PS and extruded PS (XPS) are forms of polymer that contain a high proportion of air (>95%). EPS is produced when the raw, pelletized material is expanded by heating with steam to form cellular beads. Dried particles are then fused under steam and molded into blocks or other shapes, with beads of 2–5 mm in diameter clearly visible in the final product. The air

within and between the beads gives EPS its insulating properties; however, interparticle air, as irregular gaps or voids, renders the material susceptible to (limited) water absorption. XPS is formed when PS crystals, additives, and blowing agents are extruded at high temperatures to produce a frothy liquid that is subsequently shaped in a die as it cools and expands. XPS consists of tightly packed cells that have no gaps or voids between them. This closed structure inhibits water absorption and results in a smoother surface and a higher density than EPS. Note that Styrofoam is often used synonymously with foamed PS but is strictly a trademarked brand of XPS produced for building insulation by Dow Chemical company. Foamed PS is commonly employed in home and appliance insulation, protective packaging, automobile parts, embankment filling, lightweight concrete (as an aggregate), and food packaging; with regard to the construction sector, XPS is favored over EPS where pressure, stability, and humidity are especially high. The durability, low density, and insulating properties of foamed PS have also resulted in many applications in the marine sector. Here, EPS (and less frequently, XPS) are used in fish boxes, buoys, pontoons, floating docks, net floats, life jackets, surfboards, and boat stands [189]. As a tethered floating base, EPS is used directly or for greater durability, it may be coated or covered by hard plastic or cement. Loss of foamed PS to the environment may occur via the transport, storage, or cutting of construction material, escapement of waste from controlled and historical landfill, storage or compaction of waste before or during disposal or recycling, deterioration or loss of structures in situ, and littering and fly-tipping. Waste enters the marine environment through rivers, stormwater, and WWTPs, and from direct littering and loss or structural damage at sea or in the littoral zone. Foamed PS not only is a significant contributor to marine litter worldwide, but also its lightweight and low density, ready transportation by the wind, and propensity to readily fragment, ensure that it disperses more widely and rapidly than other forms of (unfoamed) plastic, both at sea and when it is beached. With small fragments readily blown around by the wind when dry and adhering to surfaces when wet, foamed PS is also particularly difficult to retrieve during beach cleans.

1.3.2.4.1 Influence Factors of Microplastics Generation UV irradiation incorporated a large amount of oxygen functional groups (OFGs) on the PD–PS surface. The OFGs could be generated following the cleavage of C—H bonds (tertiary C atom), hydrogen abstraction of peroxy radicals (—$COO^{\cdot}$), disproportionation of alkoxy radicals (—$CO^{\cdot}$), and consecutive oxidation driven by free radicals. The persistent O-centered free radicals with a g-factor of 2.0043 (e.g. $CO^{\cdot}$, $COO^{\cdot}$) were observed on EPS. This resulted from the electron transfer initiated by the peroxides and chromophoric OFGs (e.g. C=O, O=C—H) on the polyconjugated aromatic PS matrix. Moreover, the surface wettability was transformed from hydrophobic to hydrophilic in EPS. UV exposure likely caused the release of low-molecular-weight fragments from degradation of PS backbone due to chain scission triggered by peroxy radicals [190]. The release of these organic chemicals from irradiated plastic particles could accelerate the structural fragmentation, leading to generation of mesoporous/micropores and size reduction during photooxidation. Overall, photodegradation MPs led to matrix structural collapse, size reduction, nanoparticle

production, surface oxidation, formation of persistent O-centered free radicals (PFRs), and release of endogenous pollutants.

The chemical mechanism (Figure 1.27) for the degradation of EPS products to generate MPs was deduced [86]. During thermal aging, the energy of heat is not enough to break the C—C bond and no radicals are generated to react with oxygen in the air for oxidative degradation; hence, there are no changes in morphological and structural changes of thermos-aged EPS. In general, chromophore groups such as phenyl group (Ph—) and alkylene (—C=C—) in macromolecules are responsible for initiating photochemical reactions. When exposed to UV irradiation, the benzene ring absorbs light quantum, generating PS in the excited singlet state, and then the excited state is transferred to the triplet state through intersystem crossing. Through intramolecular energy transfer, the excitation energy of the triplet state can be transferred to C—H bond, causing it to break and generate tertiary alkyl radicals ($C^{\cdot}$). The tertiary alkyl radicals are relatively more reactive and easily react with atmospheric oxygen to form the peroxyl radicals ($COO^{\cdot}$), which combine with the dissociated hydrogen proton ($H^{\cdot}$) to generate the hydroperoxide groups. Subsequently, after cleavage of hydroxyl radicals ($^{\cdot}OH$) from hydroperoxide groups, alkoxyl radicals ($CO^{\cdot}$) are formed, which dominate under UV irradiation exposure [191]. Alkoxy radicals can be decomposed by β fracture to generate carbonyl compounds. Disproportionation of alkoxy radicals leads to chain breakage in the polymer backbone and forms primary alkyl radicals and carbonyl radicals ($O=C^{\cdot}$). After being continuously oxidized, small molecular degradation chemicals such as aldehydes, ketones, and acids can be generated eventually. At the same time, the primary alkyl radicals and the alkoxyl radicals undergo radical termination and combine with each other to form an ester bond (C—O—C). With further oxidation, O—C=O groups are further generated through Norrish type I reaction and Norrish type II reaction, which mainly take place in the co-aging process. In a word, UV irradiation and heat synergistically work on EPS to cause a continuous deep photo-thermal oxidative degradation.

1.3.2.4.2 Microplastics Generation Kinetics of Foam Some studies have suggested that plastic bags and containers can take hundreds to thousands of years to be mineralized by biodegradation. Based on our previous laboratory study, tens of thousands of MP particles were produced from a plastic pellet following UV exposure and/or subsequent mechanical abrasion with sand within a few months. Other laboratory weathering experiments have confirmed that the formation of small plastic particles increases with increasing UV exposure time and that it is possible for nanosized plastic particles to be produced by only UV exposure. Once plastic items are exposed to the environment, they start to degrade and can generate NPs and MPs by photodegradation before their complete mineralization in the environment; however, there is lack of information about the fragmentation process, including how quickly and how many NPs and MPs are generated by sunlight exposure [192]. It is crucial to determine the fragmentation rate of plastic debris in the environment, especially when developing policies to decide how quickly plastic debris should be collected before it produces secondary MPs and NPs, which are more challenging to remove.

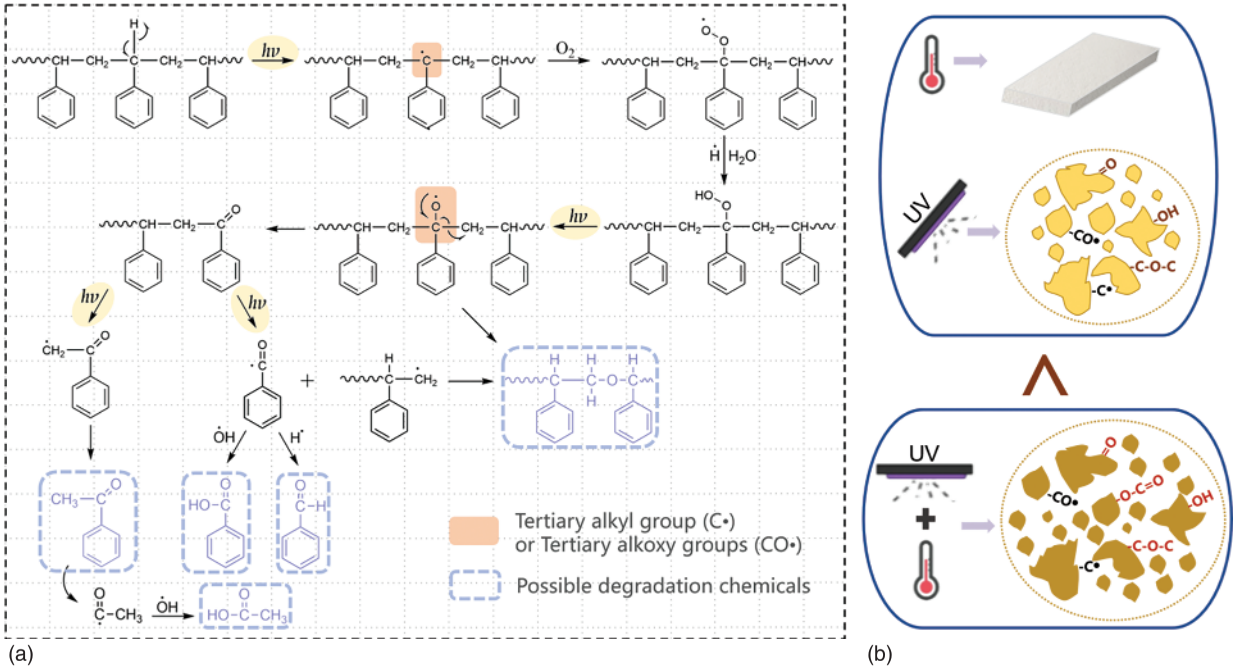

Figure 1.27 Mechanism of MPs generation. (a) Possible degradation pathway of EPS. (b) Comparison of EPS degradation degree after thermal aging, UV aging, and co-aging. Source: Reproduced from Huang et al. [86]/with permission of Elsevier.

Additionally, the fragmentation rate of plastics is an essential input in models used to estimate the emission of secondary MPs and NPs from the standing stock of plastic debris in the environment. However, it is difficult to estimate the fragmentation rate of plastics because fragmentation is a long-term process that occurs over several years of weathering and is dependent on the polymer type and environmental conditions. Based on the previous results, EPS is more vulnerable to UV exposure than PE and PP. MPs and NPs produced from EPS via sunlight exposure were identified, and the particle size distribution was determined [192]. Next, the study evaluated the fragmentation rate of EPS based on the quantitative analysis of both MP and NP particles according to the duration of sunlight exposure over a 2-year outdoor-exposure period. This fragmentation rate of EPS due to sunlight weathering can be applied to estimate the production of secondary MPs and NPs from the standing stock of macro EPS debris exposed to sunlight [188].

The abundance and size distribution of fragmented particles are produced from only the top surface, where they are directly exposed to sunlight without shading effects from the direction of sunlight. For the measurement of weight loss of EPS, particles produced from all five exposed sides, excluding the bottom of the EPS, were collected, and the weights of the samples before and after sunlight exposure were compared. The particles from the surface were collected via the following process: the surfaces of each EPS sample were soaked in a flexible aluminum dish containing 2 ml of ultrapure water to separate the particles [91]. The bottom of each EPS sample, which was the nonexposed area, was handled using only micro forceps while the samples were being washed with ultrapure water. The particles produced from the surfaces were gently washed off and collected in ultrapure water until the white surface of fresh EPS was revealed. The ultrapure water in the aluminum dish containing the particles was directly filtered through a preweighed 0.8 μm polycarbonate filter paper until no particles remained in the dish. The filter papers were dried at room temperature and weighed. The mass of the nanoparticles (Wnano) was calculated using the following equation, based on the PS density (D) and volume (V), the average radius (r), and abundance (A) of the particles, and a value of 0.1 corresponding to a flat shape represents the volume of fragmented particles in each exposure group.

$$W_{\text{nano}}\,(\text{mg cm}^{-2}) = V(0.1 \times 4/3\pi r^3 \text{nm}^3) \times D\,(1.04\text{g cm}^{-3}) \times A\,(\text{particles cm}^{-2})/18 \tag{1.26}$$

The percentage weight loss due to sunlight exposure (before particles were removed from EPS surfaces) and the final weight of an EPS sample after particles were removed were determined using Eqs. (1.27) and (1.28). W_1 is the weight of the original sample (before exposure), W_2 is the weight of the photo-degraded sample (after exposure), and W_3 is the weight of the final sample (after particles were removed from the surfaces).

$$\text{Weight loss \% due to sunlight exposure} = [(W_1 - W_2)/W_1] \times 100 \tag{1.27}$$

$$\text{Final weight (\% EPS remaining)} = [W_3/W_1] \times 100 \tag{1.28}$$

The fragmentation rate of EPS was determined by measuring the number of particles produced from each photodegraded EPS sample as a percentage of its original weight using Eq. (1.29). P_1 is the weight of the particles produced from the surfaces of each EPS sample due to weathering by sunlight (total from five sides of each sample).

$$\text{Amount of particles produced } (\%) = [P_1/W_1] \times 100 \tag{1.29}$$

The weight of air in an EPS sample cannot be ignored because the raw material was composed of 98% air and 2% PS (in volume). The weight loss of air was also determined using Eq. (1.3.2.4.5, where A_b is the weight of the air in an EPS sample before sunlight exposure, and A_f is the weight of the air in the final sample (following the removal of particles from the sample surfaces):

$$\text{Air loss } (\%) = [(A_b - A_f)/W_1] \times 100 \tag{1.30}$$

The weight of air in an EPS sample cannot be ignored because the raw material was composed of 98% air and 2% PS (in volume). The weight loss of air was also determined using Eq. (1.31). A_b is the weight of the air in an EPS sample before sunlight exposure, and A_f is the weight of the air in the final sample (following the removal of particles from the sample surfaces).

To estimate the amount of MPs and NPs produced globally from EPS boxes due to weathering following sunlight exposure, we used the following parametric equation:

$$EMNP1yr = EPS_w \times MNP1yr \tag{1.31}$$

where *EMNP1yr* is the total number of MP and NP particles produced globally from the surfaces of EPS waste by weathering following sunlight exposure for one year, EPS_w is the amount of EPS waste entering the ocean every year from rivers, and *MNP1yr* is the number of MP and NP particles produced from the surfaces of EPS boxes due to sunlight exposure for one year using the fragmentation rate determined in this study. According to the daily irradiance (mE $[cm^2$ day $nm]^{-1}$) updated and validated using solar irradiance reference spectra (0–60° latitude in the Northern Hemisphere), one EPS box with a $10 \times 10\ cm^2$ surface area would produce 1.7×10^{10} to 3.2×10^{10} micro- and nanoparticles for one year. To determine the amount of EPS waste, we used the formula (Figure 1.28):

$$EPSw = (\text{EPS packaging industry})/(\text{Global plastic production}) \times \text{Plastic waste in the ocean} \times 1/0.017 \tag{1.32}$$

The percentage of remaining EPS cube samples compared with the original (on a weight basis) following exposure to sunlight for 3, 6, 7, 9, 12, and 24 months was 96.6 ± 0.44, 93.4 ± 0.32, 91.7 ± 0.06, 85.5 ± 0.78, 79.6 ± 1.61, and $65.8 \pm 1.25\%$, respectively (Figure 1.29). Weight reduction included the weight of the air inside EPS (air loss) and fragmented particles (micro- and nanoparticles), and the weight loss of EPS by direct photodegradation. The liberation of air inside EPS samples according to the duration of sunlight exposure was 0.24 ± 0.03, 0.46 ± 0.02, 0.57 ± 0.00, 1.00 ± 0.05, 1.41 ± 0.11, and $2.38 \pm 0.09\%$ after 3, 6, 7, 9, 12, and 24 months, respectively. The particle production for 3, 6, 7, 9, 12, and 24 months of sunlight exposure was 1.32 ± 0.35, 2.52 ± 0.27, 4.12 ± 0.14, 5.93 ± 0.77, 7.57 ± 1.28,

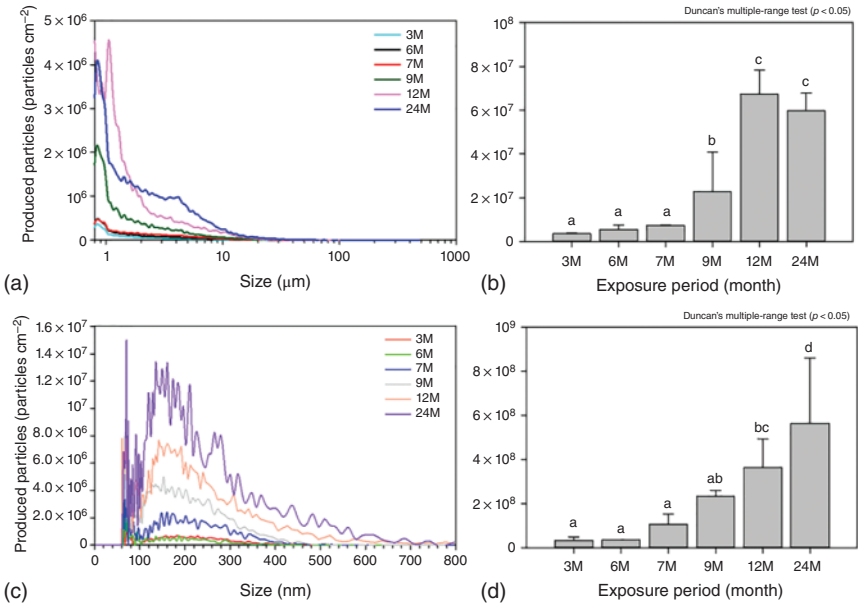

Figure 1.28 Abundance and size distribution of micro- and nano-sized expanded polystyrene (EPS) particles produced by sunlight exposure. (a) Size distribution and (b) the number of micro-sized (0.8–500 μm) EPS particles, and (c) the size distribution, and (d) the number of nano-sized EPS particles according to the sunlight exposure period (3, 6, 7, 9, and 24 months). Source: Reproduced from Song et al. [188]/with permission of American Chemical Society.

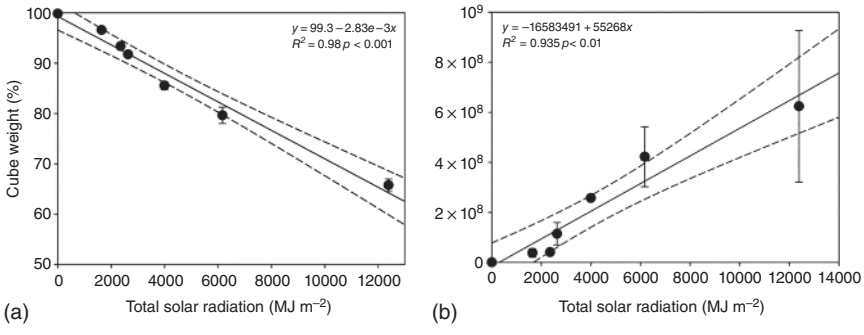

Figure 1.29 Half-life ($t_{1/2}$) of the EPS cube sample and generated particles by solar radiation. The linear regression analysis of (a) the reduced weight of expanded polystyrene cube samples and (b) particles generated by solar radiation. Short dashed lines indicate the range of uncertainty surrounding the true response, with 95% confidence intervals along the horizontal axis. Source: Reproduced from Song et al. [188]/with permission of American Chemical Society.

and $8.08 \pm 0.14\%$, respectively. The weight of nanoparticles (0.009–0.204 μg cm^{-2}) was negligible compared with the weight of microparticles (300–1100 μg cm^{-2}). The "weight loss by sunlight" exposure other than "removed air" and "produced particles" by sunlight exposure for 3, 6, 7, 9, 12, and 24 months was 1.46, 2.46, 2.9, 5.84, 9.89, and 21.34%, respectively [188]. The half-life ($t_{1/2}$) of an EPS cube sample with a $7.9 \pm 1.0\ cm^2$ surface area was calculated from Eq. (1.33). The total solar radiation for the half-life of the sample ($TSIt_{1/2}$) was derived from the linear regression given in Eq. (1.34), which describes the linear relationship between total solar radiation (x) and the weight reduction rate (y) of the sample in countries at the same latitude as Korea. In Eq. (1.34), 50% was substituted into y as the half-life of the sample ($x = TSIt_{1/2}$). The TSI($t_{1/2}$) was divided by the accumulated TSI for one year (TSIy; 4998 MJ cm^{-2}) in the sunlight exposure experiment, and it was estimated that it would take 3.5 years to lose 50% of the EPS weight due to sunlight exposure.

$$t_{1/2} = TSIt_{1/2}/TSIt_y \tag{1.33}$$

$$y = 99.3 - 0.00283x, r^2 = 0.98, p < 0.01 \tag{1.34}$$

The number of micro- and nanoparticles produced per square centimeter by sunlight exposure for one year was calculated by Eq. (1.35). This was derived from the linear relationship between total solar radiation (x) and the number of micro- and nanoparticles produced per area of EPS cube in countries at the same latitude as Korea. The TSIy was substituted into x, and it was found that approximately 25,645 973 micro- and nanoparticles cm^{-2} (y) could be produced in one year (2.6×10^8 particles $cm^{-2}\ year^{-1}$) (Figure 1.30).

$$y = -16583491 + 55268x, r^2 = 0.94, p < 0.01 \tag{1.35}$$

MPs are primarily generated from plastic products by UV irradiation, mechanical abrasion, thermal oxidation, hydrolysis, and biological breakdown. These aging processes will lead to changes in the physicochemical characteristics and mechanical properties, thus accelerating the release of MPs. Once exposed to the environment, aged plastic products will break into MPs under the natural force. By associating plastic aging with decrease in mechanical performance on a time scale

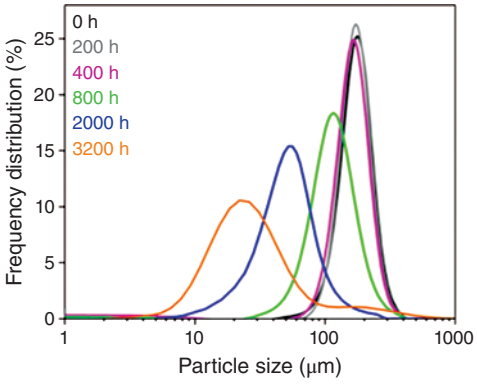

Figure 1.30 Particle size distribution of microplastics with different aging times. Source: Reproduced from Meides et al. [193]/with permission of American Chemical Society.

quantitatively, it is possible to establish an assessment method that simulates and predicts the mechanical properties of aged plastic products in service to prevent generation of MPs in advance [193]. Since natural environments consist of complex and diverse environmental conditions that vary widely, most studies conducted in outdoor environments are only of reference value for a specific single environment. Exploring the effect of different environmental factors and synergistic mechanisms quantitatively in the laboratory can help to gain insight into MPs generation behavior under the dynamic unknown environments. The aging process of plastic products is usually accompanied by the formation of microcracks and leads to a decrease in the mechanical performance of the aged samples, which tends to the propagation of microcracks and the generation of MPs under natural forces. It is essential to establish a mechanical model for predicting the decrease in mechanical properties of aged plastic products in service to prevent MPs. Herein, the one-parameter probability function of the Weibull formula is combined with Hooke's law to establish a formula to fit the stress–strain curve of the material, which can simulate the constant degradation of mechanical properties monitored in experiments [194]. In order to establish the relationship between the decrease in mechanical performance and aging time, the Weibull formula is modified by introducing the time scale t in the characteristic parameter ε_{td}. Thus, the modified Weibull formula is rewritten as follows:

$$\sigma(\varepsilon) = E \cdot \varepsilon \cdot \exp\left\{-\left[\frac{\varepsilon}{(kt+b)}\right]^m\right\} (\varepsilon > 0) \tag{1.36}$$

where t is aging time; k and b are two parameters of a linear function fitted to time using fracture strain. This model can be used to guide the prediction of mechanical properties of other types of plastic products during aging, with a view to predicting and controlling the production of MPs in advance.

1.3.2.4.3 Nanoplastics Generation from Foam Degradation proceeds in two main stages: (i) photooxidation in a near-surface layer and (ii) microcrack formation and particle rupturing. An increasing amount of MP fragments with carboxyl, peroxide, and keto groups is continuously released into the environment. In the case of particle weathering in water, simulated solar exposure and mechanical stress by stirring led to a decrease in particle size. Quantitative particle size measurements show that the decrease in particle size is combined with the broadening of the particle size distributions. The average particle size of the reference sample is ~160 μm, with particle distribution ranging from ~100 to 300 μm. It was observed that 2000 hours of weathering, however, led to a decrease in the average particle size down to 50 μm with particle sizes ranging from ~10 to 200 μm. During the first 600 hours of weathering, we observed a linear decay in size. From 600 hours onward, the trend evolves exponentially with a time constant (τ) of 930 hours. The particle breakdown accelerates, and the particle size reaches 20 μm at 3200 hours [193]. For samples weathered for 2000 hours and longer, the formation of a tail toward large particle sizes is visible within the particle size distributions. This effect is attributed to agglomeration effects as a consequence of the increased surface area and polarity. Within the first 400 hours of exposure, the primarily angular particles developed

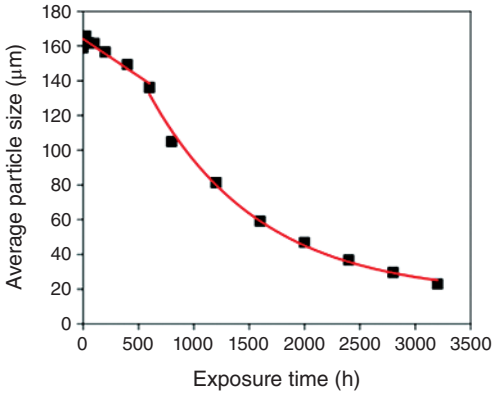

Figure 1.31 Average particle size of microplastics with different aging times. Source: Reproduced from Meides et al. [193]/with permission of American Chemical Society.

smooth surfaces and rounded shapes. Further, thin platelet-shaped fragments were ablated from the particle surfaces. Prominent fractures and deep microcracks became visible beyond 800 hours. After 2400 hours of exposure, fragments <1 μm were observed due to particle disintegration, which adheres to larger particles [188] (Figure 1.31).

EPS fragments were observed on the pellet surface after two months of UV exposure in this study, indicating that UV exposure alone, without MA, was sufficient to break EPS into microsized fragments. Although EPS has unsaturated double bonds that are susceptible to photoinitiated degradation, the foamed structure of EPS may influence both photooxidation and subsequent fragmentation. The depth of UV penetration, diffusion of radicals, and availability of oxygen are critical in the propagation and rate of photooxidation of polymers [195]. The mesoporous structure of EPS could assist photooxidation by facilitating the penetration of UV radiation and diffusion of radicals while increasing oxygen availability. Expansion of PS changes the bulk plastic into a fused small balloon-like structure with a thin PS envelope. The progression of cracks and fusion with other cracks in the thin layer more readily fragmented than the bulk plastic. In addition, the gradual decrease in the CI of the surface of EPS pellets after six months of UV exposure supported the assumption that fragmentation of the surface layer exposed the underlying relatively less oxidized surface. According to polymer type, the size of fragmented particles by chemical and mechanical weathering differed, and the rate of fragmentation was in the order of EPS > PP ≫ PE. The physicochemical properties of polymers determined the degree and rate of weathering and fragmentation in combination with environmental factors. The fragmentation of PE and PP could be impeded by additives, such as UV stabilizers and antioxidants, compared with EPS. Therefore, not only the amount of each polymer is used in production and the polymer composition of marine macroplastic debris but also the weathering and fragmentation characteristics of polymers are critical determining factors for predicting MP abundance in the environment.

In this study, the unaccounted proportion of EPS by volume after 12 months of UV exposure and two months of MA was 76.5% of the parent pellet volume. These results imply that 76.5% of EPS by volume was fragmented into particles that

could not be recovered or detected by using the current analytical method. Even if the recovery rate of PE (100–500 μm) particles was 99.4%, it is possible that the fragmented particles less than 100 μm were lost during the density separation. The low rising velocity of small plastic particles may affect their low recovery. Even at the highest magnification (×1000) of the fluorescence microscope, the smallest discernible NR-stained MPs were several micrometers wide. It is, however, likely that a large proportion of EPS was fragmented into submicron particles [196]. The continuous increase in the number of EPS particles with decreasing particle size to the lowest size class (1–50 μm) supports the existence of submicron particles, which may have been more numerous than the microsized particles. Moreover, the smaller plastic particle fraction increased with exposure time in the laboratory weathering experiment, and NPs formed from five different polymers, including PE, PP, and PS, with only UV exposure in aqueous conditions. Nanosized PS plastics have been frequently used for toxicity tests of MPs and have demonstrated toxic effects at high exposure levels.

References

1 Silva, A.B., Bastos, A.S., Justino, C.I.L. et al. (2018). Microplastics in the environment: challenges in analytical chemistry – a review. *Anal. Chim. Acta.* 1017: 1–19.

2 Wright, S.L., Thompson, R.C., and Galloway, T.S. (2013). The physical impacts of microplastics on marine organisms: a review. *Environ. Pollut.* 178: 483–492.

3 Imhof, H.K., Schmid, J., Niessner, R. et al. (2012). A novel, highly efficient method for the separation and quantification of plastic particles in sediments of aquatic environments. *Limnol. Oceanogr-Meth.* 10 (7): 524–537.

4 Galgani, F., Hanke, G., Werner, S. et al. (2013). Marine litter within the European marine strategy framework directive. *ICES J. Mar. Sci.* 70 (6): 1055–1064.

5 Lambert, S. and Wagner, M. (2016). Characterisation of nanoplastics during the degradation of polystyrene. *Chemosphere* 145: 265–268.

6 Klaine, S.J., Alvarez, P.J., Batley, G.E. et al. (2008). Nanomaterials in the environment: behavior, fate, bioavailability, and effects. *Environ. Toxicol. Chem.* 27 (9): 1825–1851.

7 Sobhani, Z., Zhang, X., Gibson, C. et al. (2020). Identification and visualisation of microplastics/nanoplastics by Raman imaging (i): down to 100 nm. *Water Res.* 174: 115658.

8 Gigault, J., Halle, A.T., Baudrimont, M. et al. (2018). Current opinion: what is a nanoplastic? *Environ. Pollut.* 235: 1030–1034.

9 Cole, M., Lindeque, P., Halsband, C. et al. (2011). Microplastics as contaminants in the marine environment: a review. *Mar. Pollut. Bull.* 62 (12): 2588–2597.

10 Arhant, M., Le Gall, M., Le Gac, P.-Y. et al. (2019). Impact of hydrolytic degradation on mechanical properties of PET - towards an understanding of microplastics formation. *Polym. Degrad. Stab.* 161: 175–182.

11 Chen, Q., Wang, Q., Zhang, C. et al. (2021). Aging simulation of thin-film plastics in different environments to examine the formation of microplastic. *Water Res.* 202: 117462.

12 Xia, B., Sui, Q., Du, Y. et al. (2022). Secondary PVC microplastics are more toxic than primary PVC microplastics to Oryzias melastigma embryos. *J. Hazard. Mater.* 424: 127421.

13 Briain, O.Ó., Marques Mendes, A.R., McCarron, S. et al. (2020). The role of wet wipes and sanitary towels as a source of white microplastic fibres in the marine environment. *Water Res.* 182: 116021.

14 Song, Y.K., Hong, S.H., Jang, M. et al. (2014). Large accumulation of micro-sized synthetic polymer particles in the sea surface microlayer. *Environ. Sci. Technol.* 48 (16): 9014–9021.

15 Mughini-Gras, L., van der Plaats, R.Q.J., van der Wielen, P. et al. (2021). Riverine microplastic and microbial community compositions: a field study in the Netherlands. *Water Res.* 192: 116852.

16 Ambrosini, R., Azzoni, R.S., Pittino, F. et al. (2019). First evidence of microplastic contamination in the supraglacial debris of an alpine glacier. *Environ. Pollut.* 253: 297–301.

17 He, P., Chen, L., Shao, L. et al. (2019). Municipal solid waste (MSW) landfill: a source of microplastics? Evidence of microplastics in landfill leachate. *Water Res.* 159: 38–45.

18 Gouin, T., Cunliffe, D., De France, J. et al. (2021). Clarifying the absence of evidence regarding human health risks to microplastic particles in drinking-water: high quality robust data wanted. *Environ. Int.* 150: 106141.

19 Andrady, A.L. (2011). Microplastics in the marine environment. *Mar. Pollut. Bull.* 62 (8): 1596–1605.

20 Rocha-Santos, T. and Duarte, A.C. (2015). A critical overview of the analytical approaches to the occurrence, the fate and the behavior of microplastics in the environment. *Trends. Analyt. Chem.* 65: 47–53.

21 Liu, L., Fokkink, R., and Koelmans, A.A. (2016). Sorption of polycyclic aromatic hydrocarbons to polystyrene nanoplastic. *Environ. Toxicol. Chem.* 35 (7): 1650–1655.

22 Beckingham, B. and Ghosh, U. (2017). Differential bioavailability of polychlorinated biphenyls associated with environmental particles: microplastic in comparison to wood, coal and biochar. *Environ. Pollut.* 220 (Pt A): 150–158.

23 Hartmann, N.B., Rist, S., Bodin, J. et al. (2017). Microplastics as vectors for environmental contaminants: exploring sorption, desorption, and transfer to biota. *Integr. Environ. Asses.* 13 (3): 488–493.

24 Jovanovic, B. (2017). Ingestion of microplastics by fish and its potential consequences from a physical perspective. *Integr. Environ. Asses.* 13 (3): 510–515.

25 Zhang, K., Hamidian, A.H., Tubic, A. et al. (2021). Understanding plastic degradation and microplastic formation in the environment: a review. *Environ. Pollut.* 274: 116554.

26 Liu, P., Shi, Y., Wu, X. et al. (2021). Review of the artificially-accelerated aging technology and ecological risk of microplastics. *Sci. Total. Environ.* 768: 144969.

27 Li, J., Liu, H., and Paul, C.J. (2018). Microplastics in freshwater systems: a review on occurrence, environmental effects, and methods for microplastics detection. *Water Res.* 137: 362–374.

28 Tunali, M., Adam, V., and Nowack, B. (2023). Probabilistic environmental risk assessment of microplastics in soils. *Geoderma.* 430: 116315.

29 Zhao, K., Wei, Y., Dong, J. et al. (2022). Separation and characterization of microplastic and nanoplastic particles in marine environment. *Environ. Pollut.* 297: 118773.

30 Weber, R., Watson, A., Forter, M. et al. (2011). Review article: persistent organic pollutants and landfills - a review of past experiences and future challenges. *Waste Manag. Res.* 29 (1): 107–121.

31 Huang, W., Wang, X., Chen, D. et al. (2021). Toxicity mechanisms of polystyrene microplastics in marine mussels revealed by high-coverage quantitative metabolomics using chemical isotope labeling liquid chromatography mass spectrometry. *J. Hazard. Mater.* 417: 126003.

32 Patterson, J., Jeyasanta, K.I., Sathish, N. et al. (2019). Profiling microplastics in the Indian edible oyster, Magallana bilineata collected from the Tuticorin coast, gulf of Mannar. *Southeastern India. Sci. Total. Environ.* 691: 727–735.

33 Fraser, M.A., Chen, L., Ashar, M. et al. (2020). Occurrence and distribution of microplastics and polychlorinated biphenyls in sediments from the Qiantang River and Hangzhou Bay. *China. Ecotoxicol. Environ. Saf.* 196: 110536.

34 Mai, L., Bao, L.J., Shi, L. et al. (2018). Polycyclic aromatic hydrocarbons affiliated with microplastics in surface waters of Bohai and Huanghai seas. *China. Environ. Pollut.* 241: 834–840.

35 Tong, H., Hu, X., Zhong, X. et al. (2021). Adsorption and desorption of Triclosan on biodegradable polyhydroxybutyrate microplastics. *Environ. Toxicol. Chem.* 40 (1): 72–78.

36 Holmes, L.A., Turner, A., and Thompson, R.C. (2012). Adsorption of trace metals to plastic resin pellets in the marine environment. *Environ. Pollut.* 160 (1): 42–48.

37 Bakir, A., Rowland, S.J., and Thompson, R.C. (2014). Enhanced desorption of persistent organic pollutants from microplastics under simulated physiological conditions. *Environ. Pollut.* 185: 16–23.

38 Jaikumar, G., Brun, N.R., Vijver, M.G. et al. (2019). Reproductive toxicity of primary and secondary microplastics to three cladocerans during chronic exposure. *Environ. Pollut.* 249: 638–646.

39 Talvitie, J., Mikola, A., Koistinen, A. et al. (2017). Solutions to microplastic pollution - removal of microplastics from wastewater effluent with advanced wastewater treatment technologies. *Water Res.* 123: 401–407.

40 Cheung, P.K. and Fok, L. (2017). Characterisation of plastic microbeads in facial scrubs and their estimated emissions in mainland China. *Water Res.* 122: 53–61.

41 van Wezel, A., Caris, I., and Kools, S.A. (2016). Release of primary microplastics from consumer products to wastewater in the Netherlands. *Environ. Toxicol. Chem.* 35 (7): 1627–1631.

42 Wang, T., Li, B., Zou, X. et al. (2019). Emission of primary microplastics in mainland China: invisible but not negligible. *Water Res.* 162: 214–224.

43 Kole, P.J., Lohr, A.J., Van Belleghem, F. et al. (2017). Wear and tear of Tyres: a stealthy source of microplastics in the environment. *Int. J. Env. Res. Pub. He.* 14 (10): 1265.

44 Azizi, N., Nasseri, S., Nodehi, R.N. et al. (2022). Evaluation of conventional wastewater treatment plants efficiency to remove microplastics in terms of abundance, size, shape, and type: a systematic review and Meta-analysis. *Mar. Pollut. Bull.* 177: 113462.

45 Wang, T., Zou, X., Li, B. et al. (2019). Preliminary study of the source apportionment and diversity of microplastics: taking floating microplastics in the South China Sea as an example. *Environ. Pollut.* 245: 965–974.

46 Wang, X., Mauzerall, D.L., Hu, Y. et al. (2005). A high-resolution emission inventory for eastern China in 2000 and three scenarios for 2020. *Atmos. Environ.* 39 (32): 5917–5933.

47 Fan, Y., Zheng, K., Zhu, Z. et al. (2019). Distribution, sedimentary record, and persistence of microplastics in the Pearl River catchment. *China. Environ. Pollut.* 251: 862–870.

48 Cox, K.D., Covernton, G.A., Davies, H.L. et al. (2019). Human consumption of microplastics. *Environ. Sci. Technol.* 53 (12): 7068–7074.

49 Bosker, T., Bouwman, L.J., Brun, N.R. et al. (2019). Microplastics accumulate on pores in seed capsule and delay germination and root growth of the terrestrial vascular plant Lepidium sativum. *Chemosphere* 226: 774–781.

50 Sanchez-Hernandez, L.J., Ramirez-Romero, P., Rodriguez-Gonzalez, F. et al. (2021). Seasonal evidences of microplastics in environmental matrices of a tourist dominated urban estuary in Gulf of Mexico, Mexico. *Chemosphere* 277: 130261.

51 Liu, M., Lu, S., Song, Y. et al. (2018). Microplastic and mesoplastic pollution in farmland soils in suburbs of Shanghai. *China. Environ. Pollut.* 242 (Pt A): 855–862.

52 Dhir, R.K., Brito, J., Mangabhai, R. et al. (2017). Production and properties of copper slag. In: *Sustainable Construction Materials: Copper Slag*, 27–86.

53 Barboza, L.G.A., Dick Vethaak, A., Lavorante, B. et al. (2018). Marine microplastic debris: An emerging issue for food security, food safety and human health. *Mar. Pollut. Bull.* 133: 336–348.

54 Carbery, M., O'Connor, W., and Palanisami, T. (2018). Trophic transfer of microplastics and mixed contaminants in the marine food web and implications for human health. *Environ. Int.* 115: 400–409.

55 Zhang, N., Li, Y.B., He, H.R. et al. (2021). You are what you eat: microplastics in the feces of young men living in Beijing. *Sci. Total. Environ.* 767: 144345.

56 Waldschlager, K., Lechthaler, S., Stauch, G. et al. (2020). The way of microplastic through the environment - application of the source-pathway-receptor model (review). *Sci. Total. Environ.* 713: 136584.

57 Khalik, W., Ibrahim, Y.S., Tuan Anuar, S. et al. (2018). Microplastics analysis in Malaysian marine waters: a field study of Kuala Nerus and Kuantan. *Mar. Pollut. Bull.* 135: 451–457.

58 Ziajahromi, S., Kumar, A., Neale, P.A. et al. (2017). Impact of microplastic beads and fibers on waterflea (*Ceriodaphnia dubia*) survival, growth, and reproduction: implications of single and mixture exposures. *Environ. Sci. Technol.* 51 (22): 13397–13406.

59 Browne, M.A., Crump, P., Niven, S.J. et al. (2011). Accumulation of microplastic on shorelines woldwide: sources and sinks. *Environ. Sci. Technol.* 45 (21): 9175–9179.

60 Dris, R., Gasperi, J., Mirande, C. et al. (2017). A first overview of textile fibers, including microplastics, in indoor and outdoor environments. *Environ. Pollut.* 221: 453–458.

61 De Falco, F., Cocca, M., Avella, M. et al. (2020). Microfiber release to water, via laundering, and to air, via everyday use: a comparison between polyester clothing with differing textile parameters. *Environ. Sci. Technol.* 54 (6): 3288–3296.

62 Zambrano, M.C., Pawlak, J.J., Daystar, J. et al. (2019). Microfibers generated from the laundering of cotton, rayon and polyester based fabrics and their aquatic biodegradation. *Mar. Pollut. Bull.* 142: 394–407.

63 Hartline, N.L., Bruce, N.J., Karba, S.N. et al. (2016). Microfiber masses recovered from conventional machine washing of new or aged garments. *Environ. Sci. Technol.* 50 (21): 11532–11538.

64 Caruso, G. (2019). Microplastics as vectors of contaminants. *Mar. Pollut. Bull.* 146: 921–924.

65 Lei, K., Qiao, F., Liu, Q. et al. (2017). Microplastics releasing from personal care and cosmetic products in China. *Mar. Pollut. Bull.* 123 (1–2): 122–126.

66 Praveena, S.M., Shaifuddin, S.N.M., and Akizuki, S. (2018). Exploration of microplastics from personal care and cosmetic products and its estimated emissions to marine environment: an evidence from Malaysia. *Mar. Pollut. Bull.* 136: 135–140.

67 Abbasi, S., Keshavarzi, B., Moore, F. et al. (2019). Distribution and potential health impacts of microplastics and microrubbers in air and street dusts from Asaluyeh County. *Iran. Environ. Pollut.* 244: 153–164.

68 Besseling, E., Quik, J.T.K., Sun, M. et al. (2017). Fate of nano- and microplastic in freshwater systems: a modeling study. *Environ. Pollut.* 220 (Pt A): 540–548.

69 Cole, M., Lindeque, P.K., Fileman, E. et al. (2016). Microplastics Alter the properties and sinking rates of Zooplankton Faecal Pellets. *Environ. Sci. Technol.* 50 (6): 3239–3246.

70 Koelmans, A.A., Bakir, A., Burton, G.A. et al. (2016). Microplastic as a vector for chemicals in the aquatic environment: critical review and model-supported reinterpretation of empirical studies. *Environ. Sci. Technol.* 50 (7): 3315–3326.

71 McDevitt, J.P., Criddle, C.S., Morse, M. et al. (2017). Addressing the issue of microplastics in the wake of the microbead-free waters act-a new standard can facilitate improved policy. *Environ. Sci. Technol.* 51 (12): 6611–6617.

72 Rochman, C.M., Kross, S.M., Armstrong, J.B. et al. (2015). Scientific evidence supports a ban on microbeads. *Environ. Sci. Technol.* 49 (18): 10759–10761.

73 Yurtsever, M. (2019). Glitters as a source of primary microplastics: an approach to environmental responsibility and ethics. *J. Agr. Environ. Ethic.* 32 (3): 459–478.

74 Julienne, F., Lagarde, F., and Delorme, N. (2019). Influence of the crystalline structure on the fragmentation of weathered polyolefines. *Polym. Degrad. Stab.* 170: 109012.

75 Phuong, N.N., Zalouk-Vergnoux, A., Poirier, L. et al. (2016). Is there any consistency between the microplastics found in the field and those used in laboratory experiments? *Environ. Pollut.* 211: 111–123.

76 Zhang, C., Li, Y., Kang, W. et al. (2021). Current advances and future perspectives of additive manufacturing for functional polymeric materials and devices. *SusMat.* 1 (1): 127–147.

77 Sorasan, C., Edo, C., Gonzalez-Pleiter, M. et al. (2022). Ageing and fragmentation of marine microplastics. *Sci. Total. Environ.* 827: 154438.

78 Geyer, R., Jambeck, J.R., and Law, K.L. (2017). Production, use, and fate of all plastics ever made. *Sci. Adv.* 3 (7): e1700782.

79 Naik, R.A., Rowles, L.S. 3rd, Hossain, A.I. et al. (2020). Microplastic particle versus fiber generation during photo-transformation in simulated seawater. *Sci. Total. Environ.* 736: 139690.

80 Kale, S.K., Deshmukh, A.G., Dudhare, M.S. et al. (2015). Microbial degradation of plastic: a review. *J. Biochem. Technol.* 6 (2): 952–961.

81 Song, Y.K., Hong, S.H., Eo, S. et al. (2022). The fragmentation of nano- and microplastic particles from thermoplastics accelerated by simulated-sunlight-mediated photooxidation. *Environ. Pollut.* 311: 119847.

82 Chamas, A., Moon, H., Zheng, J. et al. (2020). Degradation rates of plastics in the environment. *ACS Sustain. Chem. Eng.* 8 (9): 3494–3511.

83 Cooper, D.A. and Corcoran, P.L. (2010). Effects of mechanical and chemical processes on the degradation of plastic beach debris on the island of Kauai. *Hawaii. Mar. Pollut. Bull.* 60 (5): 650–654.

84 Yoshida, S., Hiraga, K., Takehana, T. et al. (2016). A bacterium that degrades and assimilates poly (ethylene terephthalate). *Science.* 351 (6278): 1196–1199.

85 Liu, L., Xu, M., Ye, Y. et al. (2022). On the degradation of (micro)plastics: degradation methods, influencing factors, environmental impacts. *Sci. Total. Environ.* 806: 151312.

86 Huang, Z., Cui, Q., Yang, X. et al. (2022). An evaluation model to predict microplastics generation from polystyrene foams and experimental verification. *J. Hazard. Mater.* 446: 130673.

87 Cui, Q., Yang, X., Li, J. et al. (2022). Microplastics generation behavior of polypropylene films with different crystalline structures under UV irradiation. *Polym. Degrad. Stab.* 199: 109916.

88 Resmerita, A.M., Coroaba, A., Darie, R. et al. (2018). Erosion as a possible mechanism for the decrease of size of plastic pieces floating in oceans. *Mar. Pollut. Bull.* 127: 387–395.

89 Enfrin, M., Lee, J., Gibert, Y. et al. (2020). Release of hazardous nanoplastic contaminants due to microplastics fragmentation under shear stress forces. *J. Hazard. Mater.* 384: 121393.

90 Tong, H., Zhong, X., Duan, Z. et al. (2022). Micro- and nanoplastics released from biodegradable and conventional plastics during degradation: formation, aging factors, and toxicity. *Sci. Total. Environ.* 833: 155275.

91 Song, Y.K., Hong, S.H., Jang, M. et al. (2017). Combined effects of UV exposure duration and mechanical abrasion on microplastic fragmentation by polymer type. *Environ. Sci. Technol.* 51 (8): 4368–4376.

92 González-Pleiter, M., Tamayo-Belda, M., Pulido-Reyes, G. et al. (2019). Secondary nanoplastics released from a biodegradable microplastic severely impact freshwater environments. *Environ. Sci. Nano.* 6 (5): 1382–1392.

93 Kalogerakis, N., Karkanorachaki, K., Kalogerakis, G.C. et al. (2017). Microplastics generation: onset of fragmentation of polyethylene films in marine environment mesocosms. *Front. Mar. Sci.* 4: 84.

94 Jaiswal, P.B., Pushkar, B.K., Maikap, K. et al. (2022). Abiotic aging assisted bio-oxidation and degradation of LLDPE/LDPE packaging polyethylene film by stimulated enrichment culture. *Polym. Degrad. Stab.* 206: 110156.

95 da Costa, J.P., Santos, P.S.M., Duarte, A.C. et al. (2016). (Nano)plastics in the environment - sources, fates and effects. *Sci. Total. Environ.* 566-567: 15–26.

96 Lambert, S. and Wagner, M. (2018). *Microplastics Are Contaminants of Emerging Concern in Freshwater Environments: An Overview*, 1–23. Springer International Publishing.

97 Lambert, S., Sinclair, C., and Boxall, A. (2014). Occurrence, degradation, and effect of polymer-based materials in the environment. *Rev. Environ. Contam. Toxicol.* 227: 1–53.

98 Lambert, S. and Wagner, M. (2016). Formation of microscopic particles during the degradation of different polymers. *Chemosphere* 161: 510–517.

99 Yang, Y., Li, Z., Yan, C. et al. (2022). Kinetics of microplastic generation from different types of mulch films in agricultural soil. *Sci. Total. Environ.* 814: 152572.

100 El Hadri, H., Gigault, J., Maxit, B. et al. (2020). Nanoplastic from mechanically degraded primary and secondary microplastics for environmental assessments. *NanoImpact* 17: 100206.

101 Koelmans, A.A. (2019). Proxies for nanoplastic. *Nat. Nanotechnol.* 14 (4): 307–308.

102 Besseling, E., Wegner, A., Foekema, E.M. et al. (2013). Effects of microplastic on fitness and PCB bioaccumulation by the lugworm *Arenicola marina* (L.). *Environ. Sci. Technol.* 47 (1): 593–600.

103 Wegner, A., Besseling, E., Foekema, E.M. et al. (2012). Effects of nanopolystyrene on the feeding behavior of the blue mussel (*Mytilus edulis* L.). *Environ. Toxicol. Chem.* 31 (11): 2490–2497.

104 Banerjee, A. and Shelver, W.L. (2021). Micro- and nanoplastic induced cellular toxicity in mammals: a review. *Sci. Total. Environ.* 755: 142518.

105 Sorensen, L., Rogers, E., Altin, D. et al. (2020). Sorption of PAHs to microplastic and their bioavailability and toxicity to marine copepods under co-exposure conditions. *Environ. Pollut.* 258: 113844.

106 Ardusso, M., Forero-Lopez, A.D., Buzzi, N.S. et al. (2021). COVID-19 pandemic repercussions on plastic and antiviral polymeric textile causing pollution on beaches and coasts of South America. *Sci. Total. Environ.* 763: 144365.

107 Sangkham, S. (2020). Face mask and medical waste disposal during the novel COVID-19 pandemic in Asia. *Case Stud. Therm. Eng.* 2: 100052.

108 Aragaw, T.A. (2020). Surgical face masks as a potential source for microplastic pollution in the COVID-19 scenario. *Mar. Pollut. Bull.* 159: 111517.

109 Rujnic-Sokele, M. and Pilipovic, A. (2017). Challenges and opportunities of biodegradable plastics: a mini review. *Waste Manag. Res.* 35 (2): 132–140.

110 Singh, B. and Sharma, N. (2008). Mechanistic implications of plastic degradation. *Polym. Degrad. Stab.* 93 (3): 561–584.

111 Kumar, M., Xiong, X., He, M. et al. (2020). Microplastics as pollutants in agricultural soils. *Environ. Pollut.* 265: 114980.

112 Cai, L., Wang, J., Peng, J. et al. (2018). Observation of the degradation of three types of plastic pellets exposed to UV irradiation in three different environments. *Sci. Total. Environ.* 628–629: 740–747.

113 Fairbrother, A., Hsueh, H.-C., Kim, J.H. et al. (2019). Temperature and light intensity effects on photodegradation of high-density polyethylene. *Polym. Degrad. Stab.* 165: 153–160.

114 Rouillon, C., Bussiere, P.O., Desnoux, E. et al. (2016). Is carbonyl index a quantitative probe to monitor polypropylene photodegradation? *Polym. Degrad. Stab.* 128: 200–208.

115 Dong, M., Zhang, Q., Xing, X. et al. (2020). Raman spectra and surface changes of microplastics weathered under natural environments. *Sci. Total. Environ.* 739: 139990.

116 Karlsson, T.M., Hassellov, M., and Jakubowicz, I. (2018). Influence of thermooxidative degradation on the in situ fate of polyethylene in temperate coastal waters. *Mar. Pollut. Bull.* 135: 187–194.

117 Wang, X., Li, Y., Zhao, J. et al. (2020). UV-induced aggregation of polystyrene nanoplastics: effects of radicals, surface functional groups and electrolyte. *Environ. Sci. Nano.* 7 (12): 3914–3926.

118 Pirsaheb, M., Hossini, H., and Makhdoumi, P. (2020). Review of microplastic occurrence and toxicological effects in marine environment: experimental evidence of inflammation. *Process Saf. Environ. Prot.* 142: 1–14.

119 Peterson, J.D., Vyazovkin, S., and Wight, C.A. (2001). Kinetics of the thermal and Thermo-oxidative degradation of polystyrene, polyethylene and poly(propylene). *Macromol. Chem. Phys.* 202 (6): 775–784.

120 Ward, C.P., Armstrong, C.J., Walsh, A.N. et al. (2019). Sunlight converts polystyrene to carbon dioxide and dissolved organic carbon. *Environ. Sci. Technol. Lett.* 6 (11): 669–674.

121 Zurier, H.S. and Goddard, J.M. (2021). Biodegradation of microplastics in food and agriculture. *Case Stud. Therm. Eng.* 37: 37–44.

122 Andrady, A.L., Hamid, H.S., and Torikai, A. (2003). Effects of climate change and UV-B on materials. *Photochem. Photobiol. Sci.* 2 (1): 68–72.

123 Kamweru, P.K., Ndiritu, F.G., Kinyanjui, T.K. et al. (2011). Study of temperature and UV wavelength range effects on degradation of photo-irradiated polyethylene films using DMA. *J. Macromol. Sci.* 50 (7): 1338–1349.

124 Deshoulles, Q., Le Gall, M., Dreanno, C. et al. (2022). Chemical coupling between oxidation and hydrolysis in polyamide 6 - a key aspect in the understanding of microplastic formation. *Polym. Degrad. Stab.* 197: 109851.

125 Deshoulles, Q., Gall, M.L., Benali, S. et al. (2022). Hydrolytic degradation of biodegradable poly(butylene adipate-co-terephthalate) (PBAT) – Towards an understanding of microplastics fragmentation. *Polym. Degrad. Stab.* 205: 110122.

126 Wang, W.-H., Huang, C.-W., Tsou, E.-Y. et al. (2021). Characterization of degradation behavior of poly(glycerol maleate) films in various aqueous environments. *Polym. Degrad. Stab.* 183: 109441.

127 Oyama, H.T., Kimura, M., Nakamura, Y. et al. (2020). Environmentally safe bioadditive allows degradation of refractory poly(lactic acid) in seawater: effect of poly(aspartic acid-co-l-lactide) on the hydrolytic degradation of PLLA at different salinity and pH conditions. *Polym. Degrad. Stab.* 178: 109216.

128 Mao, R., Lang, M., Yu, X. et al. (2020). Aging mechanism of microplastics with UV irradiation and its effects on the adsorption of heavy metals. *J. Hazard. Mater.* 393: 122515.

129 Tian, C., Lv, J., Zhang, W. et al. (2022). Accelerated degradation of microplastics at the liquid Interface of ice crystals in frozen aqueous solutions. *Angew. Chem. Int. Ed.* 61 (31): e202206947.

130 Blasing, M. and Amelung, W. (2018). Plastics in soil: analytical methods and possible sources. *Sci. Total. Environ.* 612: 422–435.

131 Ter Halle, A., Ladirat, L., Gendre, X. et al. (2016). Understanding the fragmentation pattern of marine plastic debris. *Environ. Sci. Technol.* 50 (11): 5668–5675.

132 Li, J., Song, Y., and Cai, Y. (2020). Focus topics on microplastics in soil: analytical methods, occurrence, transport, and ecological risks. *Environ. Pollut.* 257: 113570.

133 Zhou, L., Wang, T., Qu, G. et al. (2020). Probing the aging processes and mechanisms of microplastic under simulated multiple actions generated by discharge plasma. *J. Hazard. Mater.* 398: 122956.

134 Chen, X., Xiong, X., Jiang, X. et al. (2019). Sinking of floating plastic debris caused by biofilm development in a freshwater lake. *Chemosphere* 222: 856–864.

135 Cassone, B.J., Grove, H.C., Elebute, O. et al. (1922). Role of the intestinal microbiome in low-density polyethylene degradation by caterpillar larvae of the greater wax moth, Galleria mellonella. *Proc. Biol. Sci.* 2020 (287): 20200112.

136 Wu, X., Pan, J., Li, M. et al. (2019). Selective enrichment of bacterial pathogens by microplastic biofilm. *Water Res.* 165: 114979.

137 Napper, I.E. and Thompson, R.C. (2019). Environmental deterioration of biodegradable, oxo-biodegradable, compostable, and conventional plastic carrier bags in the sea, soil, and open-air over a 3-year period. *Environ. Sci. Technol.* 53 (9): 4775–4783.

138 Auta, H.S., Emenike, C.U., and Fauziah, S.H. (2017). Screening of Bacillus strains isolated from mangrove ecosystems in peninsular Malaysia for microplastic degradation. *Environ. Pollut.* 231: 1552–1559.

139 Huber, M., Archodoulaki, V.-M., Pomakhina, E. et al. (2022). Environmental degradation and formation of secondary microplastics from packaging material: a polypropylene film case study. *Polym. Degrad. Stab.* 195: 109794.

140 Julienne, F., Lagarde, F., Bardeau, J.-F. et al. (2022). Thin polyethylene (LDPE) films with controlled crystalline morphology for studying plastic weathering and microplastic generation. *Polym. Degrad. Stab.* 195: 109791.

141 Ossmann, B.E., Sarau, G., Holtmannspotter, H. et al. (2018). Small-sized microplastics and pigmented particles in bottled mineral water. *Water Res.* 141: 307–316.

142 Zuccarello, P., Ferrante, M., Cristaldi, A. et al. (2019). Exposure to microplastics (<10 mum) associated to plastic bottles mineral water consumption: the first quantitative study. *Water Res.* 157: 365–371.

143 Giese, A., Kerpen, J., Weber, F. et al. (2021). A preliminary study of microplastic abrasion from the screw cap system of reusable plastic bottles by Raman microspectroscopy. *ACS ES&T Water* 1 (6): 1363–1368.

144 Chen, Y., Xu, H., Luo, Y. et al. (2023). Plastic bottles for chilled carbonated beverages as a source of microplastics and nanoplastics. *Water Res.* 242: 120243.

145 Zhang, X., Lin, T., and Wang, X. (2022). Investigation of microplastics release behavior from ozone-exposed plastic pipe materials. *Environ. Pollut.* 296: 118758.

146 Zhang, X., Liu, C., Liu, J. et al. (2022). Release of microplastics from typical rainwater facilities during aging process. *Sci. Total. Environ.* 813: 152674.

147 He, H., Li, F., Liu, K. et al. (2023). The disinfectant residues promote the leaching of water contaminants from plastic pipe particles. *Environ. Pollut.* 327: 121577.

148 Liang, H., Ji, Y., Ge, W. et al. (2022). Release kinetics of microplastics from disposable face masks into the aqueous environment. *Sci. Total. Environ.* 816: 151650.

149 Liu, Z., Zhu, Y., Lv, S. et al. (2021). Quantifying the dynamics of polystyrene microplastics UV-aging process. *Environ. Sci. Technol. Lett.* 9 (1): 50–56.

150 Zhu, K., Sun, Y., Jiang, W. et al. (2022). Inorganic anions influenced the photoaging kinetics and mechanism of polystyrene microplastic under the simulated sunlight: role of reactive radical species. *Water Res.* 216: 118294.

151 Andrady, A.L. (2017). The plastic in microplastics: a review. *Mar. Pollut. Bull.* 119 (1): 12–22.

152 O'Brine, T. and Thompson, R.C. (2010). Degradation of plastic carrier bags in the marine environment. *Mar. Pollut. Bull.* 60 (12): 2279–2283.

153 Allen, D., Allen, S., Abbasi, S. et al. (2022). Microplastics and nanoplastics in the marine-atmosphere environment. *Nat. Rev. Earth Environ.* 3 (6): 393–405.

154 Peller, J.R., Mezyk, S.P., Shidler, S. et al. (2022). Facile nanoplastics formation from macro and microplastics in aqueous media. *Environ. Pollut.* 313: 120171.

155 Luo, Y., Al Amin, M., Gibson, C.T. et al. (2022). Raman imaging of microplastics and nanoplastics generated by cutting PVC pipe. *Environ. Pollut.* 298: 118857.

156 Wang, M., Li, Q., Shi, C. et al. (2023). Oligomer nanoparticle release from polylactic acid plastics catalysed by gut enzymes triggers acute inflammation. *Nat. Nanotechnol.* 18 (4): 403–411.

157 Shen, C., Zhao, X., Long, Y. et al. (2023). Approach for the low carbon footprint of biodegradable plastic PBAT: complete recovery of its every monomer via high-efficiency hydrolysis and separation. *ACS Sustain. Chem. Eng.* 11 (5): 2005–2013.

158 Degli-Innocenti, F., Barbale, M., Chinaglia, S. et al. (2022). Analysis of the microplastic emission potential of a starch-based biodegradable plastic material. *Polym. Degrad. Stab.* 199: 109934.

159 MacArthur, E. (2017). Beyond plastic waste. *Science* 358 (6365): 843.

160 Kemona, A. and Piotrowska, M. (2020). Polyurethane recycling and disposal: methods and prospects. *Polymers* 12 (8): 1752.

161 Xie, F., Zhang, T., Bryant, P. et al. (2019). Degradation and stabilization of polyurethane elastomers. *Prog. Polym. Sci.* 90: 211–268.

162 Rosu, D., Rosu, L., and Cascaval, C.N. (2009). IR-change and yellowing of polyurethane as a result of UV irradiation. *Polym. Degrad. and Stabil.* 94 (4): 591–596.

163 Datta, J., Kosiorek, P., and Włoch, M. (2016). Synthesis, structure and properties of poly(ether-urethane)s synthesized using a tri-functional oxypropylated glycerol as a polyol. *J. Therm. Anal. Calorim.* 128 (1): 155–167.

164 Wang, H., Wang, Y., Liu, D. et al. (2014). Effects of additives on weather-resistance properties of polyurethane films exposed to ultraviolet radiation and ozone atmosphere. *J. Nanomater.* 2014: 1–7.

165 Brzeska, J., Morawska, M., Sikorska, W. et al. (2017). Degradability of cross-linked polyurethanes based on synthetic polyhydroxybutyrate and modified with polylactide. *Chem. Zvesti.* 71 (11): 2243–2251.

166 Scholz, P., Wachtendorf, V., Panne, U. et al. (2019). Degradation of MDI-based polyether and polyester-polyurethanes in various environments – effects on molecular mass and crosslinking. *Polym. Test.* 77: 105881.

167 Gewert, B., Plassmann, M., Sandblom, O. et al. (2018). Identification of chain scission products released to water by plastic exposed to ultraviolet light. *Environ. Sci. Technol. Lett.* 5 (5): 272–276.

168 Jiang, Z., Huang, L., Fan, Y. et al. (2022). Contrasting effects of microplastic aging upon the adsorption of sulfonamides and its mechanism. *Chem. Eng. J.* 430: 132939.

169 Theiler, G., Wachtendorf, V., Elert, A. et al. (2018). Effects of UV radiation on the friction behavior of thermoplastic polyurethanes. *Polym. Test.* 70: 467–473.

170 Albergamo, V., Wohlleben, W., and Plata, D.L. (2023). Photochemical weathering of polyurethane microplastics produced complex and dynamic mixtures of dissolved organic chemicals. *Environ. Sci-Proc. Imp.* 25 (3): 432–444.

171 Zheng, T., Zheng, X., Zhan, S. et al. (2021). Study on the ozone aging mechanism of natural rubber. *Polym. Degrad. and Stabil.* 186: 109514.
172 Karekar, A., Schicktanz, C., Tariq, M. et al. (2023). Effects of artificial weathering in NR/SBR elastomer blends. *Polym. Degrad. and Stabil.* 208: 110267.
173 Wang, M., Wang, R., Chen, X. et al. (2022). Effect of non-rubber components on the crosslinking structure and thermo-oxidative degradation of natural rubber. *Polym. Degrad. and Stabil.* 196: 109845.
174 Thomas, J., Moosavian, S.K., Cutright, T. et al. (2022). Investigation of abiotic degradation of tire cryogrinds. *Polym. Degrad. and Stabil.* 195: 109814.
175 Choi, E.Y. and Kim, C.K. (2023). Degradation and lifetime prediction of thermoplastic polyurethane encapsulants in seawater for underwater acoustic sensor applications. *Polym. Degrad. and Stabil.* 209: 110281.
176 Schmidt, J., Wei, R., Oeser, T. et al. (2017). Degradation of polyester polyurethane by bacterial polyester hydrolases. *Polymers* 9 (2): 65.
177 Sipe, J.M., Bossa, N., Berger, W. et al. (2022). From bottle to microplastics: can we estimate how our plastic products are breaking down? *Sci. Total. Environ.* 814: 152460.
178 Kraibut, A., Saiwari, S., Kaewsakul, W. et al. (2022). Dynamic response and molecular chain modifications associated with degradation during mixing of silica-reinforced natural rubber compounds. *Polymers* 15 (1): 160.
179 Jung, U. and Choi, S.S. (2023). Variation in abundance ratio of isoprene and dipentene produced from wear particles composed of natural rubber by pyrolysis depending on the particle size and thermal aging. *Polymers* 15 (4): 929.
180 Moon, B., Lee, J., Park, S. et al. (2018). Study on the aging behavior of natural rubber/butadiene rubber (NR/BR) blends using a parallel spring model. *Polymers* 10 (6): 658.
181 Cai, Y., Mitrano, D.M., Hufenus, R. et al. (2021). Formation of fiber fragments during abrasion of polyester textiles. *Environ. Sci. Technol.* 55 (12): 8001–8009.
182 Sorensen, L., Groven, A.S., Hovsbakken, I.A. et al. (2021). UV degradation of natural and synthetic microfibers causes fragmentation and release of polymer degradation products and chemical additives. *Sci. Total. Environ.* 755 (Pt 2): 143170.
183 Cai, Y., Yang, T., Mitrano, D.M. et al. (2020). Systematic study of microplastic fiber release from 12 different polyester textiles during washing. *Environ. Sci. Technol.* 54 (8): 4847–4855.
184 Hernandez, E., Nowack, B., and Mitrano, D.M. (2017). Polyester textiles as a source of microplastics from households: a mechanistic study to understand microfiber release during washing. *Environ. Sci. Technol.* 51 (12): 7036–7046.
185 Kuhn, S., van Franeker, J.A., O'Donoghue, A.M. et al. (2020). Details of plastic ingestion and fibre contamination in North Sea fishes. *Environ. Pollut.* 257: 113569.
186 Kurniawan, S.B., Said, N.S.M., Imron, M.F. et al. (2021). Microplastic pollution in the environment: insights into emerging sources and potential threats. *Environ. Sci. Technol. Lett.* 23: 101790.

187 Heo, Y., Cho, W.S., Maruthupandy, M. et al. (2022). Biokinetics of fluorophore-conjugated polystyrene microplastics in marine mussels. *J. Hazard Mater.* 438: 129471.

188 Song, Y.K., Hong, S.H., Eo, S. et al. (2020). Rapid production of micro- and nanoplastics by fragmentation of expanded polystyrene exposed to sunlight. *Environ. Sci. Technol.* 54 (18): 11191–11200.

189 Schleier, J., Simons, M., Greiff, K. et al. (2022). End-of-life treatment of EPS-based building insulation material – An estimation of future waste and review of treatment options. *Resour. Conserv. Recycl.* 187: 106603.

190 Wang, Z., An, C., Chen, X. et al. (2021). Disposable masks release microplastics to the aqueous environment with exacerbation by natural weathering. *J. Hazard. Mater.* 417: 126036.

191 Zhu, K., Jia, H., Zhao, S. et al. (2019). Formation of environmentally persistent free radicals on microplastics under light irradiation. *Environ. Sci. Technol.* 53 (14): 8177–8186.

192 Wu, X., Chen, X., Jiang, R. et al. (2022). New insights into the photo-degraded polystyrene microplastic: effect on the release of volatile organic compounds. *J. Hazard. Mater.* 431: 128523.

193 Meides, N., Menzel, T., Poetzschner, B. et al. (2021). Reconstructing the environmental degradation of polystyrene by accelerated weathering. *Environ. Sci. Technol.* 55 (12): 7930–7938.

194 Miller, O., Freund, L., and Needleman, A. (1999). Modeling and simulation of dynamic fragmentation in brittle materials. *Int. J. Fracture.* 96: 101–125.

195 Liu, J., Zhang, T., Tian, L. et al. (2019). Aging significantly affects mobility and contaminant-mobilizing ability of nanoplastics in saturated loamy sand. *Environ. Sci. Technol.* 53 (10): 5805–5815.

196 Turner, A. (2020). Foamed polystyrene in the marine environment: sources, additives, transport, behavior, and impacts. *Environ. Sci. Technol.* 54 (17): 10411–10420.